AN ABSTRACT OF THE THESIS OF

Hisashi Machida for the degree of Doctor of Philosophy

in Chemistry presented on September 10, 1975

Title: A STUDY OF SIMULTANEOUS DIFFUSION OF Ca^{2+} AND Sr^{2+} IN ALKALI CHLORIDES

Abstract approved: Redacted for privacy

William J. Fredericks

The simultaneous diffusion of Ca^{2+} and Sr^{2+} ions in purified single crystals of KCl and NaCl was studied over the temperature ranges from 451°C to 669°C in KCl and from 448°C to 683°C in NaCl. A radioactive tracer technique was used in two types of measurements: diffusion from a deposited surface layer of $CaCl_2$ and $SrCl_2$ at temperatures below 580°C (the lowest melting eutectic) in the KCl system and below 500°C in the NaCl system, and diffusion from $CaCl_2$ and $SrCl_2$ vapors above 580°C in KCl and above 500°C in NaCl. The saturation diffusion coefficients, enthalpies and entropies of impurity-vacancy association were calculated using the common ion model for simultaneous diffusion of divalent ions in alkali halides.

The saturation diffusion coefficients $D_s(Ca)$ and $D_s(Sr)$ in KCl are given by

$$D_s(Ca) = 9.93 \times 10^{-5} \exp(-0.592\ eV/kT)\ cm^2/sec$$

and

$$D_s(Sr) = 1.20 \times 10^{-3} \exp(-0.871 \text{ eV}/kT) \text{ cm}^2/\text{sec}$$

for calcium and strontium, respectively.

The Gibbs free energy of association of the impurity-vacancy complex in KCl for calcium can be represented by

$$\Delta G(Ca) = -0.507 \text{ eV} + (2.25 \times 10^{-4} \text{ eV}/°K)T$$

and that for strontium by

$$\Delta G(Sr) = -0.575 \text{ eV} + (2.90 \times 10^{-4} \text{ eV}/°K)T.$$

In NaCl the saturation diffusion coefficients $D_s(Ca)$ and $D_s(Sr)$ are given by

$$D_s(Ca) = 1.14 \times 10^{-3} \exp(-0.851 \text{ eV}/kT) \text{cm}^2/\text{sec}$$

and

$$D_s(Sr) = 2.30 \times 10^{-3} \exp(-0.925 \text{ eV}/kT) \text{cm}^2/\text{sec}$$

for calcium and strontium, respectively.

The Gibbs free energy of association of the impurity-vacancy complex in NaCl for calcium can be represented by

$$\Delta G(Ca) = -0.572 \text{ eV} + (2.69 \times 10^{-4} \text{ eV}/°K)T$$

and that for strontium by

$$\Delta G(Sr) = -0.671 \text{ eV} + (3.35 \times 10^{-4} \text{ eV}/°K)T.$$

A Study of Simultaneous Diffusion of Ca^{2+} and Sr^{2+} in Alkali Chlorides

by

Hisashi Machida

A THESIS

submitted to

Oregon State University

in partial fulfillment of
the requirements for the
degree of

Doctor of Philosophy

June 1976

APPROVED:

Redacted for privacy

Professor of Chemistry

in charge of major

Redacted for privacy

Chairman of Department of Chemistry

Redacted for privacy

Dean of Graduate School

Date thesis is presented September 10, 1975

Typed by Clover Redfern for Hisashi Machida

ACKNOWLEDGMENT

I wish to express appreciation to Dr. W.J. Fredericks for suggesting the problem and for many helpful discussions on this work.

Acknowledgment is due to Ron Bennett for many useful suggestions and discussions, and for his help in proofreading this thesis.

Appreciation is due to Dr. Roman Schmitt of the O.S.U. Radiation Center for helping with radiation counting and activation analysis.

I also express thanks to the National Science Foundation for financial assistance in the form of a research assistantship.

Finally, I would like to express special gratitude to my wife, Yoko, for her understanding and encouragement which made the completion of this thesis possible.

TABLE OF CONTENTS

LIST OF TABLES

LIST OF FIGURES

A STUDY OF SIMULTANEOUS DIFFUSION OF Ca^{2+} AND Sr^{2+} IN ALKALI CHLORIDES

I. INTRODUCTION

The research presented in this thesis is a contribution to a long range program with the goal of understanding defect interactions in solids. The presence of such defects, with the sole exception of chemically different species, can only be inferred from their effect on physical properties of the solids. An addition to our knowledge of impurity-vacancy complex formation and behavior, specifically the formation of divalent cation-cation vacancy complexes in alkali halides, is the primary objective of this work.

It is known that mass transport properties of alkali halides are significantly changed by the addition of aliovalent impurity ions, that is, impurity ions which differ in charge from the corresponding solvent ion. In alkali halides a divalent cationic impurity M^{2+} is substitutionally dissolved in the cation sublattice along with a cation vacancy (a vacant site in the cation sublattice) to maintain electroneutrality (see Figure 1.1). Stasiw and Teltow (1947) postulated that the vacancies combine with the impurity ions, because of their opposite charges, to form impurity vacancy complexes. The existence of such complexes profoundly affects the diffusion and conduction properties of the alkali halides. The effect on the diffusion is

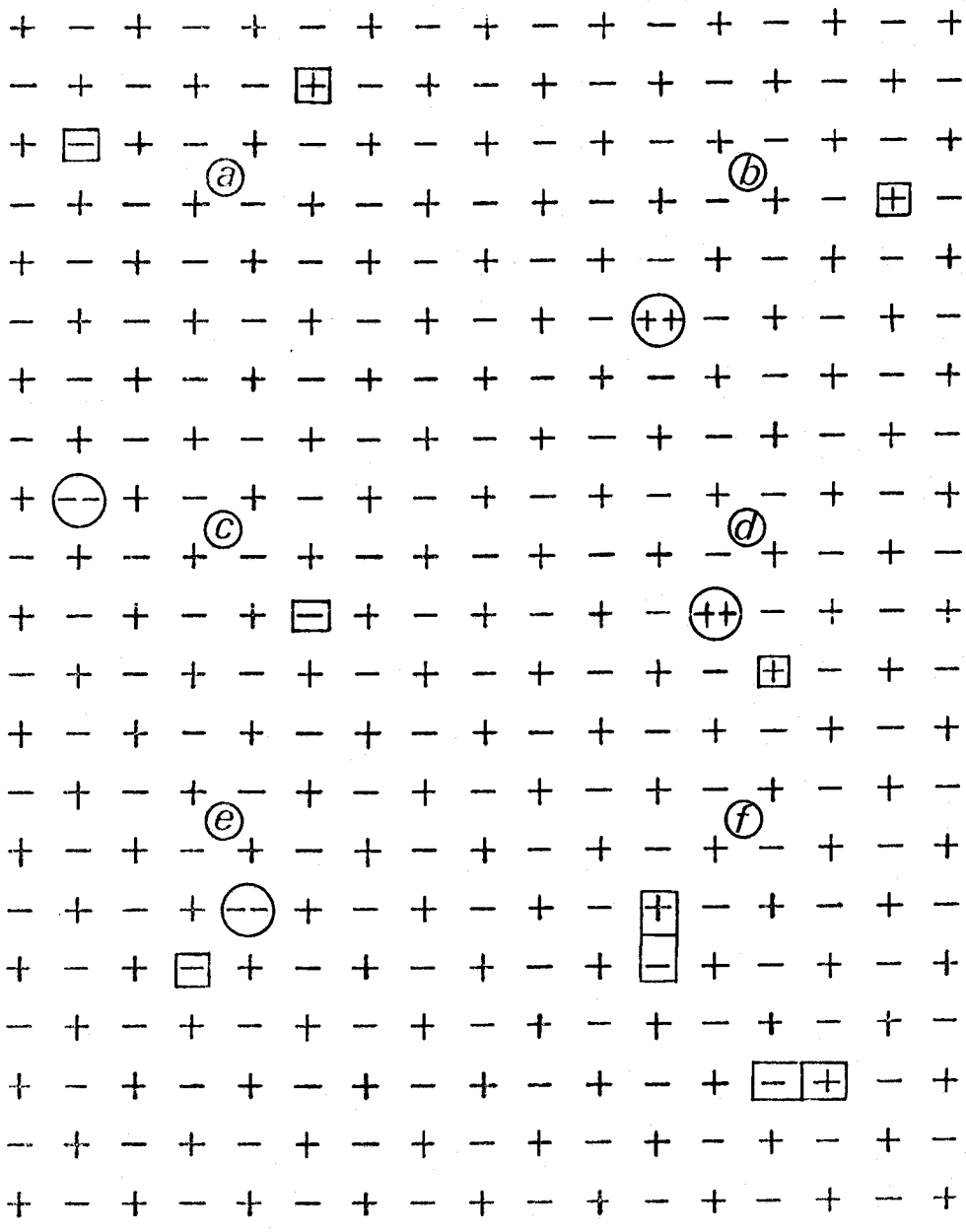

⊞ Cation vacancy. ⊟ Anion vacancy.

⊕⊕ Divalent cation impurity. ⊖⊖ Divalent anion impurity.

Figure 1.1. Point defects in the alkali halide crystal. Two-dimensional representation. a. Schottky defect. b. Divalent cation impurity. c. Divalent anion impurity. d. Divalent-cation-impurity—cation-vacancy complex. e. Divalent-anion-impurity—anion-vacancy complex. f. Vacancy pairs.

exemplified in Figure 1.2, which shows the data obtained for the Sr^{2+} diffusion from the vapor source in pure NaCl at 625°C. Line b in the figure was obtained from the vapor source solution of Fick's second law, which satisfies the boundary condition of constant surface concentration throughout the diffusion and which has the form of the error function complement (Crank, 1970, p. 19), by setting the constant diffusion coefficient $D = 1.69 \times 10^{-8}$ cm^2/sec. It is seen that the experimental penetration lies at higher concentrations than the calculated curve. The reason that the experimental data do not conform to the error function complement solution is that D is not constant but changes with the amount of Sr. The dependence of the diffusion coefficient on the concentration has been verified by a number of different workers. For example, Figure 1.3 shows data for Pb^{2+} diffusion in KCl (Keneshea and Fredericks, 1964). Note the diffusion coefficient approaches the constant value at higher concentrations.

The expected effect of impurity-vacancy complex formation on diffusion in alkali halide crystals is that the diffusion rate of the divalent cation impurity, which has a vacancy attached to it for a certain fraction of time, would be much greater than that of the monovalent cation impurity (the self-diffusion), which only makes chance encounters with the cation vacancies. It is shown in Figure 1.4 that the diffusion of Pb^{2+} in NaCl is greater than the diffusion of Na^{+}. This

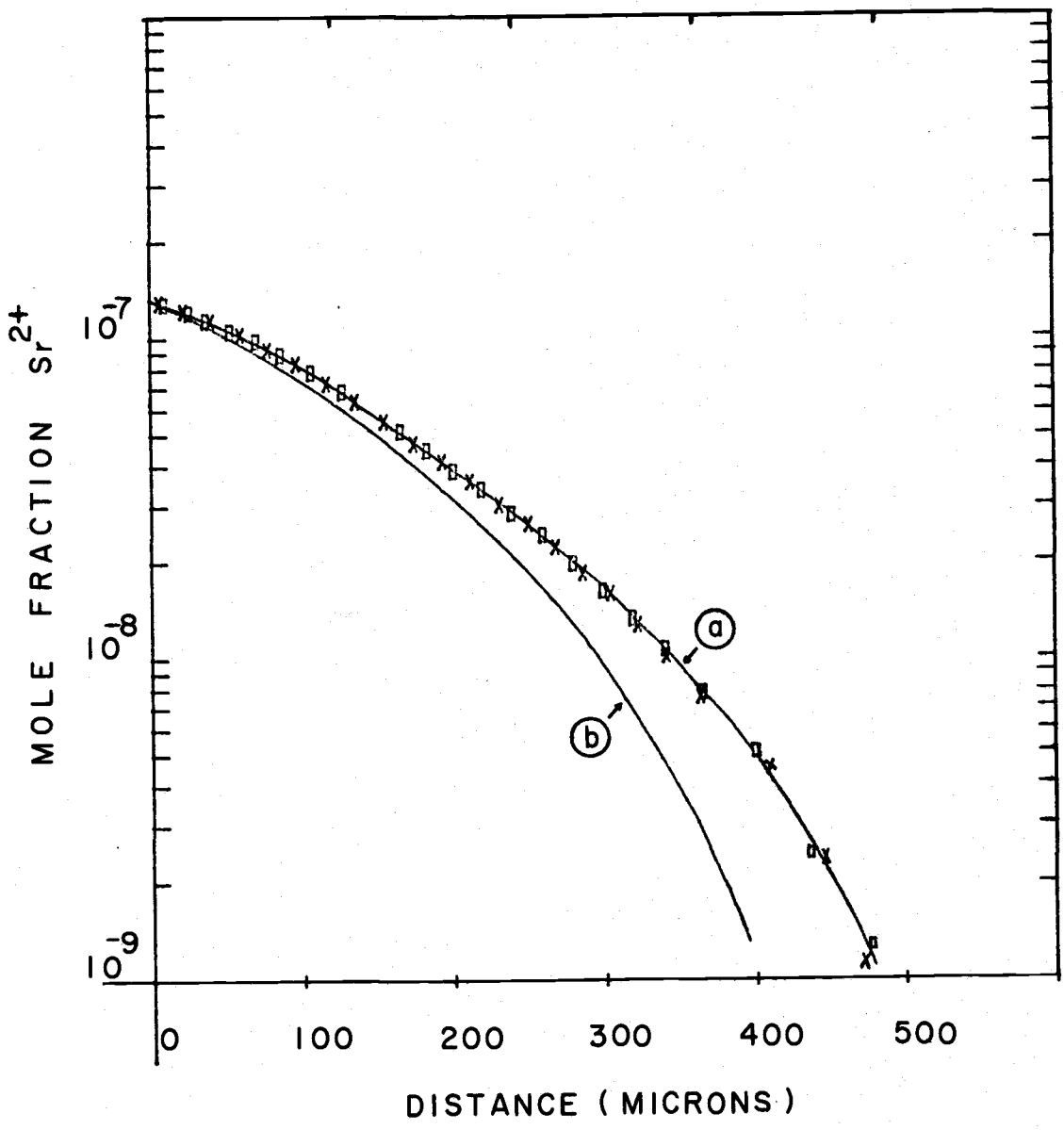

Figure 1.2. Diffusion of Sr^{2+} ions in pure NaCl from $SrCl_2$ Vapor. Temp.=625°C. Diffusion time=8.5806×10^5 sec.
a. Experimental. b. $C = C_0 \operatorname{erfc} \frac{x}{2\sqrt{Dt}}$
with $D=1.69 \times 10^{-8} cm^2/sec$.

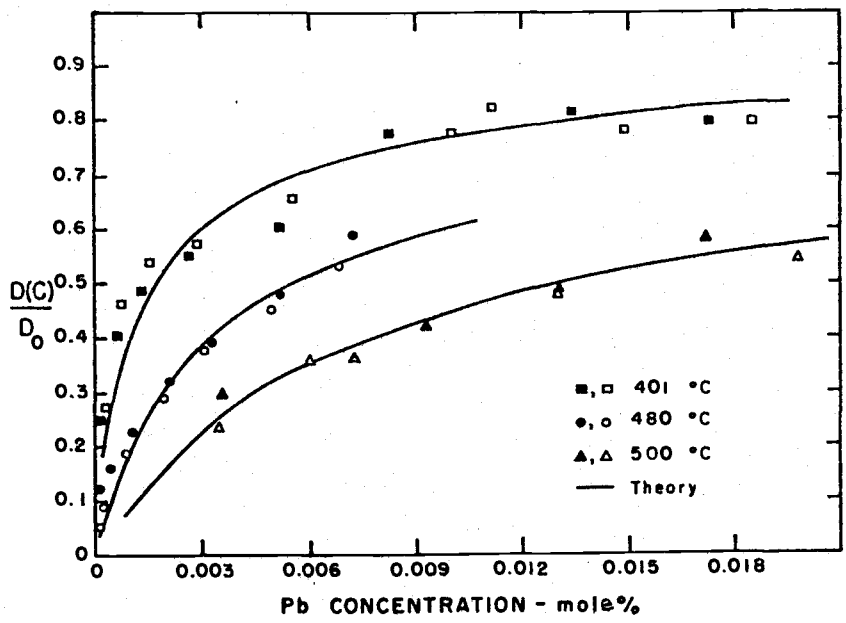

Figure 1.3. Diffusion of Pb^{2+} ions in pure KCl as a function of Pb concentration. Solid curves are theoretically calculated profiles. (Taken from Keneshea and Fredericks, 1964).

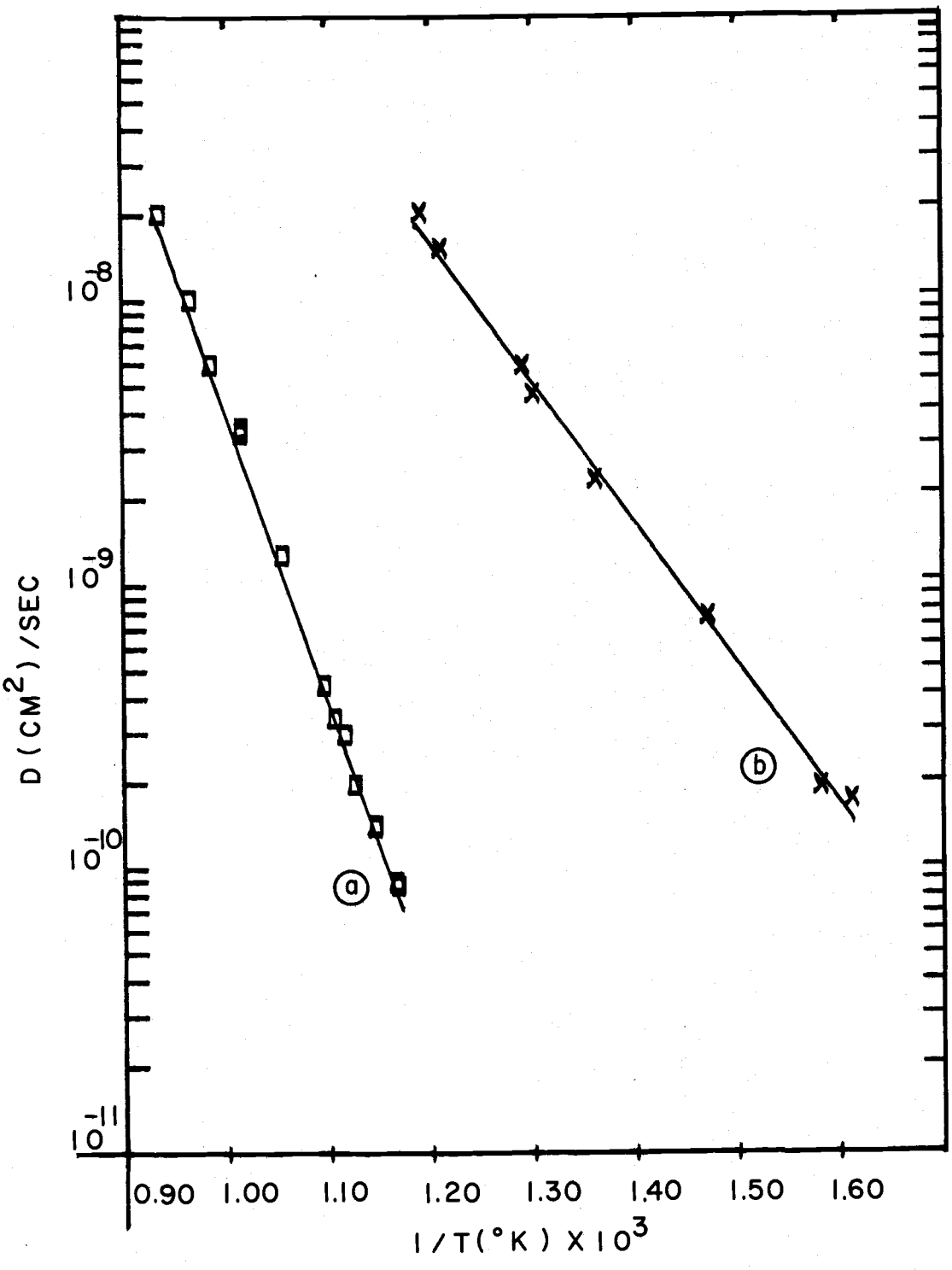

Figure 1.4. Diffusion of Pb^{2+} and Na^{+} ions in pure NaCl as a function of temperature. a. Na^{+} diffusion with U=2.04 eV(Rothman et al.,1972). b. Pb^{2+} diffusion with U=0.982 eV(Krause and Fredericks,1971).

behavior is to be expected if the divalent impurity ion forms complexes with the cation vacancies. In the figure the slopes of the straight lines give the activation energies of migration, which are a measure of the barrier energy that an ion must overcome in moving from its lattice site to the nearest neighbor vacancy. The activation energy for Na^{+} ion is 2.04 eV (Rothman et al., 1972) and for Pb^{2+} ion is 0.982 eV (Krause and Fredericks, 1971).

The formation of the divalent cation impurity-cation vacancy complex has also been verified through electron spin resonance experiments (Watkins, 1959), conductivity measurement (see, for example, Etzel and Maurer, 1950), and dielectric relaxation studies (Dreyfus, 1961).

The theory of transport properties in ionic crystals has been extensively reviewed by Lidiard (1957), Howard and Lidiard (1964), Barr and Lidiard (1970), Nowick (1972), Fuller (1972) and F. Beniere (1972). A recent review of matter transport in alkali halide crystals by Fredericks (1975) gives a detailed discussion of present theory and experimental situation of diffusion in alkali halides.

This work is concerned with the simultaneous diffusion of two divalent cations Ca^{2+} and Sr^{2+} in NaCl and KCl single crystals. The calcium and strontium ions were chosen as diffusants for several reasons. First, diffusion of divalent impurity cations in alkali halides has been studied in this laboratory for many years. More data were

needed on the relationship of the chemical nature of the diffusant and activation energy of migration and thermodynamic functions of associated divalent cation-cation vacancy complexes. Comparison of activation energies of migration, enthalpies and entropies of the complex formation, ionic radii, bond energies and ionicities of bonds between M^{2+} and Cl^{-} ions is given in Table 1.1.

Table 1.1 also illustrates the sensitivity of diffusion in these systems to uncontrolled impurities in both the host crystals and the diffusant. For example note the difference in U for the 1964 and 1973 Pb^{2+} (KCl) results. The earlier experiment used commercial host crystals which contained OH^{-}. The divalent ions form a stable compound in the host lattice with OH^{-} which retards the diffusion of the divalent ion (Allen and Fredericks, 1973). If the host crystal or the diffusant contains unknown aliovalent impurities the diffusion of the tracer can be increased or retarded from its true value (Fredericks, 1975). Although in recent experiments the host crystals are extremely pure, the tracers supplied by commercial sources may have excessive amounts of daughter products or residual ions left from preparation of the tracer isotope (Fredericks, 1975). For an illustration of how this source of impurities will affect the vacancy concentration and thus the diffusion of even monovalent ions see Rothman et al. (1972). The simultaneous diffusion method provides some correction for this problem because the major source of

Table 1.1. Values of the migration energy U, the enthalpy ΔH and the entropy ΔS of the complex formation, the bond energy and the ionicity of the bond between M^{2+} ion and Cl^- ion.

Cation	Radius (Å)[a]	U(eV)	ΔH(eV)	ΔS(eV/deg)[b]	Ionicity	BE(eV)[c]	Reference
Cd^{2+} (NaCl)	0.97	0.92	-1.085	-8.95×10^{-4}	0.806[d]	2.82	Allen et al. (1967)
Cd^{2+} (NaCl)		0.86	-0.972	-6.65×10^{-4}	0.417[e]	2.99±0.56	Krause and Fredericks (1971)[f]
Cd^{2+} (KCl)		0.54	-0.412	$+1.39\times10^{-4}$			Keneshea and Fredericks (1965)
Cd^{2+} (KCl)		0.56	-0.474	$+1.23\times10^{-4}$			Krause and Fredericks (1973)[f]
Ca^{2+} (NaCl)	0.99	0.85	-0.572	-2.69×10^{-4}	0.896[d]	2.80	This work[f]
Ca^{2+} (KCl)		0.59	-0.507	-2.25×10^{-4}	0.689[e]	6.29±1.08	This work[f]
Hg^{2+} (KCl)	1.10	0.57	$\Delta G = 0.80 - 0.75$		0.762[d]	1.04	Allen and Fredericks (1973)
					0.286[e]	3.63±0.13	
Sr^{2+} (NaCl)	1.13	0.93	-0.671	-3.35×10^{-4}	0.902[d]	3.04	This work[f]
Sr^{2+} (KCl)		0.87	-0.575	-2.90×10^{-4}	0.705[e]	6.33±0.61	This work[f]
Pb^{2+} (NaCl)	1.21	0.98	-0.780	-5.31×10^{-4}	0.724[d]	3.10	Mannion et al. (1968)
Pb^{2+} (NaCl)		0.98	-0.775	-5.29×10^{-4}	0.158[e]	3.25±0.30	Krause and Fredericks (1971)[f]
Pb^{2+} (KCl)		1.18	-1.188	-1.00×10^{-3}			Keneshea and Fredericks (1964)
Pb^{2+} (KCl)		0.91	-0.378	$+1.60\times10^{-4}$			Krause and Fredericks (1973)[f]

[a] Pauling radius (obtained using the rock salt type of structure as standard).

[b] Entropy of complex formation excluding configurational entropy.

[c] Bond energy (Vendeneyev et al., 1966). Upper values are BE of the reaction $MCl_2 \rightarrow MCl^+ + Cl^-$. Lower values are BE of the reaction $MCl^+ \rightarrow M^{2+} + Cl^-$.

[d] Ionicity of M^{2+} with octahedral bonding to six Cl^-. Calculated by Pauling's (1939) formula, $f_i' = (N/M) f_i + (1 - N/M)$.

[e] Ionicity of bond between M^{2+} and Cl^-. Calculated by Pauling's (1960) formula, $f_i = \exp(-1/4 (X_A - X_B)^2)$.

[f] Data from simultaneous diffusion experiments.

vacancies other than those introduced by the tracer or thermally is the other tracer. Thus the best values in Table 1.1 are those obtained by the simultaneous diffusion method (Krause and Fredericks, 1973). In the present work the additional precaution of purifying the tracers by ion exchange was taken.

All the ionic radii shown in Table 1.1 are Pauling (1960) radii. It has been shown that the ionic radii that were calculated by Fumi and Tosi (1964) give better results when used for point lattice calculations. However, the trends in the size of the radii are the same as those of Pauling and in diffusion the more important factor is the relative size of the diffusant compared to the ion which it substitutes.

The second reason for choosing Ca^{2+} and Sr^{2+} is that the electronic configurations of these ions are

$$Ca^{2+}[1s^2 2s^2 2p^6 3s^2 3p^6] = Ar$$

and

$$Sr^{2+}[1s^2 2s^2 2p^6 3s^2 3p^6 3d^{10} 4s^2 4p^6] = Kr,$$

respectively, and those of other divalent ions are $Cd^{2+}[Kr\ 3d^{10}]$, $Hg^{2+}[Xe\ 4f^{14} 4d^{10}]$ and $Pb^{2+}[Xe\ 4f^{14} 4d^{10} 6s^2]$. Note all the above ions have completely filled outmost orbitals, therefore all are spherical. One might assume that if a group of ions would have regular diffusion properties this group would. However, there are notable differences in the ionic properties among these ions. Note that with

the exception of Pb^{2+} they all form chlorides in which the divalent ion is surrounded by six Cl^- in the crystal (octahedral symmetry). $CaCl_2$ and $SrCl_2$ form the rutile and the fluorite structures (Wells, 1962, p. 339), respectively, and they are strongly ionic crystals. On the other hand $CdCl_2$ and $HgCl_2$ form layer structures with six coordination, and $PbCl_2$ forms a layer structure with higher coordination. An important feature of these layer structures is the unsymmetrical environment of the halogen atoms, in contrast to the symmetrical arrangement of the neighbors in the essentially ionic compounds. Thus the last three structures are characterized as less ionic crystals. The nature of simple anion-cation bonding can be estimated from the electronegativity of the separate ions (Pauling, 1960), which are given in Table 1.1. The ionicities of the M^{2+} ions octahedrally bonded to six Cl^- in a crystal structure are also given in Table 1.1. The method for calculating the ionicity will be described in Chapter V. Since there has been no method of calculating the ionicity of a divalent impurity with six surrounding Cl^- in a NaCl type lattice, the ionicity calculated from the $M^{2+}Cl_2$ crystal structure seems to be the only way to estimate the ionic properties of ions in a NaCl structure. Therefore, it was useful in determining the ionic properties that govern the differences in transport parameters to examine in two similar lattices ions of differing ionicity but similar size and ions differing both in size and ionicity.

A method of simultaneous diffusion of two divalent cations into NaCl and KCl was used in this work. This method is based on the idea that the common ion in the complex formation reactions, in this case the cation vacancy, provides the mechanisms through which the presence of other divalent cations affects the diffusion of the tracer impurity. The conditions required for fitting the two diffusion profiles are more rigorous than for the single ion diffusion because the interaction of one diffusant with the other must be taken into account. This should provide more accurate estimates of diffusion and association parameters of both diffusants. There is an additional advantage of using the simultaneous diffusion method, that is data can be obtained for two diffusants with the same number of anneals, sectionings and weighings as required for a single diffusant.

In the association reaction of the complex it is usually assumed that only nearest-neighbor defects interact strongly to form complexes, and no account is taken of the long-range Coulombic interactions among isolated defects. This theory can be improved by introducing Debye-Huckel theory of ionic solutions to include the extra interactions. If the inclusion of long-range Coulombic interactions do not change significantly the values of thermodynamic parameters and the diffusion coefficients, it can be concluded that the diffusants were below concentrations that require the correction for the Debye-Huckel effect.

Since both diffusion and ionic conductivity data have been reliable sources for obtaining thermodynamic descriptions of alkali halide-divalent cation systems, it will be interesting to compare the results from the two different types of measurements.

II. THEORY AND MATHEMATICAL SOLUTIONS

The introduction of aliovalent impurity ions into an ionic crystal results in the presence of additional defects, that is, sufficient vacancies or intersitital ions to achieve charge neutrality must also be introduced into the crystal. In an alkali halide crystal it is known that a substitutionally introduced divalent impurity cation is accompanied by a vacancy on the cation sublattice (Lidiard, 1957). The divalent cation, M^{2+} ion, possesses an effective +1 charge relative to the perfect crystal, while the cation vacancy introduces an effective -1 charge. Owing to the Coulombic attraction between such a pair of point defects they form an impurity-vacancy complex which possesses a relatively strong binding energy. If the diffusion of an aliovalent impurity ion occurs by means of a vacancy mechanism, an M^{2+} ion can only diffuse when it is associated with a vacancy. Thus, it is convenient to regard the complex as the diffusing particle. We consider a one-dimensional diffusion problem, for which the flux of the complex is given by

$$J = -D_s \, \partial(Npc)/\partial x \qquad (2.1)$$

where J is the flux of the complexes in the x direction, D_s is the diffusion coefficient of the complexes, $\partial(Npc)/\partial x$ is the gradient of concentration of the complexes, N is the number of cations per cm^3, c is the mole fraction of the aliovalent impurity, and the degree

of association p is the ratio of the concentration of complex to the total impurity concentration. By applying the chain rule Equation (2. 1) can be rewritten in the form:

$$J = -D_s[\partial(pc)/\partial c]\partial(Nc)/\partial x \tag{2.2}$$

From Equation (2. 2) we see that the impurity diffusion coefficient, which is dependent on the impurity concentration, is

$$D(c) = D_s \partial(pc)/\partial c \tag{2.3}$$

When all impurities are associated with vacancies, that is when $p = 1$, $D(c)$ becomes independent of c, approaching the saturation diffusion coefficient D_s.

In the case of the simultaneous diffusion of Ca^{2+} and Sr^{2+} ions in the NaCl type lattice, the equilibria between the associated complexes and unassociated point defects are expressed as

$$Ca^{+} + V_c^{-} \rightleftharpoons CaV_c \tag{2.4}$$

$$Sr^{+} + V_c^{-} \rightleftharpoons SrV_c \tag{2.5}$$

where V_c^{-} is the cation vacancy, and it is common to both association reactions. The charges on the defects are assigned relative to the crystal lattice. The impurity and vacancy are regarded as associated only when they are on nearest neighbor cation sites. The

association reactions (2.4) and (2.5) may then be described by the mass action equations

$$\chi_{CaV_c}/[\chi_c(c_{Ca}-\chi_{CaV_v})] = 12\exp(-\Delta G_{Ca}/kT) = K_{Ca}(T) \qquad (2.6)$$

$$\chi_{SrV_c}/[\chi_c(c_{Sr}-\chi_{SrV_c})] = 12\exp(-\Delta G_{Sr}/kT) = K_{Sr}(T) \qquad (2.7)$$

where χ_i is the concentration of the defect i in terms of mole fraction, and c_{Ca} and c_{Sr} are the analytical concentration of calcium ion and of strontium ion, respectively. The number 12 appears because of the number of equivalent orientations of a complex in the NaCl type lattice and it is the configurational entropy term. The ΔG's are the Gibbs free energies of association of the complexes in the standard state, defined as the work gained in bringing a vacancy from a distant position to a particular nearest neighbor position of an impurity ion at constant temperature and pressure. Here the standard state is defined as one defect per cm^3. It should be emphasized that the ΔG's do not include the configurational entropy. $K_{Ca}(T)$ and $K_{Sr}(T)$ are the mass action constants and k is the Boltzmann constant.

In a pure alkali halide crystal the concentration of vacancies is governed by the Schottky product

$$\chi_c\chi_a = B\exp(-h_s/kT) = K_s(T) \qquad (2.8)$$

where B is the entropy and h_s is the enthalpy of formation for a Schottky defect, and χ_a is the concentration of anion vacancies in mole fraction. The charge neutrality condition for the system requires the following defect balance

$$\chi_c = c_{C_a} - \chi_{CaV_c} + c_{Sr} - \chi_{SrV_c} + \chi_a \tag{2.9}$$

We now define the degrees of association p_{Ca} and p_{Sr} of the complexes of Ca^{2+} and Sr^{2+} as follows:

$$p_{Ca} = \chi_{CaV_c}/c_{Ca} \tag{2.10}$$

$$p_{Sr} = \chi_{SrV_c}/c_{Sr} \tag{2.11}$$

Then Equations (2.6), (2.7) and (2.9) may be expressed for the cation vacancy χ_c as follows:

$$\chi_c = p_{Ca}/K_{Ca}(1-p_{Ca}) \tag{2.12}$$

$$\chi_c = p_{Sr}/K_{Sr}(p-p_{Sr}) \tag{2.13}$$

$$\chi_c = (1-p_{Ca})c_{Ca} + (1-p_{Sr})c_{Sr} + \chi_a \tag{2.14}$$

Equations (2.12), (2.13) and (2.14) together with (2.8) can be combined to form a set that describes the effect of one cationic impurity on the association of the other and vice versa. In obtaining the p_{Ca}

and p_{Sr} the following successive approximations method developed by Krause (Thesis) was used:

$$[z] = (1-p_{Ca})c_{Ca} + (1-p_{Sr})c_{Sr} \tag{2.15}$$

$$\chi_a = -[z]/2 + ([z]^2+K_s)^{1/2}/2 \tag{2.16}$$

$$p_{Ca} = K_{Ca}([z]+\chi_a)/1 + K_{Ca}([z]+\chi_a) \tag{2.17}$$

$$p_{Sr} = K_{Sr}([z]+\chi_a)/1 + K_{Sr}([z]+\chi_a) \tag{2.18}$$

Remembering the diffusing species are the complexes, not isolated divalent cation impurities, then the coupled differential equations of Fick's second law which describe the diffusion of the two complexes in one dimension are expressed by

$$\partial(p_{Ca}c_{Ca})/\partial t = \partial[D_s(Ca)\partial(p_{Ca}c_{Ca})/\partial x]\partial x \tag{2.19}$$

and

$$\partial(p_{Sr}c_{Sr})/\partial t = \partial[D_s(Sr)\partial(p_{Sr}c_{Sr})/\partial x]\partial x \tag{2.20}$$

where $(p_{Ca}c_{Ca})$ and $(p_{Sr}c_{Sr})$ are the concentrations of the Ca^{2+} and Sr^{2+} complexes, respectively, and the D_s's are the saturation diffusion coefficients, which are constant.

The differential equations (2.19) and (2.20) were solved numerically by the Schmidt (1924) method of finite differences. These two equations must be solved simultaneously because they are mutually

related through the degrees of association p_{Ca} (2.17) and p_{Sr} (2.18). The Schmidt method of finite differences was fully discussed by Krause (Thesis). Thus, only the final forms of the solution to the differential equations (2.19) and (2.20) are given here. They are expressed by

$$(c_{Ca})'_m = (c_{Ca})_m + D_s(Ca)\ \delta t/(\delta x)^2[p_{Ca}(c_{Ca})_{m+1} - 2p_{Ca}(c_{Ca})_m + p_{Ca}(c_{Ca})_{m-1}] \tag{2.21}$$

for the calcium ion, where δx and δt are the equal space interval and time interval, and $(c_{Ca})_{m-1}$, $(c_{Ca})_m$ and $(c_{Ca})_{m+1}$ are the concentrations at the points $(m-1)\delta x$, $m\delta x$ and $(m+1)\delta x$ respectively at time $t = n\delta t$, and $(c_{Ca})'_m$ is the concentration at the point $x = m\delta x$ at time $t = (n+1)\delta t$, and

$$(c_{Sr})'_m = (c_{Sr})_m + D_s(Sr)\ \delta t/(\delta x)^2[p_{Sr}(c_{Sr})_{m+1} - 2p_{Sr}(c_{Sr})_m + p_{Sr}(c_{Sr})_{m-1}] \tag{2.22}$$

for the strontium ion. Similar definitions as those of Ca are also given to Sr.

Here second and higher order terms have been neglected. When identical time interval δt and space interval δx are used in Equations (2.21) and (2.22) the diffusion profiles generated are the simultaneous solutions to Equations (2.19) and (2.20). It has been

shown that the Schmidt method is a satisfactory approximation and accurate enough for many practical problems (Crank, 1970, p. 189). The validity of neglecting higher order terms in the calculation of the simultaneous diffusion experiments was checked by Krause (Thesis), and it was shown to be accurate to the fourth significant figure when one generated profile was compared with another which had been generated by using smaller intervals of time and space. The diffusion profile generated by equations such as (2.21) and (2.22) behaves normal as long as the value $D_s \delta t/(\delta x)^2$ is chosen to be one-half or less (Dusinberre, 1961).

The initial and boundary conditions of the differential equations (2.19) and (2.20) are different for the diffusion from a vapor source and from a deposited surface source.

In the vapor source diffusion the boundary conditions are given by

$$c = c_1 \quad \text{for} \quad t > 0 \quad \text{at} \quad x = 0 \tag{2.23}$$

$$\partial c/\partial x = 0 \quad \text{at} \quad x = \infty \quad \text{and} \quad t = t_t \tag{2.24}$$

and the initial condition by

$$c = c_1 \text{ for } x < 0, \quad c = 0 \text{ for } x > 0 \text{ at } t = 0 \tag{2.25}$$

where t_t is the total time of the diffusion anneal, and c_1 is a constant concentration. Note the concentration of the diffusant at the

surface is constant throughout the vapor source diffusion. On the other hand, in the surface deposit experiment the concentration of the diffusant at the surface decreases with time, and the boundary conditions are represented by

$$c \neq c_1 \quad \text{for} \quad t > 0 \quad \text{at} \quad x = 0 \tag{2.26}$$

$$\partial c/\partial x = 0 \quad \text{at} \quad x = \infty \quad \text{and} \quad t = t_t \tag{2.27}$$

and the initial condition by

$$c = c_1 \quad \text{for} \quad x < 0, \quad c = 0 \quad \text{for} \quad x > 0 \quad \text{at} \quad t = 0 \tag{2.28}$$

As far as the diffusion coefficient D_s is constant the Schmidt method of finite differences can be used for experiments with two different sets of boundary conditions, because the concentration at the point x at time $t + \delta t$ with small time interval δt is calculated from the concentrations at the neighboring points $x \pm \delta x$ at time t, and it is controlled by the second terms in Equations (2.21) and (2.22), that is the terms following $D_s \, \delta t/(\delta x)^2$. The final diffusion profile at $t = t_t$ (total diffusion time) is generated in an accumulative manner at each point along the distance.

At each experimental temperature the values of K_{Ca} and K_{Sr} were calculated for initial trial values of $\Delta G(Ca)$ and $\Delta G(Sr)$ from Equations (2.6) and (2.7). The Schottky product K_s for the same temperature was computed from Equation (2.8) using

$B = 2.080 \times 10^3$ and $h_s = 2.49$ eV in KCl from Fuller's et al. (1968) results, and $B = 1.719 \times 10^4$ and $h_s = 2.48$ eV in NaCl from Allnatt's et al. (1971) results. Then the degrees of association p_{Ca} and p_{Sr} were calculated from Equations (2.15), (2.16), (2.17) and (2.18) by successive approximation. The p's were accepted when two successive values agreed in their sixth decimal place. The experimental data points of the concentration versus distance curve were extrapolated to the zero distance to obtain the surface concentrations $(c_{Ca})_{x=0}$ and $(c_{Sr})_{x=0}$. Using the p_{Ca}, p_{Sr}, $(c_{Ca})_{x=0}$, $(c_{Sr})_{x=0}$, together with trial values of $D_s(Ca)$ and $D_s(S_r)$, Equations (2.21) and (2.22) were computed to generate the calcium and strontium diffusion profiles. The initial trial values of $\Delta G(Ca)$, $\Delta G(Sr)$, $D_s(Ca)$ and $D_s(Sr)$ were chosen by an "educated guess" on basis of earlier completed experiments and varied automatically by a computer program until the generated profiles satisfactorily fitted the experimental profiles. The variations of the four parameters were done by a non-linear regression method developed by Rosenbrock (1960). The fitting was made by minimizing the sum of the squares of the differences between the experimental and computed values, that is minimizing a function $f(x) = \Sigma(x_{expt.} - x_{calc.})^2$. A rather critical question of whether the "best values" of four parameters actually correspond to a true minimum in the sum of the squares of the deviations, and not just another minimum, could be asked.

Hence the "best values" were calculated using starting values of $-\Delta G$ and D_s both greater and less than the expected "best values." The calculated "best values" of $-\Delta G$ and D_s agreed in their fourth decimal place. All the computations were done with a Control Data Computer Model 3300 at Oregon State University Computer Center. The block diagram of the computer program is shown in Figure 2. 1.

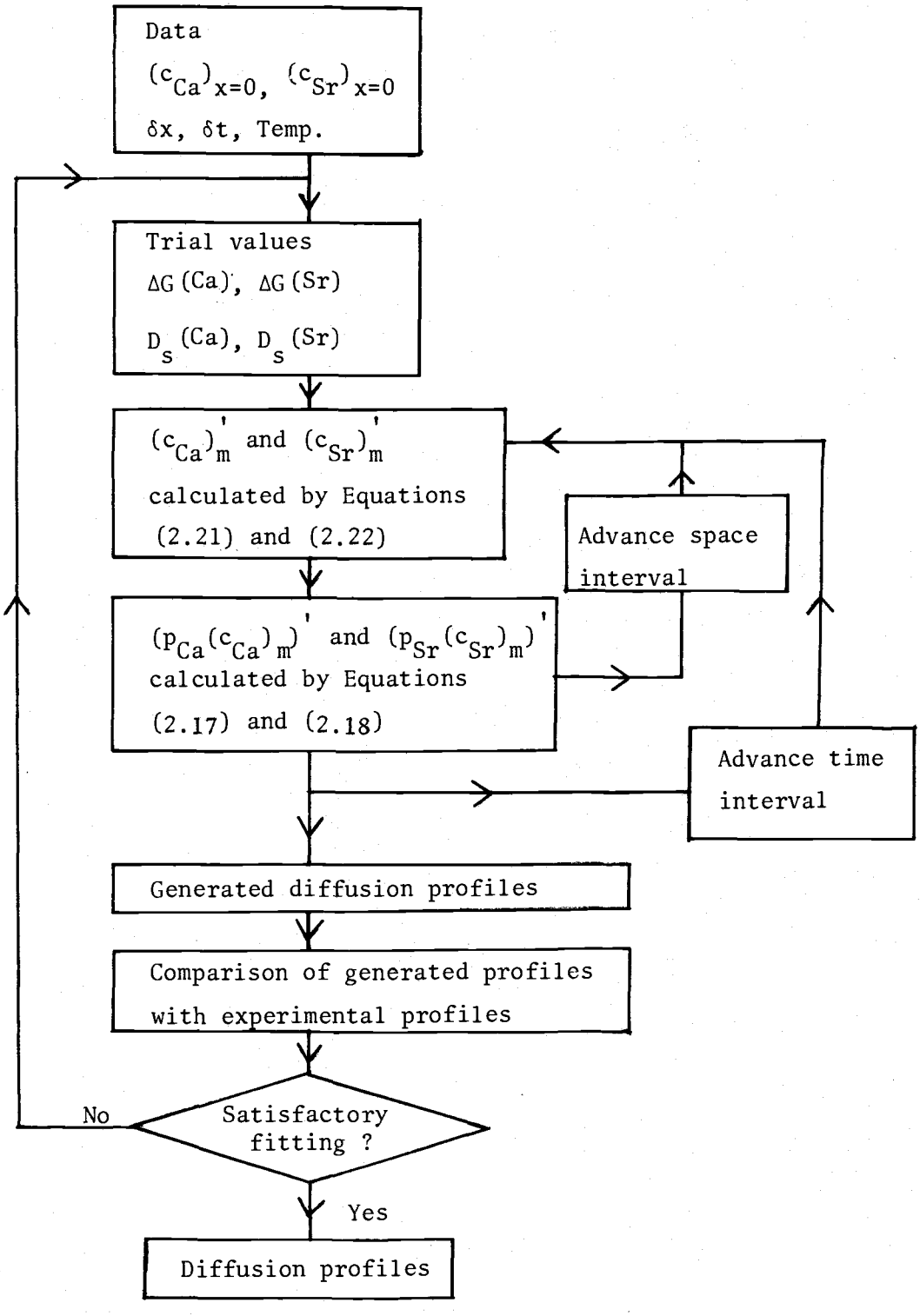

Figure 2.1. Block diagram of the computer program used to generate diffusion profiles.

III. EXPERIMENTAL

The simultaneous diffusion of Ca^{2+} and Sr^{2+} ions into crystals of KCl and NaCl was carried out using radioactive ^{45}Ca and ^{85}Sr as tracers to follow the penetration of the Ca and Sr into the crystal. Because the vapor pressures of $CaCl_2$ and $SrCl_2$ are not high at the temperatures of the cooler diffusion anneals, two types of diffusion experiments were necessary. At lower temperatures the Ca and Sr were allowed to diffuse from a thin surface layer of $CaCl_2$ and $SrCl_2$, while at the higher temperatures the Ca and Sr diffused into the crystal from $CaCl_2$ and $SrCl_2$ vapor. Surface layer sources were used in diffusion anneals that were made at temperatures below the lowest melting binary eutectic of the system being studied. These eutectics are: KCl - $SrCl_2$ at 580°C (Vortisch, 1914), KCl - $CaCl_2$ at 597°C (Lantsberry and Page, 1920), NaCl - $SrCl_2$ at 570°C (Vortisch, 1914), NaCl - $CaCl_2$ at 500°C (Menge, 1911). Unfortunately the phase equilibria of these ternary systems have not been reported, but the $CaCl_2$ - $SrCl_2$ system has the eutectic at 646°C (Sandonnini, 1914).

The pure KCl and NaCl single crystals used in these experiments were grown from the reagent grade salts which had been purified by the ion-exchange method (Fredericks et al., 1966). The KCl single crystals were grown under one-third atmosphere of HCl by the

Kyropoulos method. Single crystals of NaCl were grown under one-sixth atmosphere of HCl in a quartz growth tube by the Stockbarger-Bridgman method. Since the NaCl single crystals were slightly strained, they were annealed at 700°C for ten hours and cooled at 1/3°C per minute in at atmosphere of Cl_2 (1/3 atm.).

Results of analysis of crystals grown from the ion-exchange purified salt are shown in Table 3.1. The OH^- content was measured spectrophotometrically using the OH^- absorption band at 204 nm in KCl and at 185 nm in NaCl (Gie and Klein, 1963).

The radioisotopes were obtained from the New England Nuclear Corporation and also from the ICN in the form of $^{45}Ca(t_{1/2} = 165d)$ and $^{85}Sr(t_{1/2} = 64d)$ hydrochloric acid solutions. A 99+ % radiometric purity was given for both isotopes. The specific activities of 15.5 mCi/mg Ca and 3.88 mCi/mg Sr were given by the former supplier, and those of 20.1 mCi/mg Ca and 15.2 mCi/mg Sr by the latter.

The ^{45}Ca decays to the stable isotope ^{45}Sc by beta emission and ^{85}Sr decays to the stable isotope ^{85}Rb by electron capture (Table of Isotopes by Lederer et al.). The scandium exists in the form of a trivalent Sc^{3+} ion in the substitutionally incorporated lattice site, and the rubidium as a monovalent Rb^+ ion. Substitutional trivalent ions such as Sc^{3+} must introduce two cation vacancies to maintain the charge neutrality of the crystal; but the substitutional monovalent Rb^+ does not perturb the vacancy concentration very much, because Rb^+

Table 3.1. Analysis of ion-exchange purified KCl and NaCl single crystals. Taken from data by Krause and Fredericks (1973).

Impurity Ion	KCl	NaCl	Methods[a]
Ag^+	<0.001[b]	<0.01[b]	3
K^+	NA[c]	<1[b]	1
Na^+	3 ± 1	NA	1
Rb^+	8.740	0.012	1
Tl^+	<0.001[b]	<0.01[b]	3
Br^-	3.5 ± 0.5	0.95	1
BO_2^-	<0.01[b]	NA	3
I^-	<0.4[b]	NA	3
OH^-	<0.001[b]	0.23	3
Co^{2+}	0.00001	0.00005	1
Fe^{2+}	0.010 ± .002	0.127	1
Mg^{2+}	<0.5[b]	NA	2
Mn^{2+}	<0.004[b]	<0.003[b]	1
Pb^{2+}	<0.004[b]	<0.01[b]	3
Zn^{2+}	0.0001	0.0003	1
Ca^{2+}	<1.0[b]	NA	2

All values reported in ppm.

[a] 1. Neutron activation analysis. 2. Atomic absorption spectroscopy. 3. Optical absorption spectroscopy.

[b] Set by detection limit of analytical procedure.

[c] Not analyzed.

ions simply substitute either K^+ ions or Na^+ ions in the host crystals. An effort was made to obtain freshly prepared isotopes to minimize the decay products present. However it was still necessary to purify the commercial isotopes to remove any residual impurities left from their production and any decay products formed. This was done using a HNO_3 elution from ion-exchange columns. A similar method has been given by Rane and Bhatki (1966). Here Bio-Rad Laboratories Ag-50W-X8 (200-400 mesh) cation exchange resins packed in disposable polypropylene columns were used. The dimensions of the column are 0.7 cm I.D. and 4 cm in height. The volume of the resin bed was about 3 ml. The ^{45}Ca hydrochloric acid stock solution (20 ml) was evaporated to dryness in a beaker and a few drops of 2.1 moles per liter nitric acid were added to it. The solution containing most of the activity was transferred to a resin column which had been previously equilibrated with 10 ml of the same acid that was used to dissolve the tracers. The adsorbed activities were then eluted with 2.1 M nitric acid at a flow rate of 0.4 ml/min. The activity of the effluent was continuously monitored by a Baird Atomic Model 420 G.M. Surveymeter. The initial effluent was passed to carry away monovalent ions. Then when activity appeared in the effluent it was collected in a beaker until most of the ^{45}Ca activity had been eluted from the resin, leaving ^{45}Sc adsorbed in the column. This nitric acid solution containing pure ^{45}Ca was evaporated to dryness; then conc.

HCl was added to convert the nitric acid form of the ^{45}Ca to the hydrochloric acid one. This evaporation and conversion step was repeated once again, and the hydrochloric acid solution was taken to dryness. Finally the dried substances were dissolved in 3 N HCl. The solution containing only ^{45}Ca as a tracer was used in the diffusion experiments. A similar procedure was carried out to separate ^{85}Rb from ^{85}Sr.

As mentioned previously, the diffusion of Ca^{2+} and Sr^{2+} ions in both KCl and NaCl was carried out in two ways. The surface layer diffusion was made at temperatures below the eutectic points, that is, 580° C in KCl system and 500° C in NaCl system. Above these temperatures vapor phase diffusion must be used to keep the boundary conditions constant by avoiding the formation of a very thin region of eutectic composition in the surface layer rather than the sharp boundary required. When surface source experiments were performed below eutectics the first section removed contained anomalously high tracer concentration, but this did not persist into the crystal as is typical of eutectic melting (Keneshea and Fredericks, 1963).

The surface layer method was carried out as follows. A mixture of carrier and tracer solutions was evaporated to dryness. This was dissolved in five to six small (about 0.1 ml) portions of a solution of 95 percent ethyl alcohol saturated with KCl or NaCl. These

tracer solutions were deposited on the crystal and evaporated to dryness under a heat lamp. The ratios of tracer to carrier were 0.100 mCi/mg for the $CaCl_2$ and 0.079 mCi/mg for the $SrCl_2$. A crystal prepared in this way and an uncoated crystal were put together in such a manner that a layer of diffusants were sandwiched between two crystals. These crystals were placed on a quartz pedestal in a quartz diffusion ampoule with a second quartz pedestal placed on top as a weight and sealed under one-third atmosphere of Cl_2. A diagram of the arrangement is shown in Figure (3.1A). The diffusion ampoule was then put in the preheated diffusion furnace.

In the vapor phase diffusion experiments $^{45}CaCl_2$ and $^{85}SrCl_2$ aliquots, together with carrier $CaCl_2$ and $SrCl_2$ solutions, were evaporated to dryness in the bottom of the quartz diffusion ampoule by passing nitrogen over the surface of the hydrochloric solution while heating the solution at 70°C. The ratios of tracer to carrier were 0.398 mCi/mg for the $CaCl_2$ and 0.127 mCi/mg for the $SrCl_2$. A quartz pedestal was placed in the ampoule and the alkali halide crystal (an approximate size of 1 cm x 1.5 cm x 0.5 cm) balanced on the pedestal. The tube was treated with HCl gas several times, then sealed under one-third atmosphere of Cl_2. A diagram of the arrangement is shown in Figure (3.1B). Next the ampoule was placed in the preheated diffusion furnace, while the bottom part of it was cooled for the first 30 minutes with a water cooling coil (Krause and

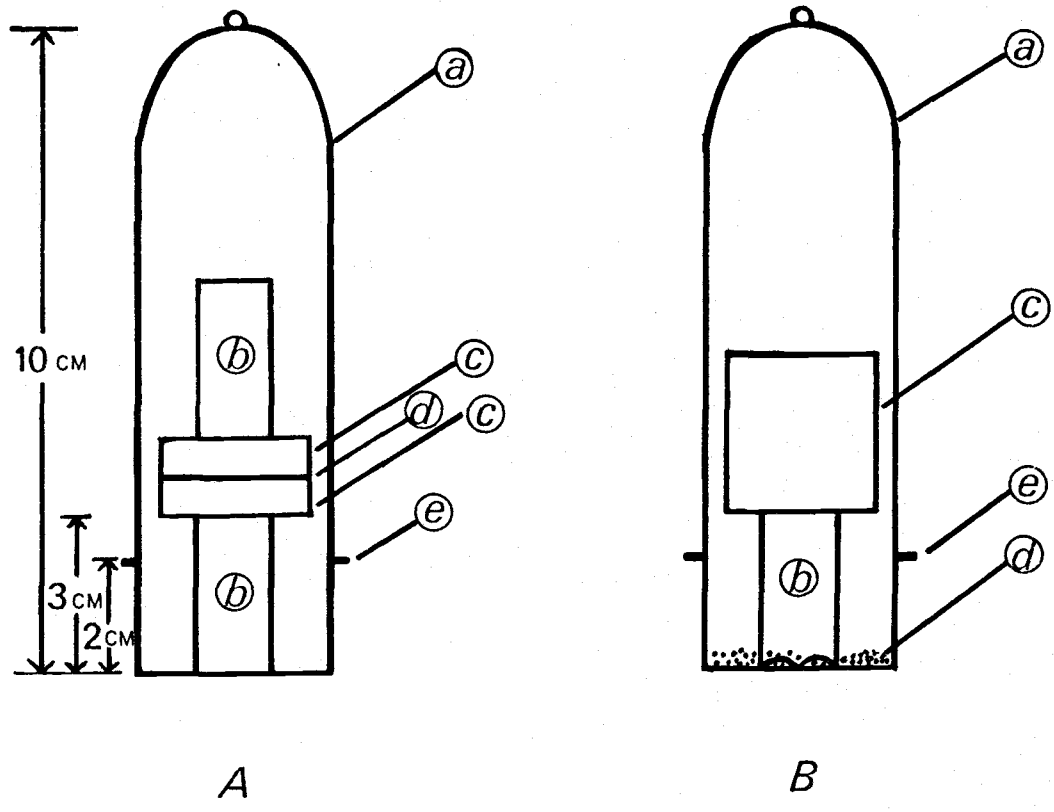

Figure 3.1. A. Diffusion ampoule used in surface layer diffusion.
B. Diffusion ampoule used in vapor phase diffusion.
a. Quartz tube. b. Quartz pedestal. c. Crystal.
d. Diffusants. e. Positioning projections.

Fredericks, 1971). In the vapor phase diffusion experiments the amount of the diffusants was large enough to insure that the $CaCl_2$ and $SrCl_2$ vapor was always in equilibrium with solid $CaCl_2$ and $SrCl_2$ during the diffusion. Thus the amount of $CaCl_2$ and $SrCl_2$ in the vapor remained constant throughout the experiment.

The furnaces (Marshall Testing Furnaces) used for the diffusion anneals had been previously adjusted to provide the uniform temperature region required and were electronically controlled by a Model 407 Wheelco temperature controller. Temperatures of the samples were measured with Pt-Pt 13% Rh thermocouples. Temperature variations were within ±1° C. A diagram of diffusion anneal apparatus, which is taken from the thesis of J. L. Krause (1970), is shown in Figure 3.2.

In all experiments after the diffusion anneals were completed the ampoules were removed from the furnace and dropped into ice water, then put in liquid nitrogen in order to quench the diffusion process as efficiently as possible. When cool the crystals were taken out of the ampoules. The vapor source diffusion samples were divided in half by cleaving the crystal parallel to the large faces. In this way two samples were obtained from each diffusion run. Two millimeter sections were cleaved from the four thin sides of the crystal. Thus a one directional diffusion sample was obtained. The final crystal dimensions were measured with micrometer calipers to obtain the cross sectional area.

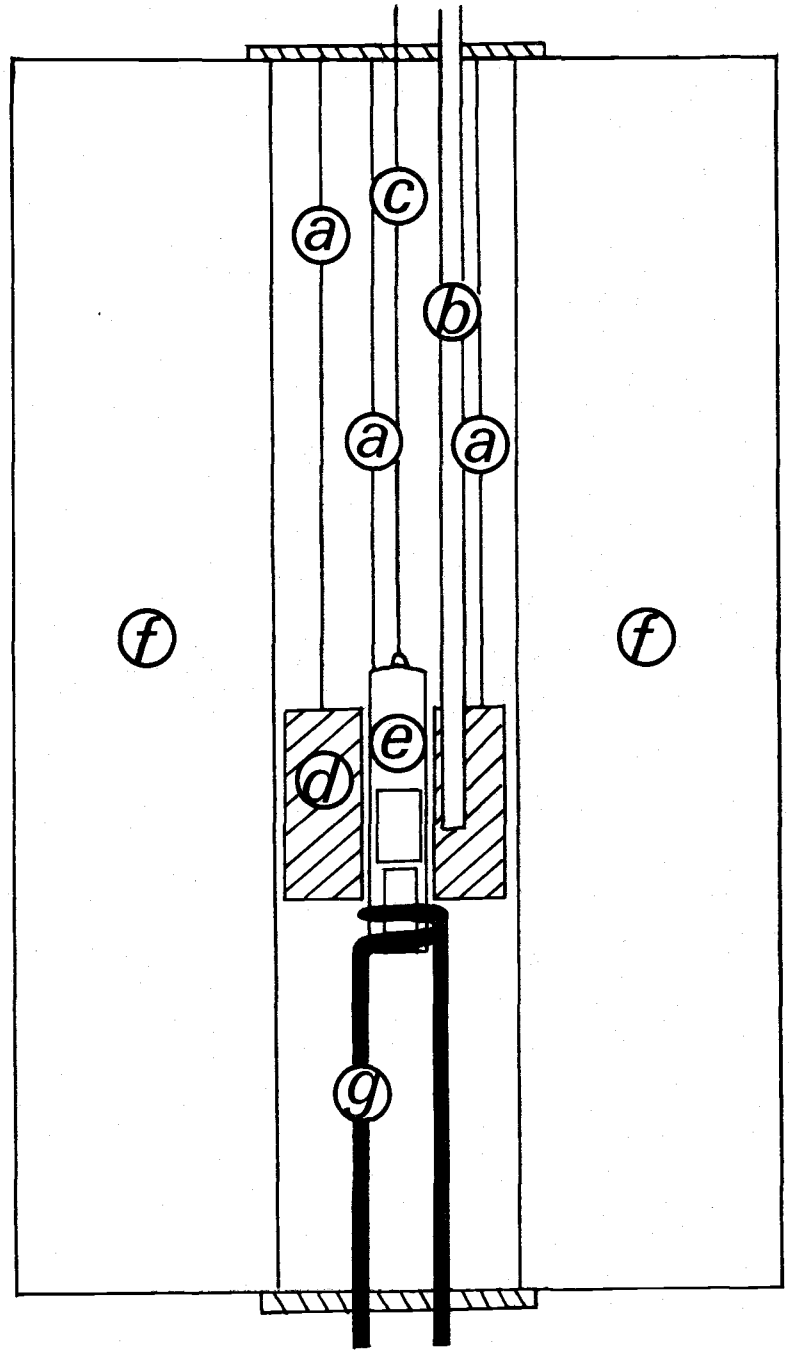

Figure 3.2. Diffusion anneal apparatus. a. Support wire for carbon block. b. Thermocouple. c. Support wire for ampoule. d. Carbon block. e. Ampoule. f. Furnace. g. Cooling coil.

The crystal was mounted in an American Optical Company Model 860 Microtome and slices were cut parallel to the surface through which diffusion took place. The surface of the crystal was aligned parallel to the plane of the knife edge by placing a small lamp behind the crystal and knife edge, and observing with a binocular microscope the shape of the slit and uniformity of the interference pattern between the crystal face and the stationary knife edge. Sections were collected in preweighed 2 ml glass vials in the KCl diffusion experiments; but in the NaCl experiments they were collected in one-half dram plastic vials. The knife edge and the holder were cleaned between slices with Kimwipes wet with acetone and wiped dry to avoid cross-contamination. It was observed that a plastic vial needed less time to weigh than a glass one did. This is probably because a plastic vial adsorbs moisture much less strongly than a glass vial because of the nonpolar nature of the plastic surface. Thus it reaches equilibrium with the balance atmosphere more quickly than does the glass vial. The glass vials were cleaned with chromic acid and rinsed several times with deionized water. The plastic vials were cleaned with the labtone solution and rinsed with deionized water in an ultrasonic cleaner.

After collecting the sections the glass vials and samples were dried at 110°C for five hours and weighed on a Mettler Microbalance Model M5. The plastic vials with samples were dried at 80°C for seven hours. From the slice weight and area the slice thickness was

calculated using values of 1.987 gm/cm^3 for the density of KCl (Hutchison, 1944) and 2.165 gm/cm^3 for NaCl (Handbook of Chemistry and Physics, 53rd edition, CRC Press, 1972).

The ^{85}Sr decays to the stable isotope ^{85}Rb by electron capture with the emission of a gamma photon with an energy of 514 keV, and the ^{45}Ca decays to the stable isotope ^{45}Sc by emitting beta particles with the maximum energy of 252 keV. The gamma radiation of ^{85}Sr at the 514 keV photopeak was counted by placing the vials in a 3 in. x 3 in. NaI well-type scintillation detector with a multichannel analyzer. The 10 keV/channel window was used in the gamma radiation counting. Samples having activities well above the background were counted long enough to give a standard deviation no greater than 3%. Because of lower impurity concentrations, samples in the vapor source diffusion needed to be counted for much longer times than those in the surface layer diffusion. The beta energy of ^{45}Ca was counted with a Packard Co. Tri-Carb Liquid Scintillation Spectrometer Model 3375. The sample was dissolved in 1 ml deionized water and the vial was placed in a large beta counting glass vial, and then 20 ml New England Nuclear Aquasol as a scintillation liquid was added into it. The counting vial with the small vial, the sample and the fluor solution in it was shaken well to insure that the resulting solution was uniform. It was observed that the suspension solution was transparent. The blank for the background counting was prepared by dissolving 5 mg

of the host crystal with deionized water and adding the fluor solution. The standard solution was made in the same way except adding either 0.002 ml, 0.005 ml or 0.010 ml of $^{45}CaCl_2$ stock solution. In the liquid scintillation counting the quench corrections were made by the channels ratio method (Wang and Willis, 1965).

All the activities were corrected for the decay by using the half-life periods of 64 days for ^{85}Sr and 165 days for the ^{45}Ca. After all the corrections had been made, the mole fractions of each ion were calculated by the following equation

$$\text{Mole fraction}_M = (A_M MW_{solvent} C_c V_c V_{st.})/(MW_{solute} V_t A_{st.} w) \tag{3.1}$$

where A_M and $A_{st.}$ are the activities of the sample and the standard, $MW_{solvent}$ and MW_{solute} the molecular weights of the host crystal and the solute, C_c and V_c the concentration and volume of the carrier used in the experiment, $V_{st.}$ and V_t the volumes of the tracer solution used in making the standard and the tracer solution used as the diffusant, and w the weight of the sample.

IV. RESULTS

Simultaneous Diffusion of Ca^{2+} and Sr^{2+} in KCl

Figures 4.1 through 4.7 show the concentrations of calcium and strontium as a function of distance into a single crystal of potassium chloride for the temperature range from 451°C to 669°C. The concentrations are given in terms of mole fractions of calcium and strontium ions in KCl. The solid curves through the experimental data points are the calculated profiles by the Schmidt method with the parameters shown in the figures. The surface layer diffusion was performed at 451°C, 504°C and 558°C. The diffusions at 572°C, 595°C, 602°C and 669°C were done by the vapor phase diffusion. In calculating the Schottky product K_s for each annealing temperature in KCl, the values of B and h_s in Equation (2.8) were taken from the results of Fuller et al. (1968), and the K_s is expressed as

$$K_s = 2.080 \times 10^3 \exp(-2.49\ eV/kT) \qquad (4.1)$$

There have been reported other values of B and h_s by several workers. Those values together with calculated values of K_s at the lowest (451°C) and the highest (669°C) temperatures of this work are compared in Table 4.1. Note the differences in the values of K_s calculated do not affect the vacancy concentrations significantly, because the concentration of the cation vacancies are controlled

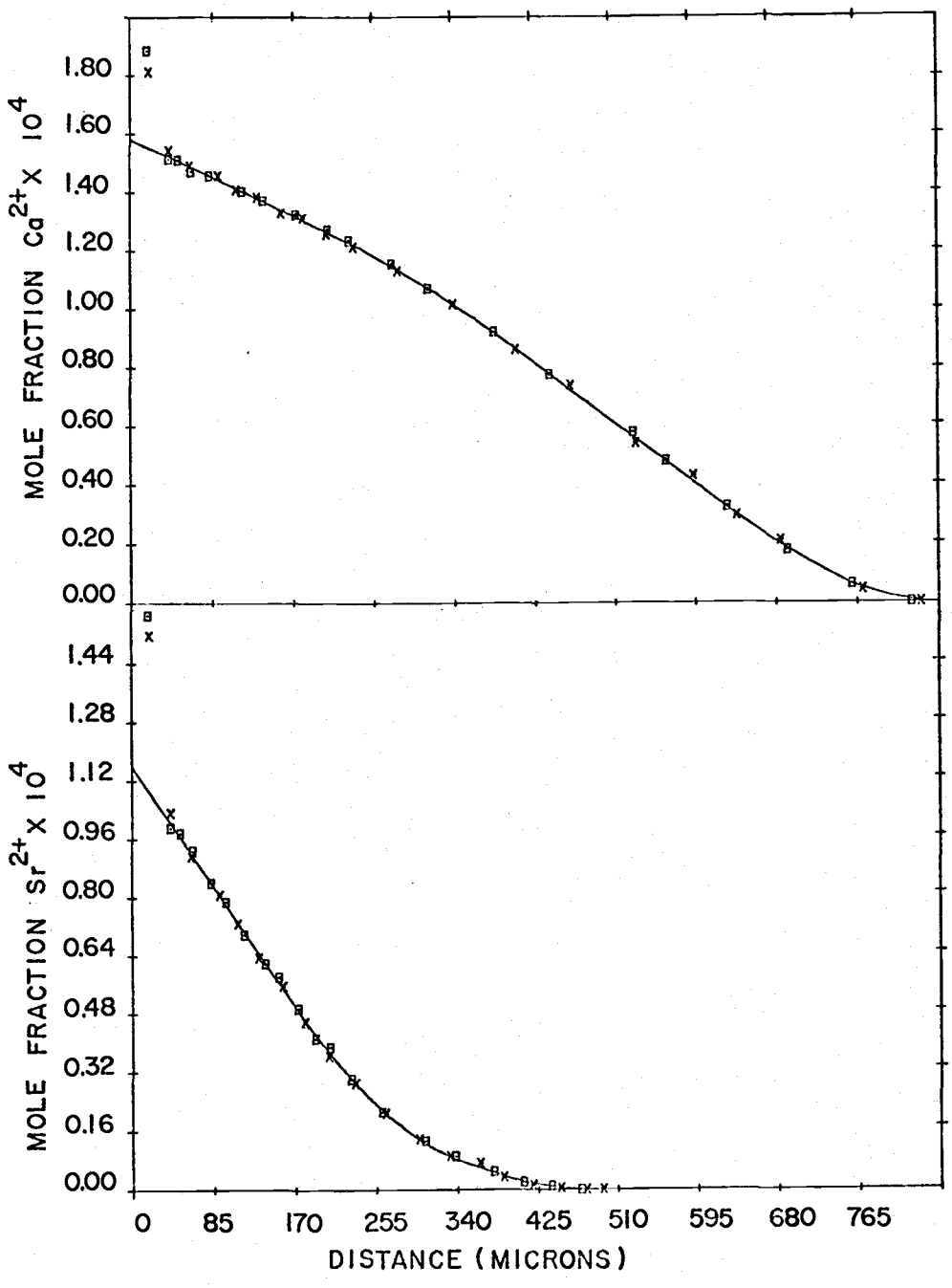

Figure 4.1. Penetration profiles of Ca^{2+} and Sr^{2+} in KCl at 451°C. Surface source. t_t=4.28760x10^{5}sec. X:Crystal A. □:Crystal B. +:Errors. Solid curves are profiles generated by Equations (2.21) and (2.22) using the following parameters.

$\Delta G(Ca)$ = -0.347 eV $D_s(Ca)$ = 7.51x10^{-9}cm^2/sec

$\Delta G(Sr)$ = -0.366 eV $D_s(Sr)$ = 1.05x10^{-9}cm^2/sec

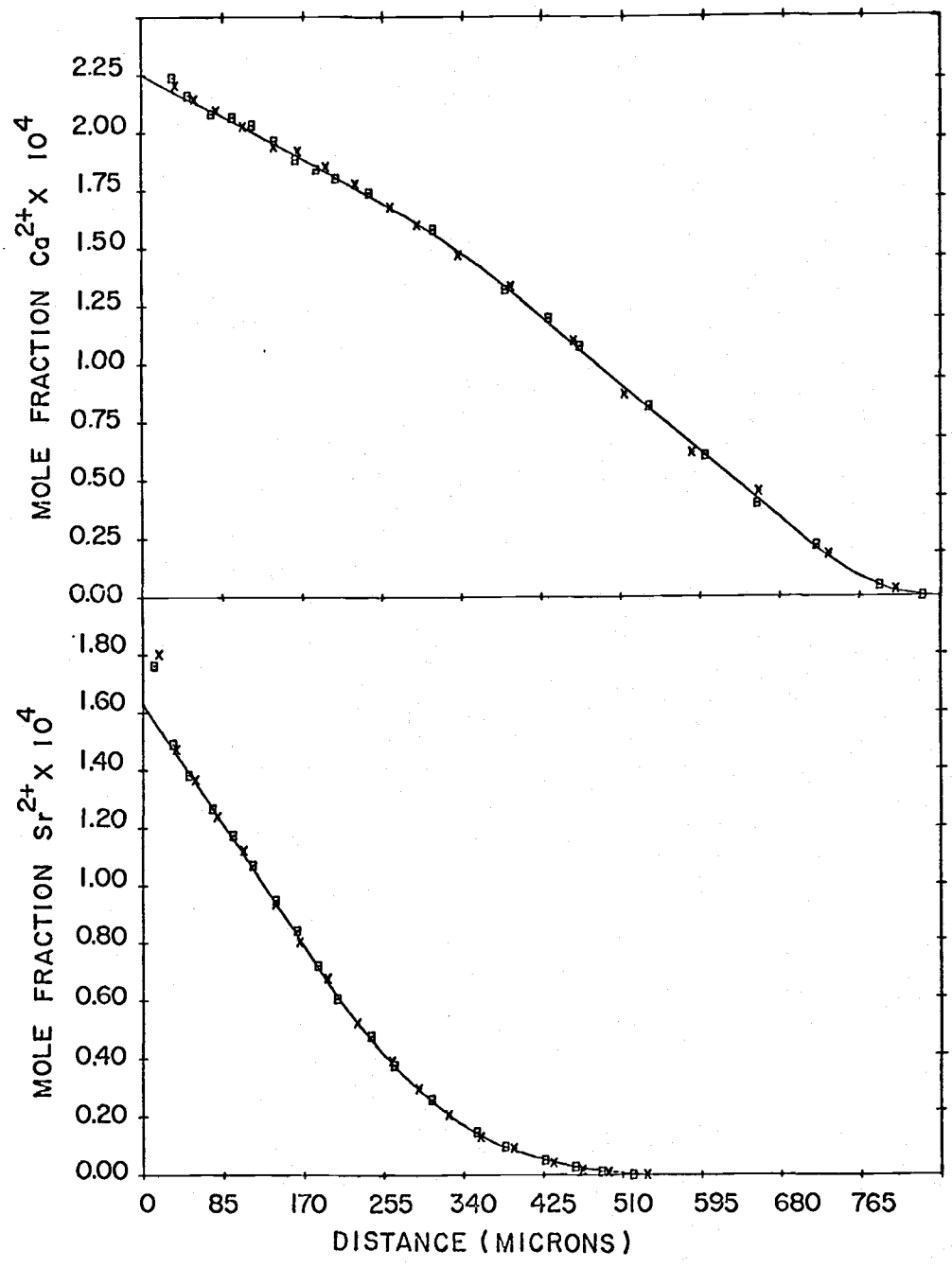

Figure 4.2. Penetration profiles of Ca^{2+} and Sr^{2+} in KCl at 504°C. Surface source. t_t=2.67000x10^{5}sec. X:Crystal A. □:Crystal B. +:Errors. Solid curves are profiles generated by Equations (2.21) and (2.22) using the following parameters.

$\Delta G(Ca)$ = -0.334 eV $D_s(Ca)$ = 1.39x10^{-8}cm^2/sec

$\Delta G(Sr)$ = -0.347 eV $D_s(Sr)$ = 2.45x10^{-9}cm^2/sec

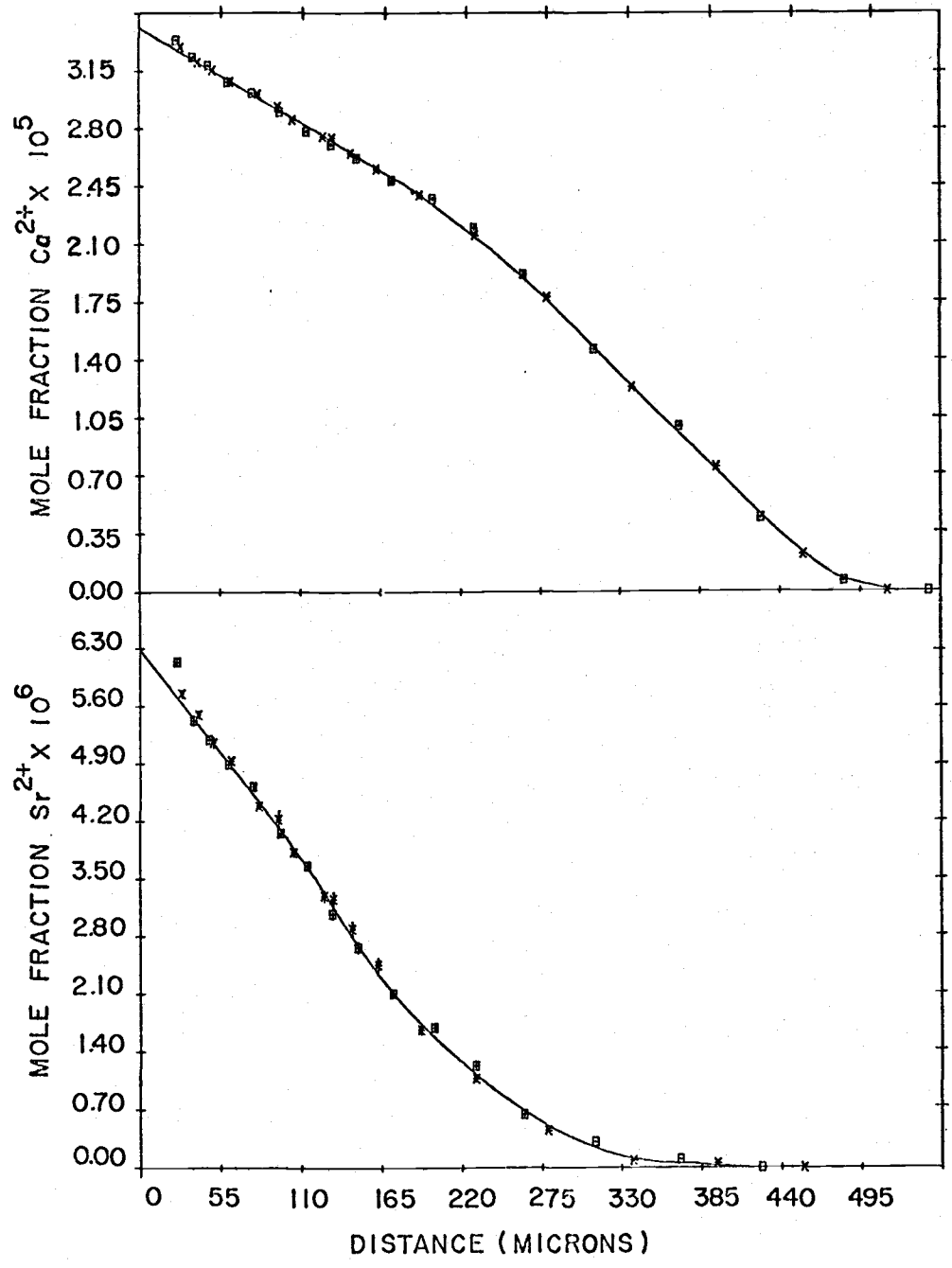

Figure 4.3. Penetration profiles of Ca^{2+} and Sr^{2+} in KCl at 558°C. Surface source. t_t=4.14300x10^5sec. X:Crystal A. □:Crystal B. ┼:Errors. Solid curves are profiles generated by Equations (2.21) and (2.22) using the following parameters.

$\Delta G(Ca)$ = -0.318 eV $D_s(Ca)$ = 2.73x10^{-8}cm^2/sec

$\Delta G(Sr)$ = -0.337 eV $D_s(Sr)$ = 6.44x10^{-9}cm^2/sec

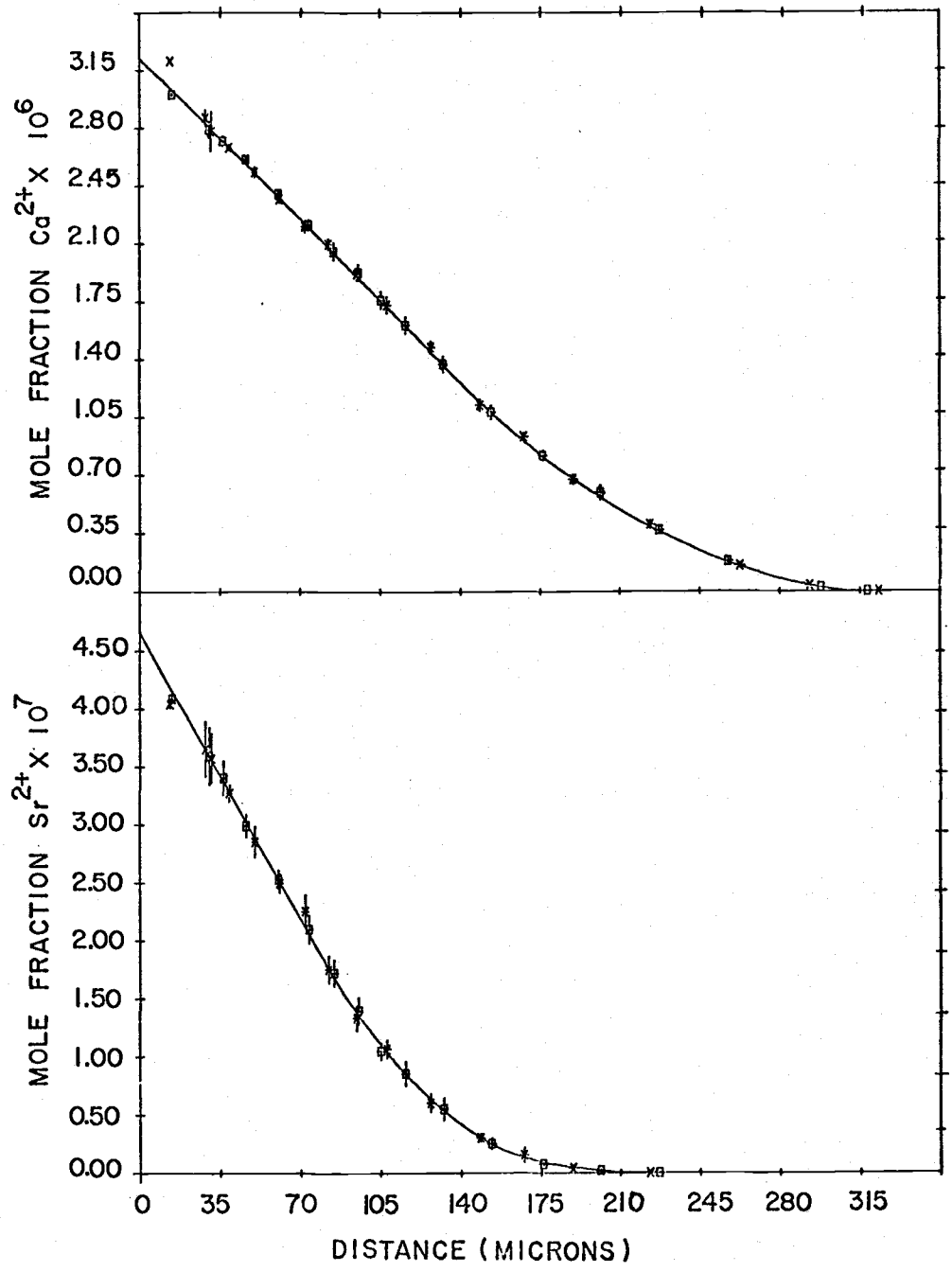

Figure 4.4. Penetration profiles of Ca^{2+} and Sr^{2+} in KCl at 572°C. Vapor source. t_t=6.31200x10^5sec. X:Crystal A. □:Crystal B. ┼:Errors. Solid curves are profiles generated by Equations (2.21) and (2.22) using the following parameters.

$\Delta G(Ca)$ = -0.315 eV $D_s(Ca)$ = 2.86x10^{-8} cm^2/sec

$\Delta G(Sr)$ = -0.329 eV $D_s(Sr)$ = 7.41x10^{-9} cm^2/sec

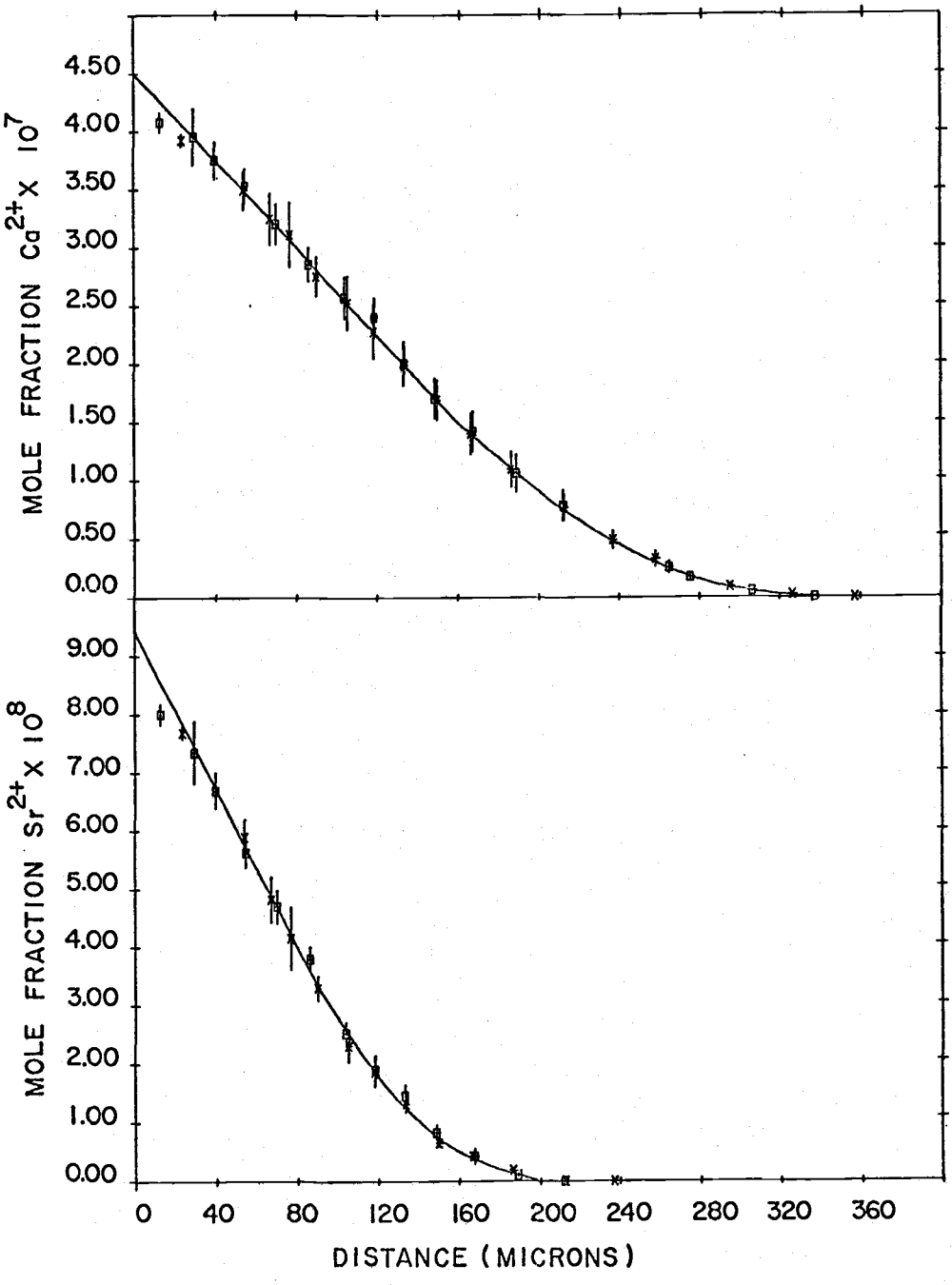

Figure 4.5. Penetration profiles of Ca^{2+} and Sr^{2+} in KCl at 595°C. Vapor source. t_t=8.59500x10^5sec. X:Crystal A. □:Crystal B. +:Errors. Solid curves are profiles generated by Equations (2.21) and (2.22) using the following parameters.

$\Delta G(Ca)$ = -0.312 eV $D_s(Ca)$ = 3.41x10^{-8}cm^2/sec

$\Delta G(Sr)$ = -0.323 eV $D_s(Sr)$ = 1.10x10^{-8}cm^2/sec

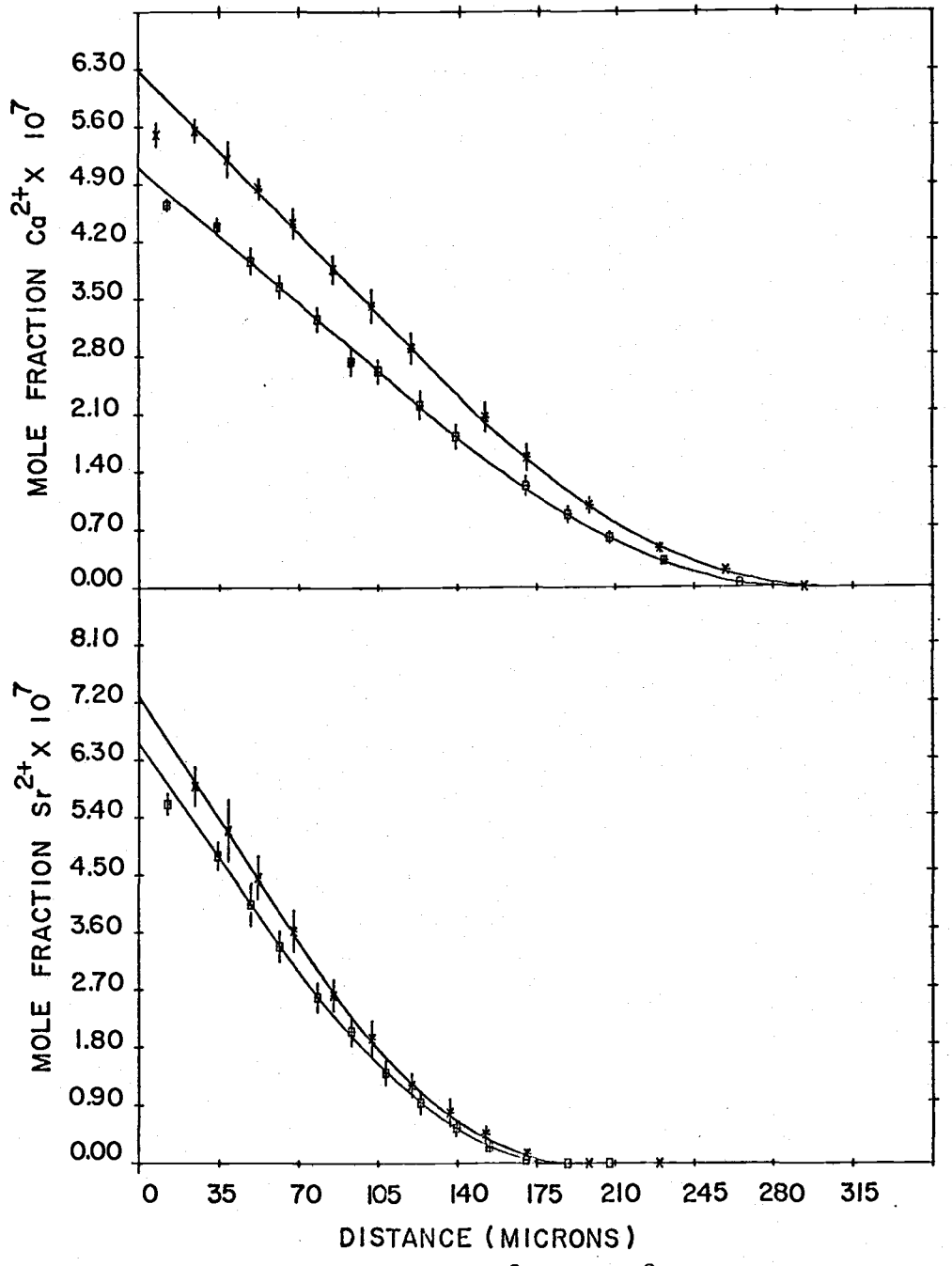

Figure 4.6. Penetration profiles of Ca^{2+} and Sr^{2+} in KCl at 602°C. Vapor source. t_t=5.52720x10^5sec. X:Crystal A. □:Crystal B. +:Errors. Solid curves are profiles generated by Equations (2.21) and (2.22) using the following parameters.

(A) $\Delta G(Ca)$ = -0.311 eV $D_s(Ca)$ = 3.92x10^{-8}cm^2/sec
$\Delta G(Sr)$ = -0.319 eV $D_s(Sr)$ = 1.23x10^{-8}cm^2/sec

(B) $\Delta G(Ca)$ = -0.311 eV $D_s(Ca)$ = 3.85x10^{-8}cm^2/sec
$\Delta G(Sr)$ = -0.319 eV $D_s(Sr)$ = 1.17x10^{-8}cm^2/sec

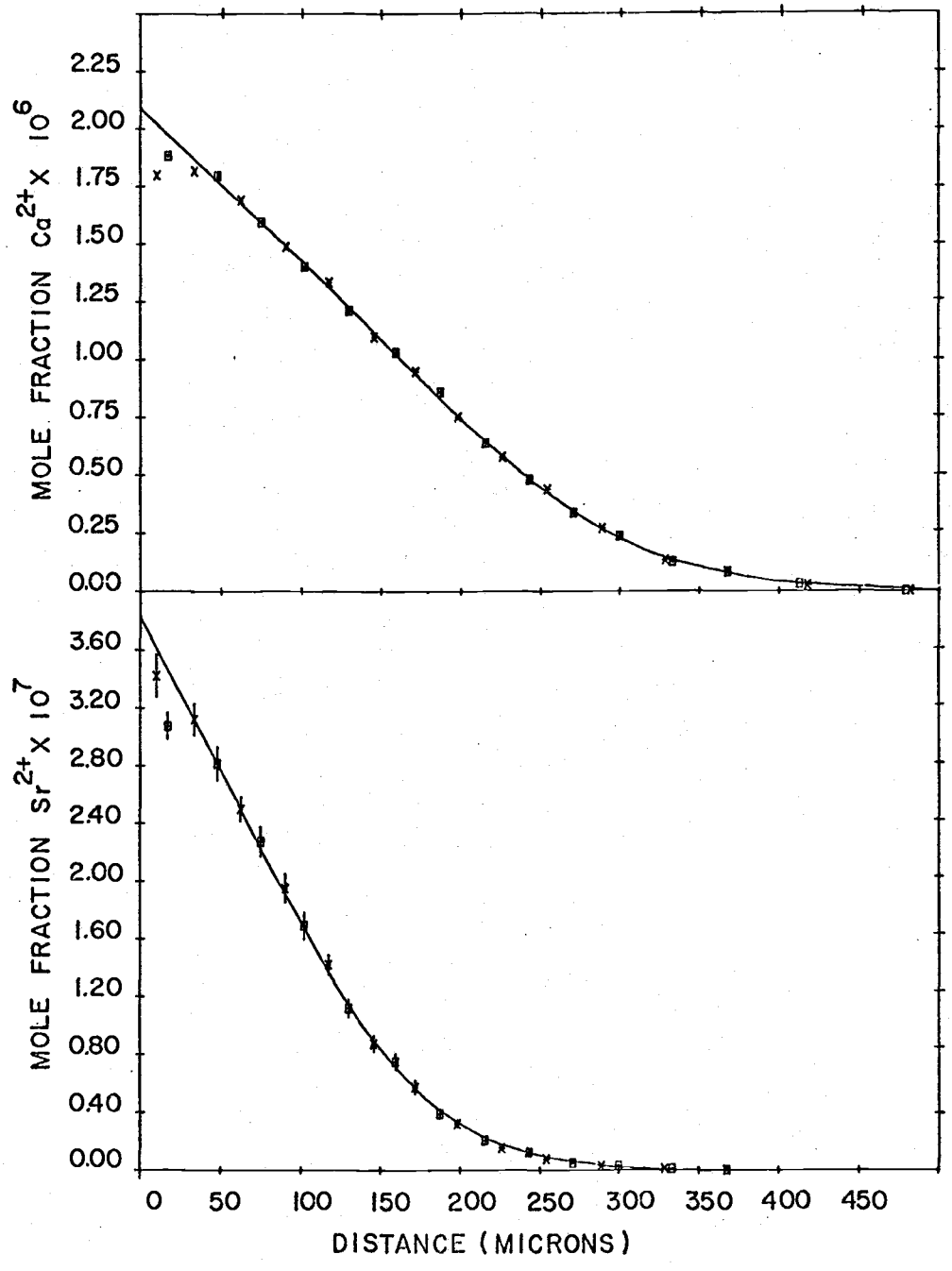

Figure 4.7. Penetration profiles of Ca^{2+} and Sr^{2+} in KCl at 669°C. Vapor source. t_t=5.05800x10^5sec. X:Crystal A. □:Crystal B. +:Errors. Solid curves are profiles generated by Equations (2.21) and (2.22) using the following parameters.

$\Delta G(Ca)$ = -0.299 eV $D_s(Ca)$ = 6.76x10^{-8}cm^2/sec

$\Delta G(Sr)$ = -0.303 eV $D_s(Sr)$ = 2.41x10^{-8}cm^2/sec

mainly by the divalent cation impurities introduced.

Table 4.1. Values of B, h_s and K_s at 451°C and 669°C in KCl.

B	h_s (eV)	K_s (451°C)	K_s (669°C)	Reference
2.080×10^{3}	2.49	9.65×10^{-15}	9.86×10^{-11}	Fuller et al. (1968)
5.404×10^{4}	2.64	2.26×10^{-14}	4.05×10^{-10}	M. Beniere et al. (1970)
1.490×10^{4}	2.59	1.39×10^{-14}	2.07×10^{-10}	Chandra and Rolfe (1970)
6.373×10^{1}	2.302	6.01×10^{-15}	3.07×10^{-11}	Jacobs and Pantelis (1971)

The limits of error in both mole fraction and distance are included in the diffusion profiles. Here the limit of error with "one percent confidence limits," which is defined such that an error is expected to lie outside the limits $(-\lambda, \lambda)$ only one percent of the time, was adopted (Shoemaker and Garland, 1967, p. 22). The limit of error λ may be compared with the standard deviation σ such that $\lambda = 2.5758\sigma$. The limit of error $\lambda(M)$ in the mole fraction M was determined by the equation of propagation of errors (Shoemaker and Garland, 1967, p. 34):

$$\lambda(M) = M[(\lambda(A_M)/AM)^2+(\lambda(MW_1)/MW_1)^2+(\lambda(C_c)/C_c)^2 + (\lambda(V_c)/V_c)^2+(\lambda(V_{st.})/V_{st.})^2+(\lambda(MW_2)/MW_2)^2 + (\lambda(V_t)/V_t)^2+(\lambda(A_{st.})/A_{st.})^2+(\lambda(w)/w)^2]^{1/2} \qquad (4.2)$$

where the λ's are the limits of error in measured quantities in the parentheses, whose meanings are defined in Equation (3.1). Note $MW_{solvent}$ and MW_{solute} are abbreviated by MW_1 and MW_2, respectively. The leading term in Equation (4.2), which contributes most to the uncertainty in the mole fraction, is the first term, $(\lambda(A_M)/A_M)^2$, namely the limit of error in the activity of the sample. This quantity $\lambda(A_M)$ was determined by the following equation (Wang and Willis, 1965, p. 189):

$$\lambda(A_M) = 2.5758\sigma(A_M) = 2.5758(r_g/t_g + r_b/t_b)^{1/2} \qquad (4.3)$$

where r_g is the gross sample count rate, t_g the time of gross sample counting, r_b the background count rate and t_b the time of background counting.

The limit of error in the distance was determined by the following equation

$$\lambda(r_n) = [(n-1)(\lambda_T)^2 + (\tfrac{1}{2}\lambda_T)^2]^{1/2}; \quad n = 1, 2, 3, \ldots \qquad (4.4)$$

where $\lambda(r_n)$ is the limit of error in the distance of nth slice, and λ_T the limit of error in the thickness of each slice.

The statistical error limits are generally larger in the vapor phase diffusions than the surface layer ones due to the lower activities of the samples. Note that the error limits in the calcium concentrations are smaller than those in the strontium. This is accounted for by

the high efficiency of the beta scintillation countings for the ^{45}Ca. Because of this advantage ^{45}Ca countings are much faster and more accurate from the statistical point of view.

Surface layer diffusions show rather peculiar penetration profiles, but the calculated profiles follow the experimental profiles very well. In the vapor phase diffusions, especially at higher temperatures (595°C, 602°C and 669°C), the first few slices show abnormally low concentrations near the surface. It is considered to be due to the desorption of the diffusing materials from the host crystal during the quenching process. A similar desorption problem was reported by Krause and Fredericks (1971) and shown to be a function of quenching time and to be due to desorption. However the experimental points deep in the crystal show normal behavior. Therefore the points deeper in the crystal were extrapolated to zero distance while the first few points were neglected when the surface anomaly occurred. There was one diffusion anneal, that is at 602°C, which showed the differing surface concentrations of the diffusants. In spite of the two differing penetration profiles from one diffusion anneal, the free energies of association $\Delta G(Ca)$ and $\Delta G(Sr)$ did not alter, but the diffusion coefficients $D_s(Ca)$ and $C_s(Sr)$ changed.

The plotting of the diffusion profiles including the experimental conditions and the values of ΔG and D_s were done by a Hewlett-Packard Model 9820A calculator with Model 9862A Calculator Plotter.

Table 4.2 summarizes the values of ΔG and D_s used to generate the diffusion profiles of Ca^{2+} and Sr^{2+} in KCl.

Figure 4.8 is an Arrhenius plot of D_s vs. $1/T$ ($^\circ K^{-1}$) for Ca^{2+} and Sr^{2+} in KCl. The straight lines through the experimental points were obtained by a least squares fit of the data. The values of D_s at various temperatures are given by

$$D_s = D_0 \exp(-U/kT) \tag{4.5}$$

where D_0 is a pre-exponential term, which is a temperature independent constant; U is the migration energy for the impurity-vacancy complex, or in other words, the activation energy required for a divalent cation and an associated vacancy to exchange places in the lattice. If $\log D_s$ is plotted against $1/T$, a value for U may be found from the slope of the straight line and D_0 from the intercept.

The saturation diffusion coefficients $D_s(Ca)$ and $D_s(Sr)$ are given by

$$D_s(Ca) = 9.93 \times 10^{-5} \exp(-0.592 \text{ eV}/kT) \text{ cm}^2/\text{sec} \tag{4.6}$$

for calcium and

$$D_s(Sr) = 1.20 \times 10^{-3} \exp(-0.871 \text{ eV}/kT) \text{ cm}^2/\text{sec} \tag{4.7}$$

for strontium.

Table 4.2. Values of ΔG and D_s used to generate diffusion of Ca^{2+} and Sr^{2+} in KCl.

T (°C)	ΔG(Ca) (eV)	ΔG(Sr) (eV)	D_s(Ca) (cm^2/sec)	D_s(Sr) (cm^2/sec)	Expt.[a]
451	-0.347	-0.366	7.51×10^{-9}	1.05×10^{-9}	S
504	-0.334	-0.347	1.39×10^{-8}	2.45×10^{-9}	S
558	-0.318	-0.337	2.73×10^{-8}	6.44×10^{-9}	S
572	-0.315	-0.329	2.86×10^{-8}	7.41×10^{-9}	V
595	-0.312	-0.323	3.41×10^{-8}	1.10×10^{-8}	V
602	-0.311	-0.319	3.92×10^{-8}	1.23×10^{-8}	V
602	-0.311	-0.319	3.85×10^{-8}	1.17×10^{-8}	V
669	-0.299	-0.303	6.76×10^{-8}	2.41×10^{-8}	V

[a] S is surface layer diffusion. V is vapor phase diffusion.

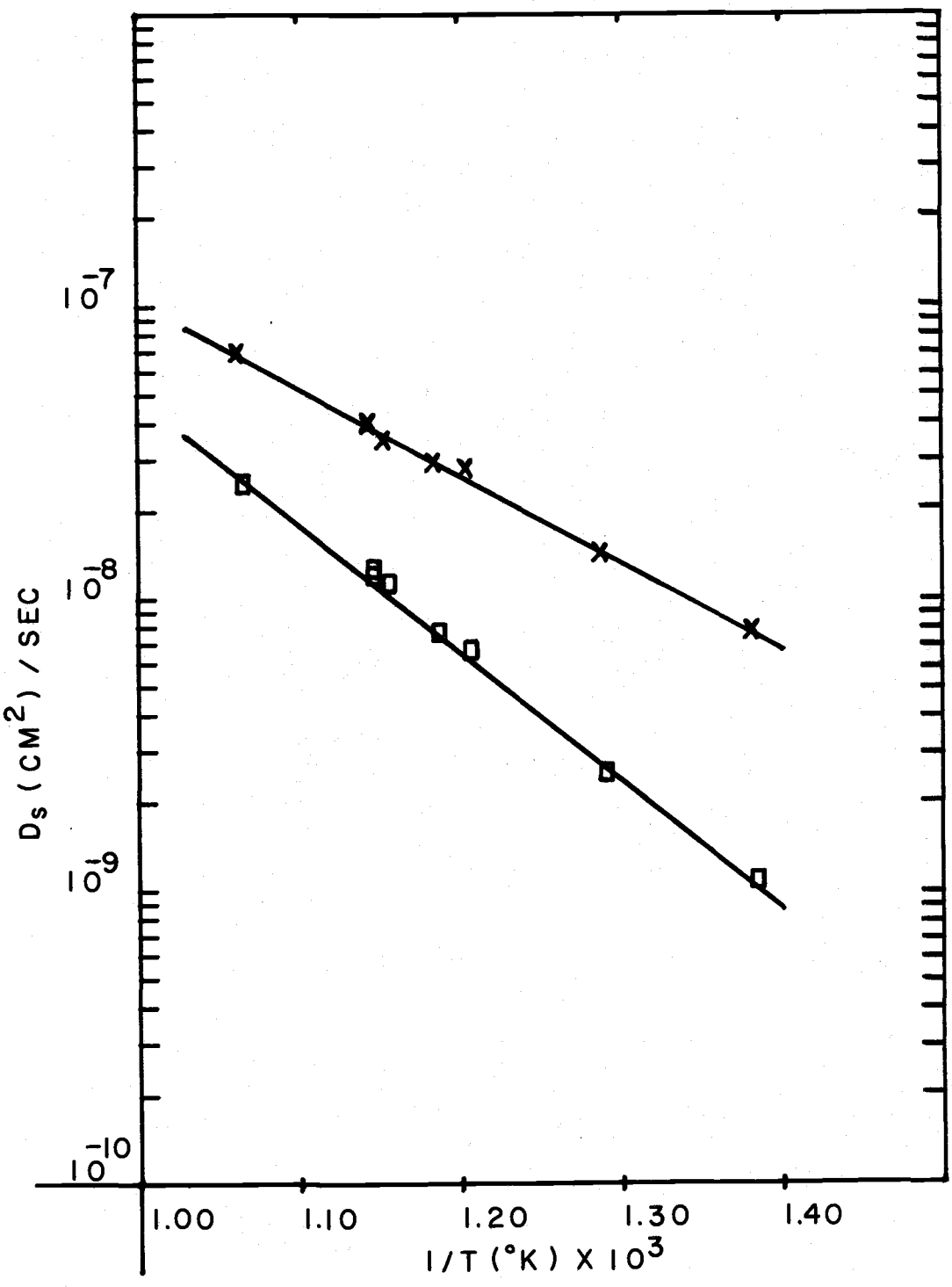

Figure 4.8. Log D_s vs. 1/T from diffusion in KCl.
X:Ca^{2+}. □ :Sr^{2+}. Solid lines with
D_o(Ca) = 9.93×10^{-5} cm^2/sec U(Ca) = 0.592 eV
D_o(Sr) = 1.20×10^{-3} cm^2/sec U(Sr) = 0.871 eV

The Gibbs free energy of association of the two complexes $-\Delta G(Ca)$ and $-\Delta G(Sr)$ are shown in Figure 4.9 as a function of temperature in degrees Kelvin. The straight lines were obtained by a least squares fit of the data. The values of $-\Delta G$ at different temperatures are fitted to

$$\Delta G = \Delta H - T\Delta S \tag{4.8}$$

where ΔH and ΔS are the enthalpy and entropy of formation for the complex, and T is in degrees Kelvin. It is emphasized that ΔS does not include the configurational entropy which is accounted for by the factor of 12 in Equations (2.6) and (2.7). From the straight lines the Gibbs free energies of association of the two complexes may be expressed as

$$\Delta G(Ca) = -0.507 \text{ eV} + (2.25 \times 10^{-4} \text{ ev/°K})T \tag{4.9}$$

and

$$\Delta G(Sr) = -0.575 \text{ eV} + (2.90 \times 10^{-4} \text{ eV/°K})T \tag{4.10}$$

Simultaneous Diffusion of Ca^{2+} and Sr^{2+} in NaCl

Figures 4.10 through 4.17 show the concentrations of calcium and strontium as a function of distance into a single crystal of sodium chloride for the temperature range from 448°C to 683°C. Table 4.3 shows the values of ΔG and D_s used to generate the diffusion of Ca^{2+} and Sr^{2+} in NaCl. The surface layer diffusions were carried out

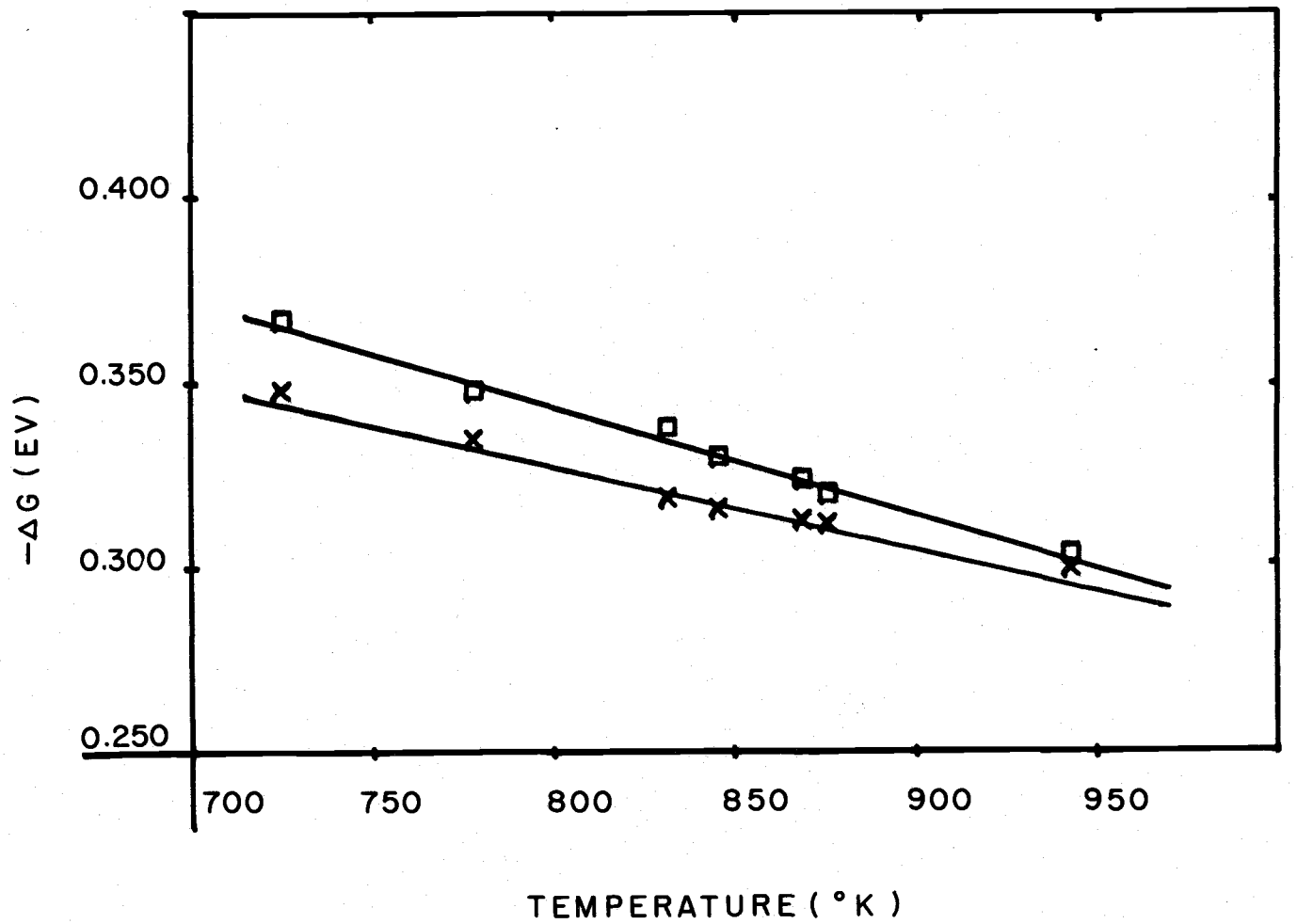

Figure 4.9. Gibbs free energies of association in KCl. X:Ca^{2+}. □:Sr^{2+}. Solid lines with

$\Delta H(Ca) = -0.507$ eV $\quad \Delta S(Ca) = -2.25 \times 10^{-4}$ eV/°K

$\Delta H(Sr) = -0.575$ eV $\quad \Delta S(Sr) = -2.90 \times 10^{-4}$ eV/°K

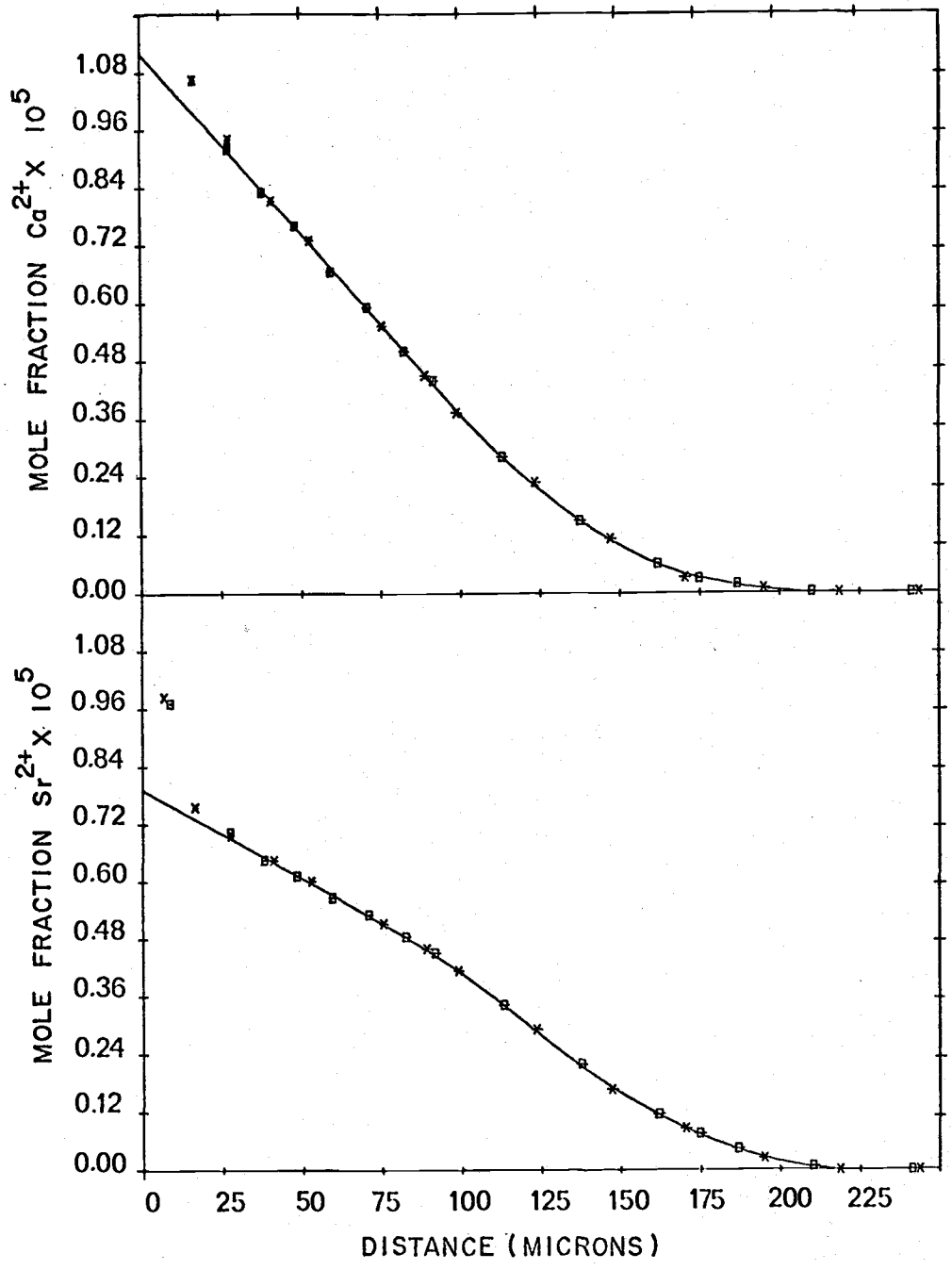

Figure 4.10. Penetration profiles of Ca^{2+} and Sr^{2+} in NaCl at 448°C. Surface source. t_t=6.89820x10^5sec. X:Crystal A. □:Crystal B. +:Errors. Solid curves are profiles generated by Equations (2.21) and (2.22) using the following parameters.

$\Delta G(Ca)$ = -0.377 eV $D_s(Ca)$ = 1.28x10^{-9}cm^2/sec

$\Delta G(Sr)$ = -0.429 eV $D_s(Sr)$ = 9.63x10^{-10}cm^2/sec

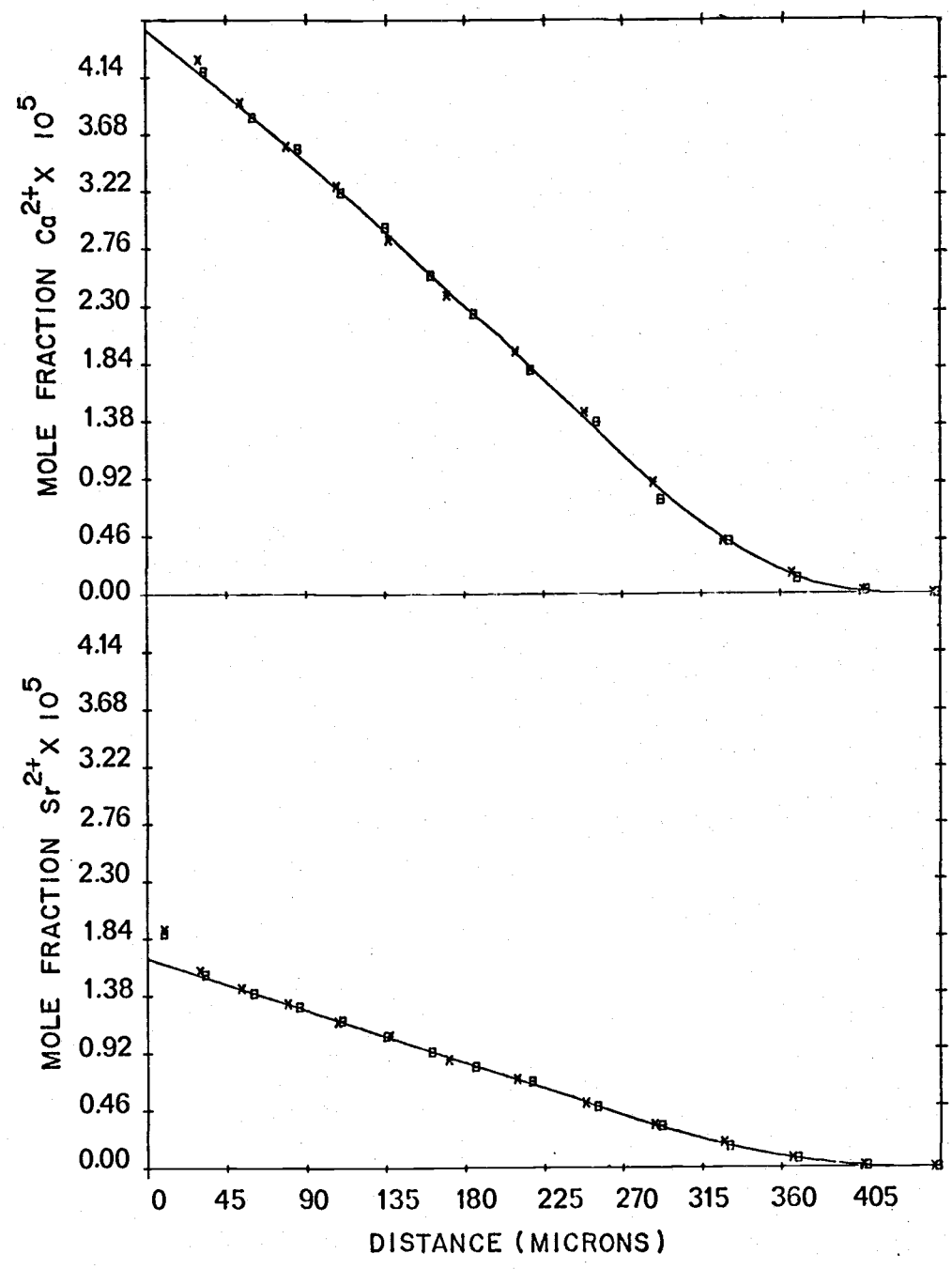

Figure 4.11. Penetration profiles of Ca^{2+} and Sr^{2+} in NaCl at 481°C. Surface source. t_t=6.91680x10^5sec. X:Crystal A. □:Crystal B. +:Errors. Solid curves are profiles generated by Equations (2.21) and (2.22) using the following parameters.

$\Delta G(Ca)$ = -0.372 eV $D_s(Ca)$ = 2.01x10^{-9}cm^2/sec

$\Delta G(Sr)$ = -0.416 eV $D_s(Sr)$ = 1.19x10^{-9}cm^2/sec

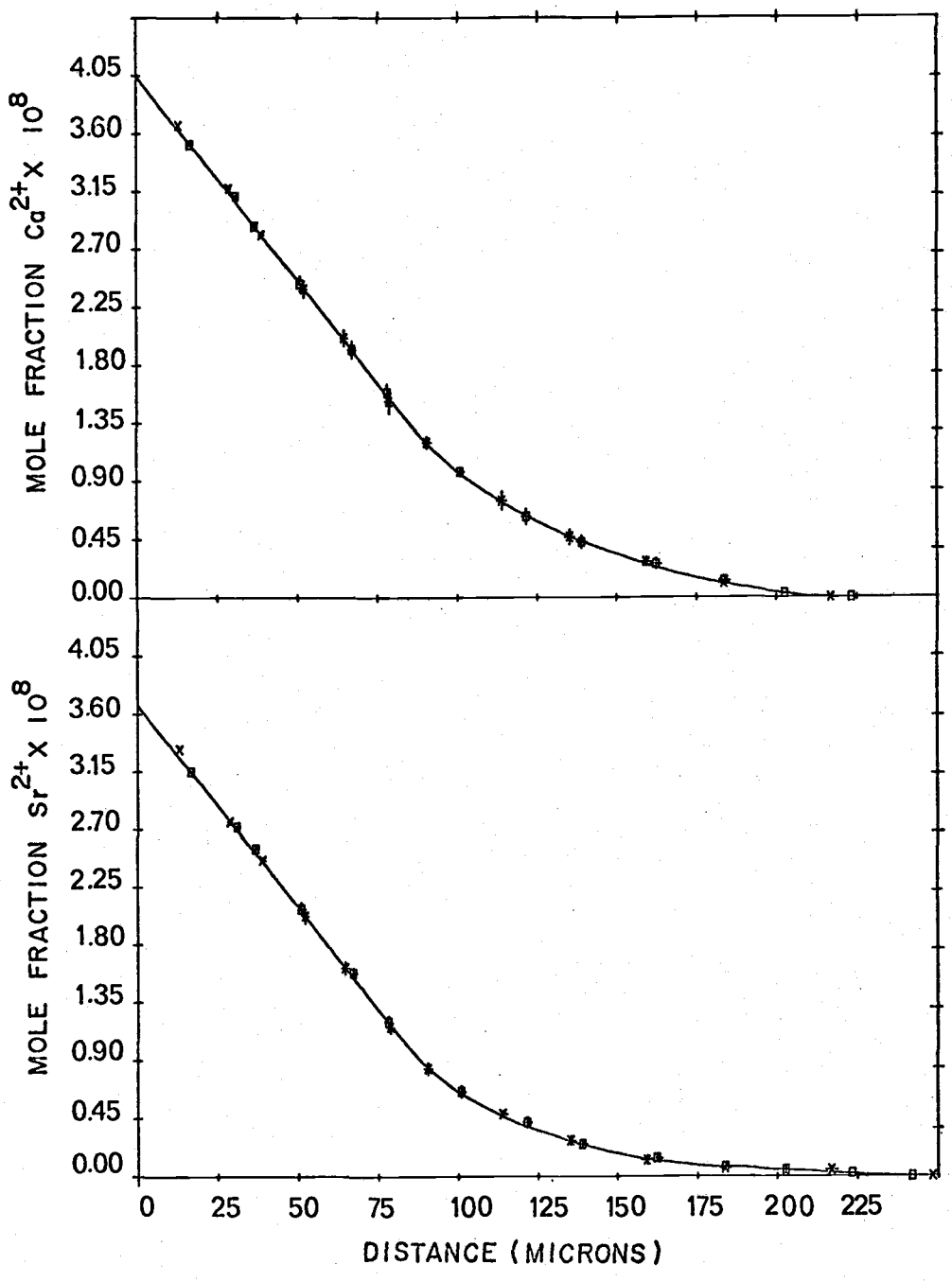

Figure 4.12. Penetration profiles of Ca^{2+} and Sr^{2+} in NaCl at 517°C. Vapor source. t_t=1.28478x10^6sec. X:Crystal A. □:Crystal B. ┼:Errors. Solid curves are profiles generated by Equations (2.21) and (2.22) using the following parameters.

$\Delta G(Ca)$ = -0.354 eV $D_s(Ca)$ = 5.42x10^{-9} cm^2/sec

$\Delta G(Sr)$ = -0.406 eV $D_s(Sr)$ = 2.75x10^{-9} cm^2/sec

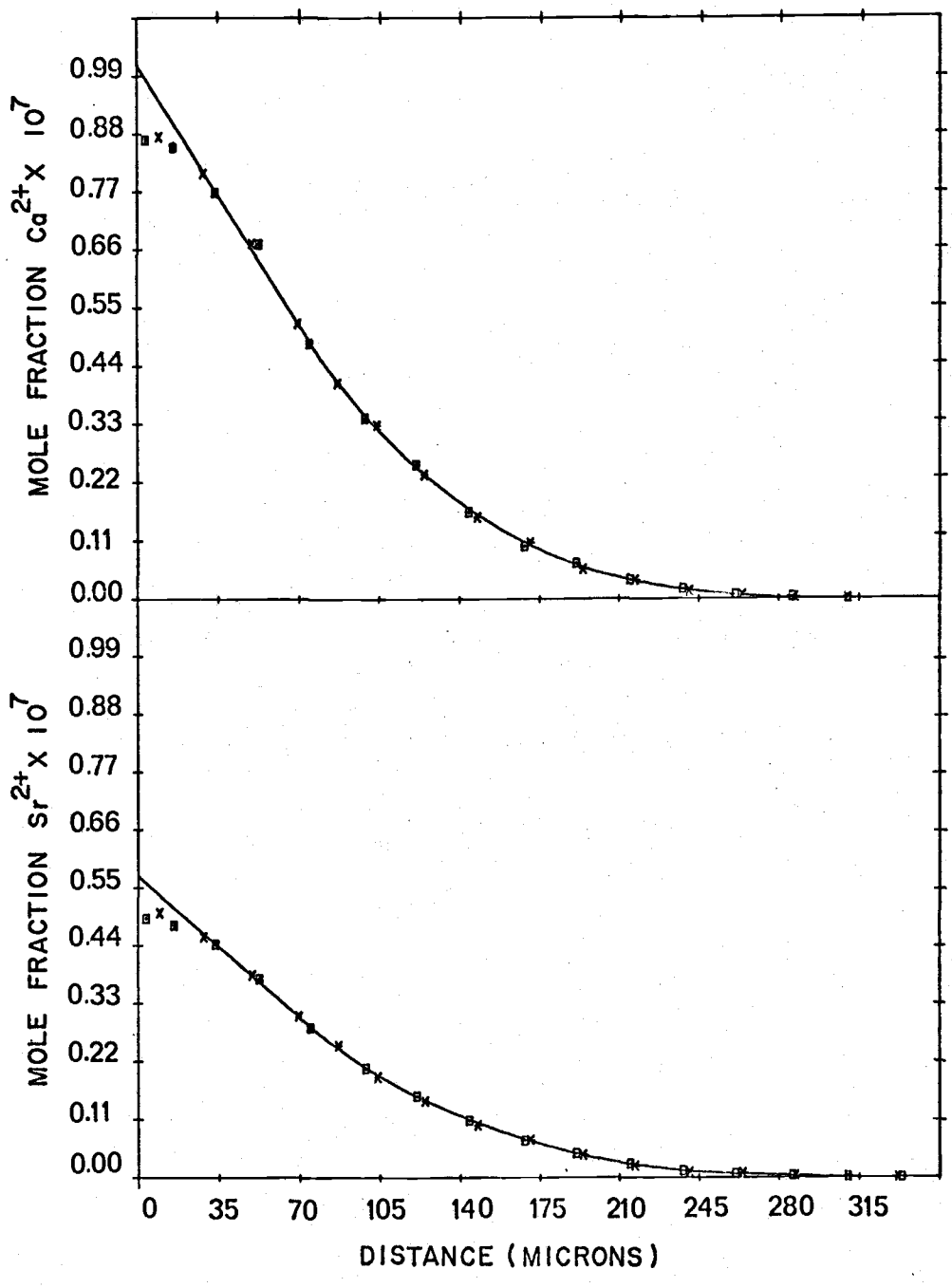

Figure 4.13. Penetration profiles of Ca^{2+} and Sr^{2+} in NaCl at 558°C. Vapor source. t_t=1.05918x10^6sec. X:Crystal A. □:Crystal B. +:Errors. Solid curves are profiles generated by Equations (2.21) and (2.22) using the following parameters.

$\Delta G(Ca)$ = -0.348 eV $D_s(Ca)$ = 7.59x10^{-9}cm^2/sec

$\Delta G(Sr)$ = -0.401 eV $D_s(Sr)$ = 5.65x10^{-9}cm^2/sec

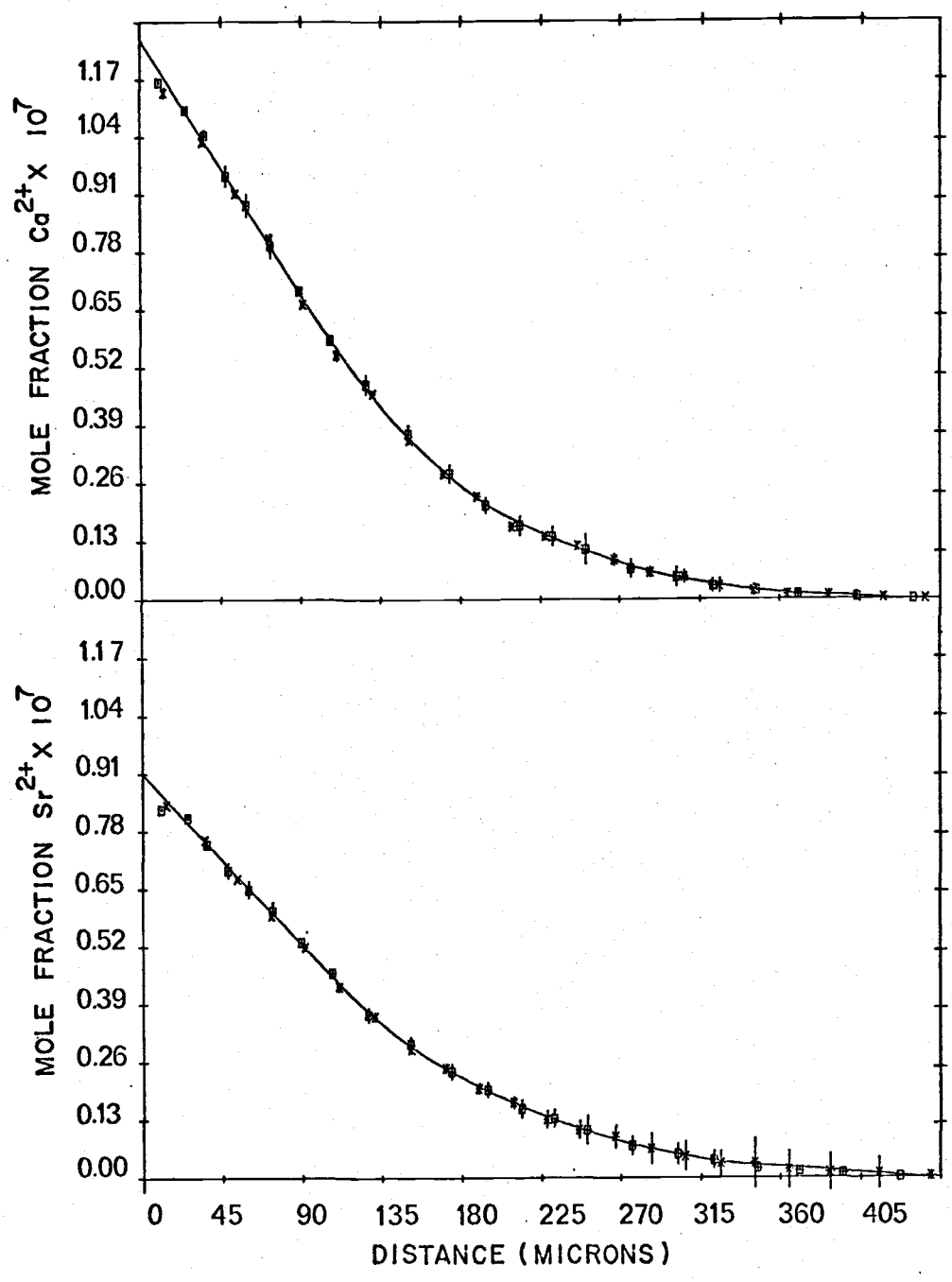

Figure 4.14. Penetration profiles of Ca^{2+} and Sr^{2+} in NaCl at 601°C. Vapor source. t_t=9.44640x10^{5}sec. X:Crystal A. □:Crystal B. +:Errors. Solid curves are profiles generated by Equations (2.21) and (2.22) using the following parameters.

$\Delta G(Ca)$ = -0.340 eV $D_s(Ca)$ = 1.30x10^{-8}cm^2/sec

$\Delta G(Sr)$ = -0.378 eV $D_s(Sr)$ = 1.09x10^{-8}cm^2/sec

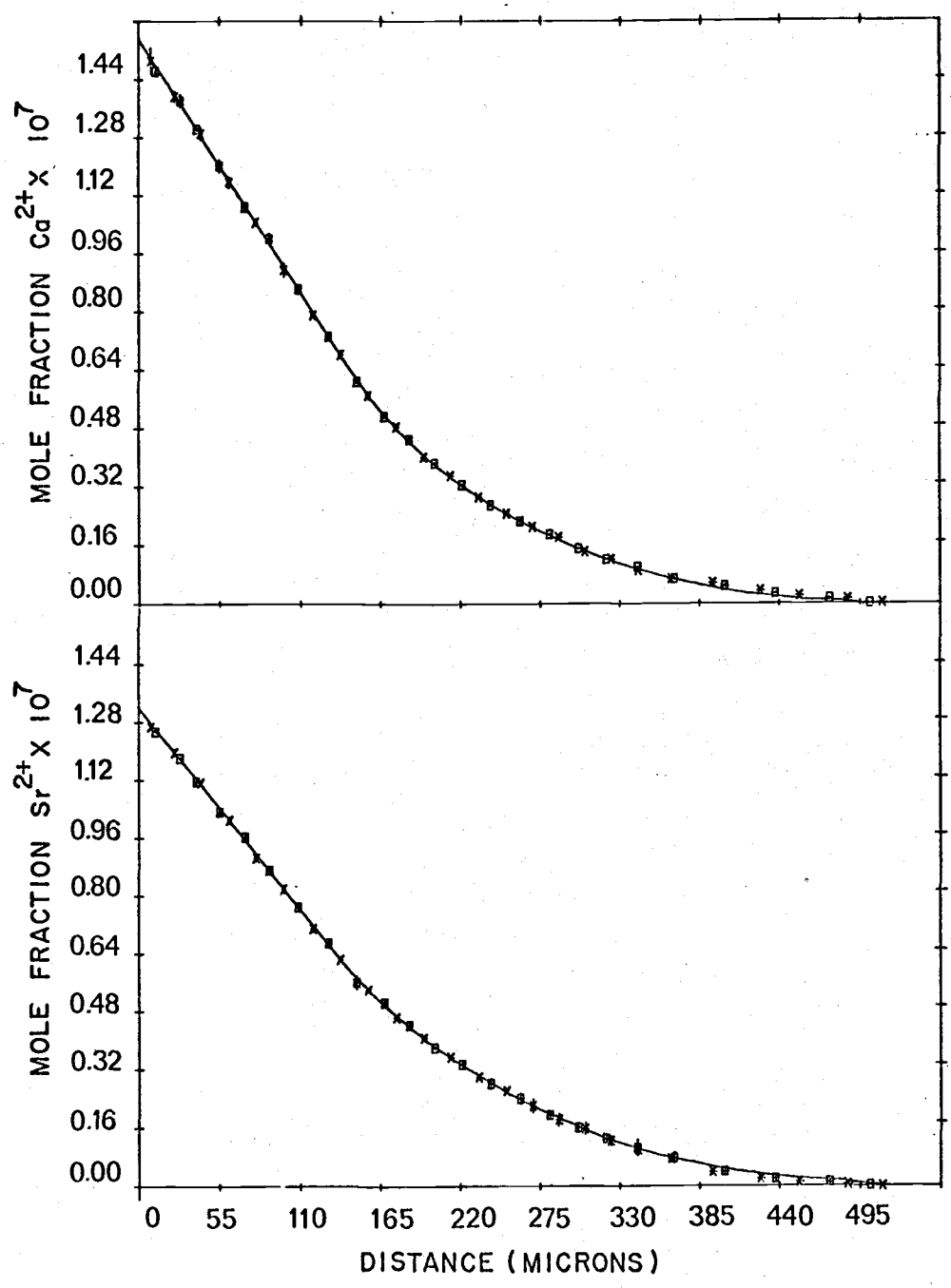

Figure 4.15. Penetration profiles of Ca^{2+} and Sr^{2+} in NaCl at 625°C. Vapor source. t_t=8.58060x10^5sec. X:Crystal A. □:Crystal B. +:Errors. Solid curves are profiles generated by Equations (2.21) and (2.22) using the following parameters.

$\Delta G(Ca)$ = -0.331 eV $D_s(Ca)$ = 1.99x10^{-8}cm^2/sec

$\Delta G(Sr)$ = -0.367 eV $D_s(Sr)$ = 1.69x10^{-8}cm^2/sec

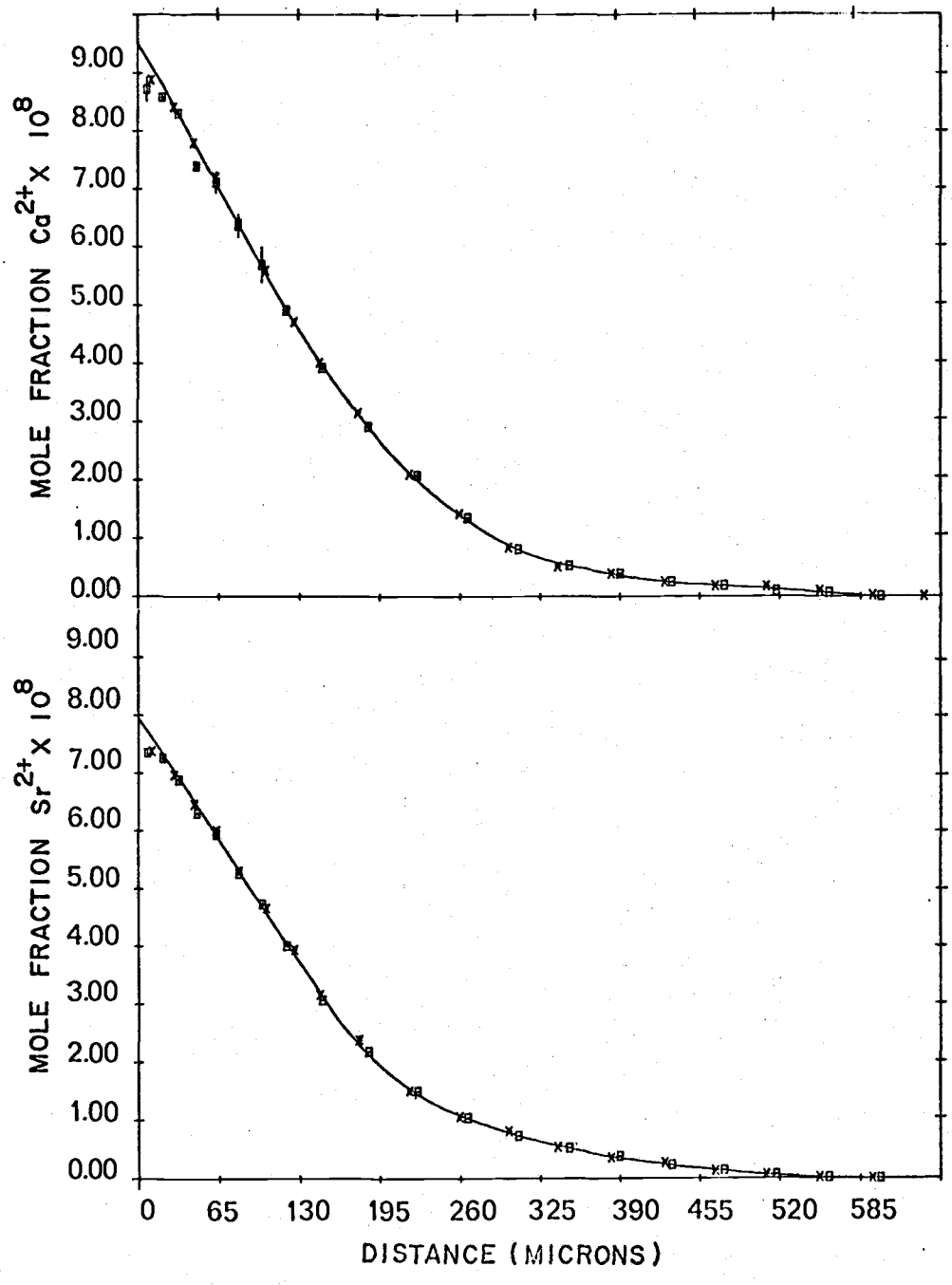

Figure 4.16. Penetration profiles of Ca^{2+} and Sr^{2+} in NaCl at 654°C. Vapor source. t_t=5.65440x10^{5}sec. X:Crystal A. □:Crystal B. ┼:Errors. Solid curves are profiles generated by Equations (2.21) and (2.22) using the following parameters.

$\Delta G(Ca)$ = -0.327 eV $D_s(Ca)$ = 2.54x10^{-8}cm^2/sec

$\Delta G(Sr)$ = -0.356 eV $D_s(Sr)$ = 1.97x10^{-8}cm^2/sec

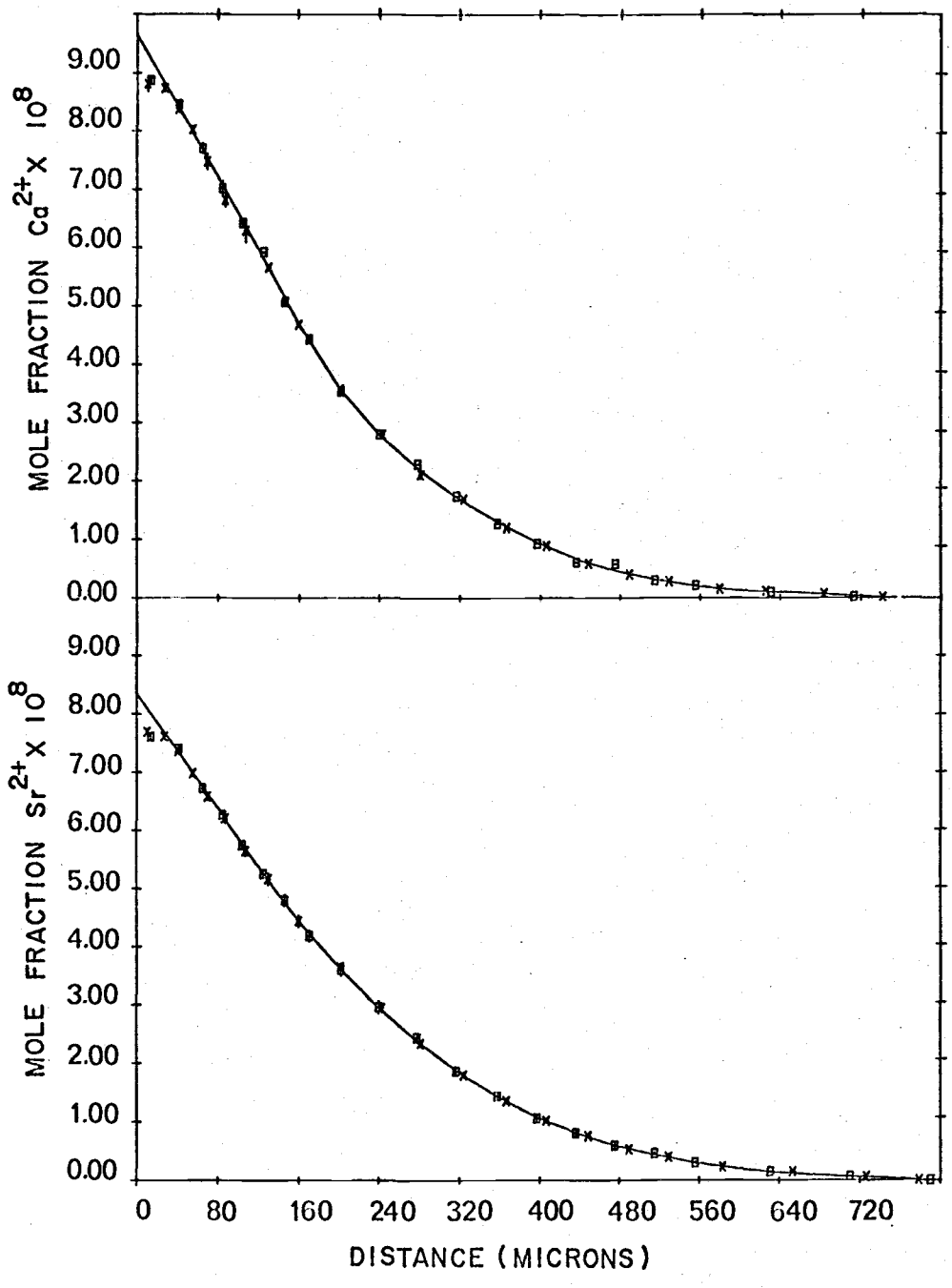

Figure 4.17. Penetration profiles of Ca^{2+} and Sr^{2+} in NaCl at 683°C. Vapor source. t_t=5.62380x10^5sec. X:Crystal A. □:Crys-B. +:Errors. Solid curves are profiles generated by Equations (2.21) and (2.22) using the following parameters.

$\Delta G(Ca)$ = -0.309 eV $D_s(Ca)$ = 3.84x10^{-8}cm^2/sec

$\Delta G(Sr)$ = -0.354 eV $D_s(Sr)$ = 3.11x10^{-8}cm^2/sec

Table 4.3. Values of ΔG and D_s used to generate diffusion of Ca^{2+} and Sr^{2+} in NaCl.

T (°C)	ΔG(Ca) (eV)	ΔG(Sr) (eV)	D_s(Ca) (cm^2/sec)	D_s(Sr) (cm^2/sec)	Expt.[a]
448	-0.377	-0.429	1.28×10^{-9}	9.63×10^{-10}	S
481	-0.372	-0.416	2.01×10^{-9}	1.19×10^{-9}	S
517	-0.354	-0.406	5.42×10^{-9}	2.75×10^{-9}	V
558	-0.348	-0.401	7.59×10^{-9}	5.65×10^{-9}	V
601	-0.340	-0.378	1.30×10^{-8}	1.09×10^{-8}	V
625	-0.331	-0.367	1.99×10^{-8}	1.69×10^{-8}	V
654	-0.327	-0.356	2.54×10^{-8}	1.97×10^{-8}	V
683	-0.309	-0.354	3.84×10^{-8}	3.11×10^{-8}	V

[a] S is surface layer diffusion. V is vapor phase diffusion.

at 448°C and 481°C, while the vapor phase diffusions were performed at 517°C, 558°C, 601°C, 625°C, 654°C and 683°C. The values of B and h_s for calculating the Schottky product K_s in the pure NaCl were taken from the results of Allnatt et al. (1971), and K_s is represented by

$$K_s = 1.719 \times 10^4 \exp(-2.48\ eV/kT) \qquad (4.11)$$

F. Beniere et al. (1970) also reported the values of B and h_s in NaCl. Table 4.4. shows the values of B and h_s with calculated K_s at 448°C and 683°C in NaCl. As mentioned in the case of KCl the differences in using the different values of B and h_s do not alter the concentration of the cation vacancies significantly, because they are controlled mainly by the amount of impurities introduced.

Table 4.4. Values of B, h_s and K_s at 448°C and 683°C in NaCl.

B	h_s (eV)	K_s (448°C)	K_s (683°C)	Reference
1.719×10^4	2.48	7.92×10^{-14}	1.45×10^{-9}	Allnatt et al. (1972)
6.895×10^4	2.5	2.30×10^{-13}	4.55×10^{-9}	F. Beniere et al. (1970)

The limits of error in mole fraction and distance were calculated as before and are included in the penetration profiles. Note that the surface layer diffusions (448°C and 481°C) show similar profiles to those which appeared in KCl. But, again, the calculated profiles

agree very well with the experimental penetration profiles.

Figure 4.18 shows the saturation coefficient D_s plotted versus $1/T$ ($^\circ K^{-1}$). From the straight lines obtained by a least squares fit $D_s(Ca)$ and $D_s(Sr)$ are found to be given by

$$D_s(Ca) = 1.14 \times 10^{-3} \exp(-0.851 \text{ eV}/kT) \text{ cm}^2/\text{sec} \qquad (4.12)$$

and

$$D_s(Sr) = 2.30 \times 10^{-3} \exp(-0.925 \text{ eV}/kT) \text{ cm}^2/\text{sec} \qquad (4.13)$$

where 1.14×10^{-3} cm^2/sec and 2.30×10^{-3} cm^2/sec are the values of the pre-exponential terms for calcium and strontium, respectively, and 0.851 eV and 0.925 eV are the migration energies of the calcium- and strontium-vacancy complex, respectively.

Figure 4.19 shows the Gibbs free energies of association of the two complexes $-\Delta G(Ca)$ and $-\Delta G(Sr)$ as a function of temperature. The straight lines are the least squares fit to the experimental data and are given by

$$\Delta G(Ca) = -0.572 \text{ eV} + (2.69 \times 10^{-4} \text{ eV}/^\circ K)T \qquad (4.14)$$

and

$$\Delta G(Sr) = -0.671 \text{ eV} + (3.35 \times 10^{-4} \text{ eV}/^\circ K)T \qquad (4.15)$$

Here -0.572 eV and -0.671 eV are the values of the enthalpy of complex formation for the calcium and strontium, respectively, and

2.69×10^{-4} eV/°K and 3.35×10^{-4} eV/°K the values of the entropy of complex formation for the calcium and strontium, respectively.

The raw data necessary to calculate the experimental profiles are given in Appendix I.

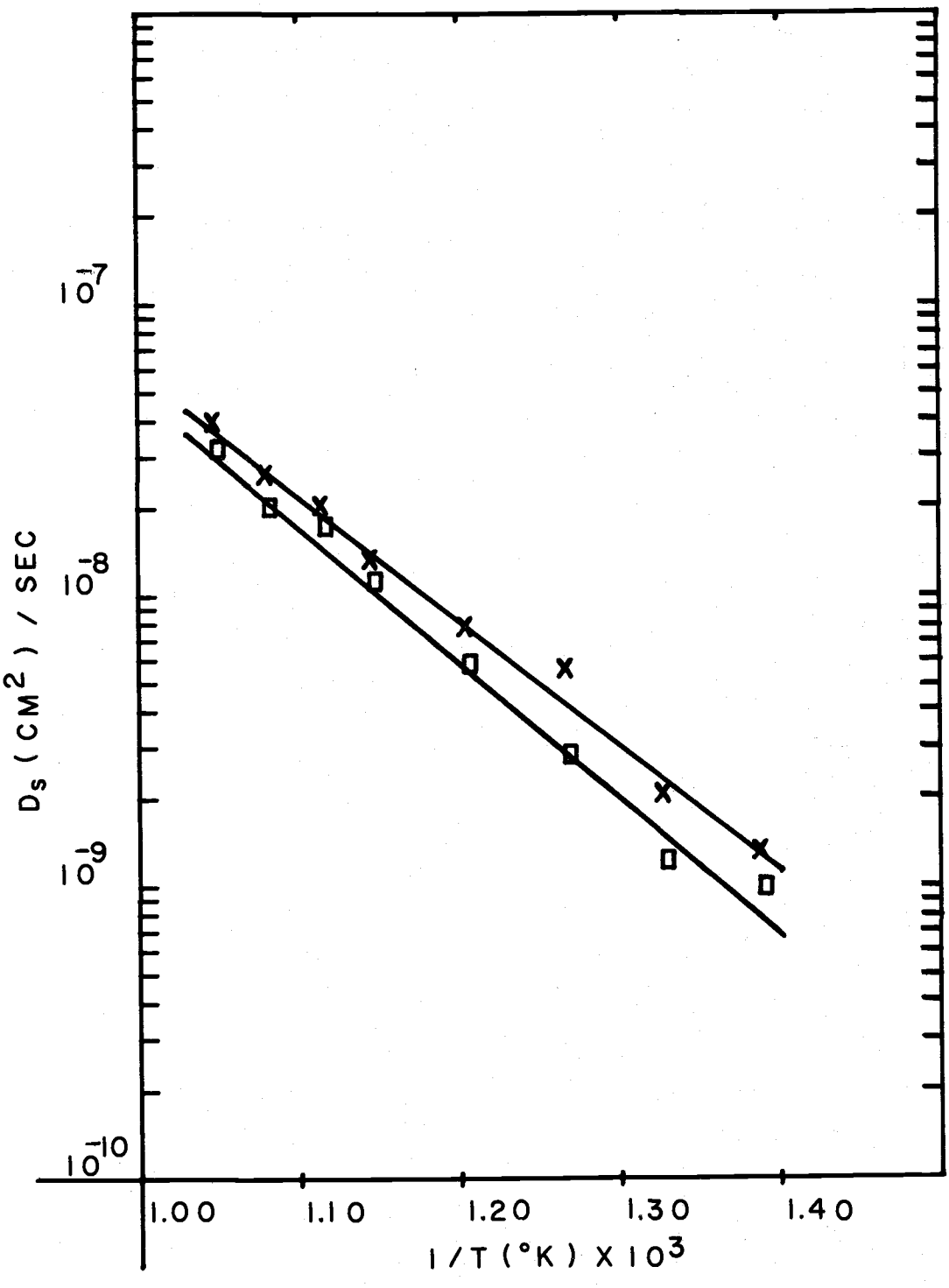

Figure 4.18. Log D_s vs. 1/T from diffusion in NaCl.
X:Ca^{2+}. □:Sr^{2+}. Solid lines with
$D_o(Ca) = 1.14 \times 10^{-3} cm^2/sec$ U(Ca) = 0.851 eV
$D_o(Sr) = 2.30 \times 10^{-3} cm^2/sec$ U(Sr) = 0.925 eV

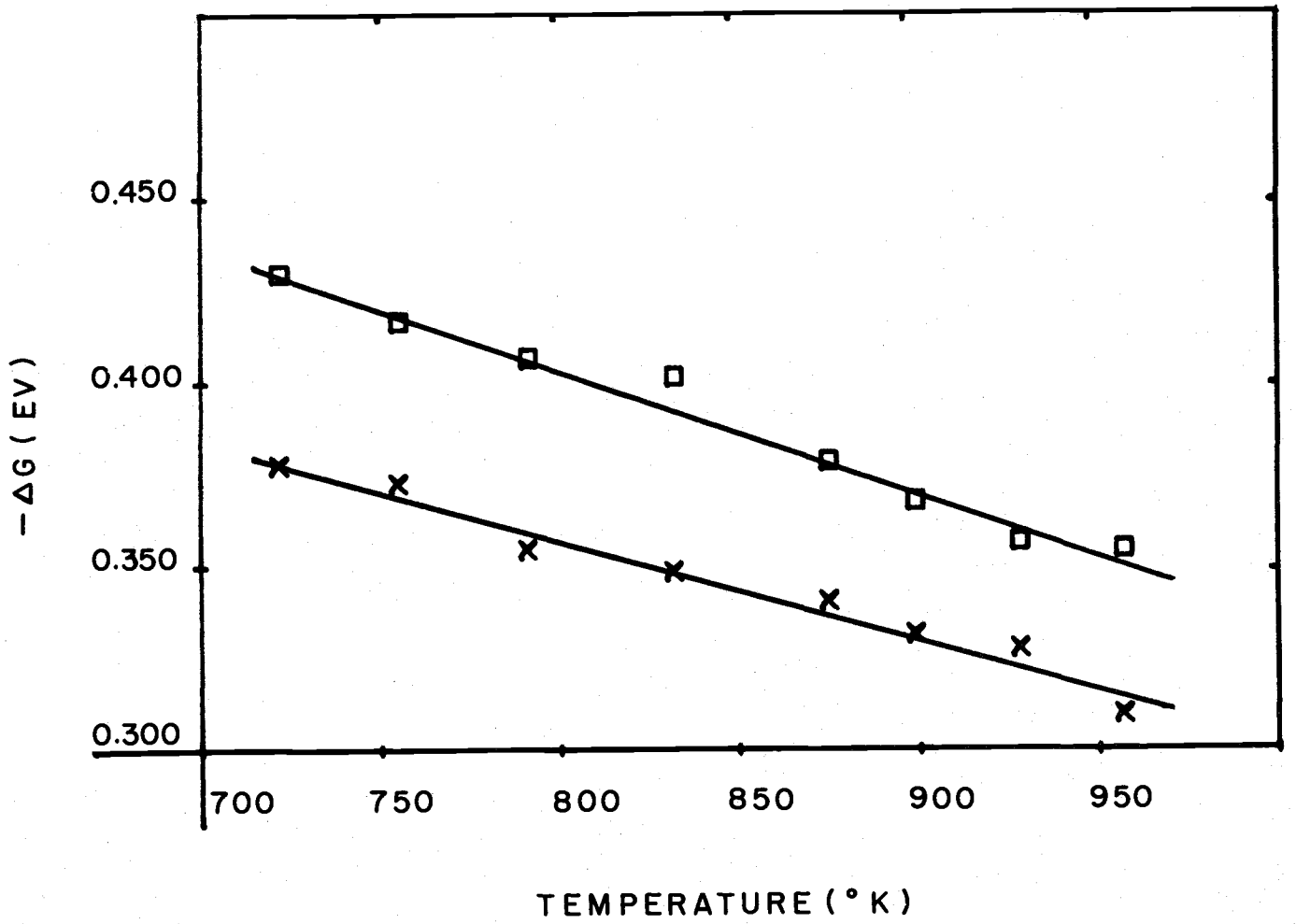

Figure 4.19. Gibbs free energies of association in NaCl. X:Ca^{2+}. □:Sr^{2+}. Solid lines with

$\Delta H(Ca) = -0.572$ eV $\quad \Delta S(Ca) = -2.69 \times 10^{-4}$ eV/°K

$\Delta H(Sr) = -0.671$ eV $\quad \Delta S(Sr) = -3.35 \times 10^{-4}$ eV/°K

V. DISCUSSION

The comparison of the pre-exponential factors D_0 and the migration energies U of available data on calcium diffusion in NaCl is shown in Table 5.1, and on strontium in NaCl shown in Table 5.2. Since calcium and strontium diffusion data in KCl have not been reported, such a comparison is not possible. Under the "Notes" column the limiting conditions, under which the diffusion parameters were determined, are shown. It should be emphasized that $D_{p\to 1}$ and $D_{c\to\infty}$ must be distinguished clearly. In the case of $D_{p\to 1}$ the concentration of the diffusing impurity varies from $c \to 0$ to near saturation, while in $D_{c\to\infty}$, the concentration of an impurity indistinguishable from the tracer diffusant is high over the entire host crystal. Note that the migration energies of Ca^{2+} in NaCl by Slifkin and Brebec (1968), and of Sr^{2+} in NaCl by Allnatt and Pantelis (1968) are considerably higher than other values. In their cases the migration energy U is not the enthalpy of migration $h_m(M^{2+})$, but it is the sum of enthalpy terms $U = h_m(M^{2+}) + h_k + h_s/2$, where h_k is the enthalpy of the impurity-vacancy association and h_s the enthalpy of the Schottky vacancy formation.

It is possible to approximate the pre-exponential factor D_0 theoretically and the calculated values for Ca and Sr are also listed in Table 5.1 and Table 5.2. The theoretical values of D_0 were

Table 5.1. Pre-exponential factors D_0 and migration energies U for Ca^{2+} diffusion in NaCl.

D_0 (cm^2/sec)	U (eV)	Method	Notes	Reference
NA[a]	0.702	Dielectric relaxation	b	Dreyfus (1961)
1.14×10^{-3}	0.851	Simultaneous diffusion with Sr^{2+}	c	This work
6.0×10^{-3}	0.90	Drift experiment	d	Banasevich et al. (1960)
NA	0.96	Diffusion	e	Murin et al. (1962)
0.94×10^{-3}	1.14	Diffusion	f	F. Beniere et al. (1969)
0.13	1.55	Diffusion	g	Slifkin and Brebec (1968)
4.73×10^{-3}		Theoretical calculation	h	

[a]Not available.

[b]Pre-exponential factor is treated as constant and independent of impurity radius.

[c]$D_{p \to 1}$.

[d]Surface deposit. D is not dependent on concentration.

[e]The host NaCl is doped with 0.2 mole % $CaCl_2$. Bent log D vs. 1/T curve.

[f]$D_{c \to \infty}$. D is not treated as concentration dependent.

[g]$U = h_m(Ca) + h_k + h_s/2$, where h_m is enthalpy of migration, h_k enthalpy of complex formation, and h_s Schottky enthalpy.

[h]$D_0 = (1/3)fa^2\nu_2 \exp(\Delta S_2/k)$.

Table 5.2. Pre-exponential factors D_0 and migration energies U for Sr^{2+} diffusion in NaCl.

D_0 (cm^2/sec)	U (eV)	Method	Notes	Reference
NA[a]	0.705	Dielectric relaxation	b	Dreyfus (1961)
1.1×10^{-3}	0.91	Drift experiment	c	Chemla (1956)
2.30×10^{-3}	0.925	Simultaneous diffusion with Ca^{2+}	d	This work
7.6×10^{-3}	1.25	Diffusion	e	F. Beniere et al. (1969)
1.7×10^{-3}	1.31	Diffusion	f	F. Beniere (1970)
41.3×10^{-3}	1.36	Simultaneous diffusion with Co^{2+}	g	Allnatt and Pantelis (1968)
3.33×10^{-3}		Theoretical calculation	h	

[a] Not available.

[b] Pre-exponential factor is treated as constant and independent of impurity radius.

[c] Surface deposit.

[d] $D_{p \to 1}$.

[e] $D_{c \to \infty}$. D is not treated as concentration dependent.

[f] $D_{c \to \infty}$. D is not treated as concentration dependent.

[g] D is not concentration dependent. $U = h_m(Sr) + h_k + h_s/2$, where h_m is enthalpy of migration, h_k enthalpy of complex formation, and h_s Schottky enthalpy.

[h] $D_0 = (1/3)fa^2\nu_2 \exp(\Delta S_2/k)$.

calculated as follows. The diffusion coefficient of a divalent impurity in the NaCl type lattice at concentrations sufficiently high for all ions to be associated with vacancies, that is when $p = 1$, is represented by

$$D_s = \frac{1}{3} f a^2 \omega_2$$

$$= \frac{1}{3} f a^2 \nu_2 \exp(\Delta S_2/k) \exp(-\Delta h_2/kT) \qquad (5.1)$$

where the following expression was used for ω_2,

$$\omega_2 = \nu_2 \exp(-\Delta g_2/kT)$$

Here ω_2 and ν_2 are the jump frequency and the effective vibrational frequency of the impurity ion, respectively. The Δg_2 is the free energy of activation for the impurity jump into an adjacent vacant site and it is expressed in terms of the enthalpy Δh_2 and the entropy ΔS_2 of activation in the usual manner. In Equation (5.1) the subscript 2 refers to the impurity-vacancy exchange, and f is the correlation factor which accounts for the non-randomness of impurity jumps in the NaCl lattice, and a is the nearest anion-cation separation. From the above Equation (5.1) the pre-exponential factor D_0, which is independent of the temperature, is given by

$$D_0 = \frac{1}{3} f a^2 \nu_2 \exp(\Delta S_2/k) \qquad (5.2)$$

The vibrational frequency ν_2 can be obtained in the classical harmonic approximation that as an impurity ion moves from the equilibrium position to an adjacent vacant site, its potential energy varies in a simple sinusoidal manner (Wert and Zener, 1949). Thus we may assume that

$$V(x) = \frac{1}{2} E(1-\cos 2\pi x/\lambda) \tag{5.3}$$

where $V(x)$ is the potential energy, and x is the coordinate along this path. The E is the height of the potential barrier, which may be taken as approximately equal to the enthalpy of activation Δh_2, and λ is the jump distance. The vibrational frequency ν_2 is then, according to this approximation, given by

$$\nu_2 = (\Delta h_2/2m\,\lambda^2)^{1/2} \tag{5.4}$$

where m is the mass of the moving species. It should be emphasized that the dependence of the pre-exponential factor D_0 on the mass of the diffusing species varies as $m^{-1/2}$. This $m^{-1/2}$ dependence of D_0 has been shown theoretically more recently by Franklin (1972). If we calculate ν_2, for example, in the case of Sr^{2+} diffusion in NaCl with the experimental value of Δh_2 (0.925 eV), the mass of the strontium (1.4555×10^{-22} gm) and the jump distance λ (3.9796×10^{-8} cm), the vibrational frequency ν_2 will be

1.79×10^{12} sec^{-1}. Taking the literature value of $\Delta S_2 = 2.2k$ from Dreyfus' (1961) results, the pre-exponential factor D_0 for the Sr^{2+} diffusion in NaCl is then calculated from Equation (5.2) using $\nu_2 = 1.79 \times 10^{12}$ sec^{-1}, $f = 0.7815$ (LeClaire, 1970) and $a = 2.814 \times 10^{-8}$ cm (Pauling, 1960, p. 526). Note that the correlation factor f of 0.7815 is the value of f for the self-diffusion of Na^+ in NaCl or of K^+ in KCl. The f for the Sr^{2+} ion is a function of various jump frequencies, but no reliable data on the jump frequencies is available at present. However the value of f for the Sr^{2+} ion should be close to this value. The value that we obtain for D_0 ($NaCl:Sr^{2+}$) is 3.33×10^{-3} cm^2/sec. This theoretical value agrees well with the experimental value of 2.30×10^{-3} cm^2/sec of this work.

The enthalpies ΔH and entropies ΔS of formation of Ca^{2+} complex in NaCl are shown in Table 5.3, and those of Sr^{2+} complex in NaCl shown in Table 5.4. The values of ΔH and ΔS of Ca^{2+} and Sr^{2+} complexes in KCl are shown in Table 5.5 and Table 5.6. The theoretical binding energies (not enthalpies) of the Ca^{2+}- and Sr^{2+}-vacancy complexes by Bassani and Fumi (1954) are also listed in those tables. The enthalpy of Ca^{2+}-vacancy complex formation in NaCl of this work agrees very well with the conductivity data of F. Beniere et al. (1969), and also the highest value of Slifkin and Brebec (1968). The enthalpy of the Sr-vacancy association in NaCl is

Table 5.3. Enthalpies of formation ΔH and entropies of formation ΔS of Ca^{2+} complex in NaCl.

ΔH (eV)	ΔS (eV/deg)[a]	Method	Notes	Reference
-0.31	NA[b]	Conductivity	c	Kanzaki et al. (1965)
-0.52 to -0.57	NA	Diffusion	d	Slifkin and Brebec (1968)
-0.57	NA	Conductivity	e	F. Beniere et al. (1969)
-0.57	-2.69×10^{-4}	Simultaneous diffusion with Sr^{2+}	f	This work
-0.67	-4.9×10^{-4}	Diffusion	g	Murin et al. (1962)
-0.38		Theoretical calculation	h	Bassani and Fumi (1954)
	-2.5×10^{-4}	Empirical calculation	i	

[a] Entropy of complex formation excluding configurational entropy.

[b] Not available.

[c] $c \rightarrow \infty$.

[d] NaCl doped with $CaCl_2$.

[e] $C \rightarrow \infty$ (heavily doped crystal).

[f] $p \rightarrow 1$.

[g] The host NaCl is doped with 0.2 mole % $CaCl_2$.

[h] Binding energy (not enthalpy).

[i] $\Delta S = 4\alpha\Delta H$ (lawson, 1957).

Table 5.4. Enthalpies of formation ΔH and entropies of formation ΔS of Sr^{2+} complex in NaCl.

ΔH (eV)	ΔS (eV)[a]	Method	Notes	Reference
-0.53	-1.5×10^{-4}	Conductivity	b	Brown and Hoodless (1967)
-0.55	-0.95×10^{-4}	Conductivity	c	Laredo et al. (1970)
-0.64 to -0.91	-1.8×10^{-4}	Conductivity	d	Allnatt et al. (1971)
-0.67	-3.35×10^{-4}	Simultaneous diffusion with Ca^{2+}	e	This work
-0.45		Theoretical calculation	f	Bassani and Fumi (1954)
	-3.0×10^{-4}	Empirical calculation	g	

[a] Entropy of complex formation excluding configurational entropy.

[b] Slight curvature in ΔG vs. $c/(\Delta G - 1/\Delta G)$.

[c] $c \rightarrow \infty$ (heavily doped crystal).

[d] Debye-Huckel effects are included.

[e] $p \rightarrow 1$.

[f] Binding energy (not enthalpy).

[g] $\Delta S = 4\alpha\Delta H$ (Lawson, 1957).

Table 5.5. Enthalpies of formation ΔH and entropies of formation ΔS of Ca^{2+} complex in KCl.

ΔH (eV)	ΔS (eV)[a]	Method	Notes	Reference
-0.51	-2.25×10^{-4}	Simultaneous diffusion with Sr^{2+}	b	This work
-0.52	NA[c]	Conductivity	d	Grundig (1960)
-0.32		Theoretical calculation	e	Bassani and Fumi (1954)
	-2.1×10^{-4}	Empirical calculation	f	

[a] Entropy of complex formation excluding configurational entropy.

[b] $p \rightarrow 1$.

[c] Not available.

[d] KCl doped with 0.5×10^{-4} mole fraction of $CaCl_2$.

[e] Binding energy (not enthalpy).

[f] $\Delta S = 4\alpha\Delta H$ (Lawson, 1957).

Table 5.6. Enthalpies of formation ΔH and entropies of formation ΔS of Sr^{2+} complex in KCl.

ΔH (eV)	ΔS (eV)[a]	Method	Note	Reference
-0.42	b	Conductivity	c	Beaumont and Jacobs (1966)
-0.56	-0.93×10^{-4}	Conductivity	d	M. Beniere (1974)
-0,57[e]	-1.62×10^{-4} e	Conductivity	f	Fuller et al. (1968)
-0.36[g]	-0.45×10^{-4} g	Conductivity	f	Fuller et al. (1968)
-0.58	-2.90×10^{-4}	Simultaneous diffusion with Ca^{2+}	h	This work
-0.58	-1.12×10^{-4}	Conductivity	i	Chandra and Rolfe (1970)
-0.59	-0.48×10^{-4}	Conductivity	j	Jacobs and Pantelis (1971)
-0.39		Theoretical calculation	k	Bassani and Fumi (1954)
	-2.3×10^{-4}	Empirical calculation	l	

[a] Entropy of complex formation excluding configurational entropy.

[b] ΔS is assumed negligible.

[c] ΔG is assumed to be independent of temperature. Not including long-range Coulomb interactions.

[d] Including long-range Coulomb interactions.

[e] By Lidiard theory including long-range Coulomb interactions.

[f] Nonrandom deviation between theoretical values and experimental ones.

[g] By simple theory including association.

[h] $p \rightarrow 1$.

[i] Including long-range Coulomb interactions.

[j] Including long-range Coulomb interactions.

[k] Binding energy (not enthalpy).

[l] $\Delta S = 4\alpha \Delta H$ (Lawson, 1957).

comparable with Allnatt's et al. (1971) conductivity value which includes the Debye-Huckel effects. Grundig's (1960) conductivity result for Ca^{2+}-vacancy complex in KCl agrees quite well with the enthalpy value of this work. Values for the enthalpy of Sr^{2+}-vacancy complex in KCl have been reported by many workers, for example, Beaumont and Jacobs (1966), Fuller et al. (1968), Chandra and Rolfe (1970), Jacobs and Pantelis (1971), M. Beniere (1974), and their values, except Beaumont and Jacobs' (1966) agree very well with the result of this work. It is seen that the enthalpy of association for Sr^{2+} is greater than that for Ca^{2+} in both NaCl and KCl. This agrees with the trend, predicted by Bassani and Fumi (1954), toward a larger association energy with increasing ionic radius. Bassani and Fumi also predicted in their work that the binding energy increases for the same ion when going from KCl to NaCl. The results of this work and of the works listed in Tables 5.3, 5.4, 5.5 and 5.6 agree with this generalization.

Usuaully it is assumed that the binding energy ΔE is approximately equal to the enthalpy of the complex formation ΔH, that is in the following equation

$$\Delta H = \Delta E + \Delta(PV) \qquad (5.5)$$

the pressure-volume work $\Delta(PV)$ is considered small. This assumption can be verified as follows. It has been shown (Keyes,

1958) that the volume changes associated with the formation of the defects can be related approximately to the enthalpy of formation by the following empirical equation

$$\Delta V = 4\beta\Delta H \qquad (5.6)$$

where ΔV is the volume change, and ΔH is the enthalpy of formation of the complex. The β is the isothermal compressibility. When the experimental value of $\Delta H = 0.671$ eV for the Sr^{2+}-vacancy complex in NaCl and the literature value of $\beta = 4.17 \times 10^{-12}$ cm^2/dyne $= 1.75 \times 10^{-4}$ cm^3/cal (Tosi, 1964) are used, the volume change ΔV will be calculated as $\Delta V = 10.8$ cm^3/mole. Similarly the volume change in the Ca^{2+}-vancancy complex formation in NaCl is calculated as $\Delta V = 9.2$ cm^3/mole. Using the values of β in KCl (Tosi, 1964) the volume changes in the Ca^{2+}- and Sr^{2+}-vacancy complex formation are calculated as $\Delta V = 11.2$ cm^3/mole and $\Delta V = 12.7$ cm^3/mole, respectively. If it is assumed that the pressure P is 1 atmosphere (1.050×10^{-6} eV/cm^3) in Equation (5.5), the value of $P(\Delta V)$ in the case of Sr^{2+}-vacancy complex formation in NaCl will be calculated as $P\Delta V = 1.13 \times 10^{-5}$ eV/mole. This value of $P\Delta V$ is compared with the theoretical binding energy of $\Delta E = 0.45$ eV/mole (Bassani and Fumi, 1954). From this comparison it is clear that the usual assumption of neglecting the pressure-volume work in Equation (5.5) is valid.

Recently, Martin et al. (1973) reported the experimental value of the volume change in the formation of a vacancy in NaCl. They obtained a value of $+2.2V_m$ for the formation of a vacancy by measuring the pressure dependence of the ^{22}Na diffusion coefficient D, that is, by their definition, $\Delta V = -RT(\partial \ln D/\partial P)_T$, where V_m is the molar volume and is 27 cm^3/mole for NaCl. This value may be compared with the theoretical value of $-0.69V_m$ calculated by Faux and Lidiard (1971). It can be seen that the discrepancy between theoretical and experimental values is quite large. This suggests that the theoretical calculation of the volume change in the defect formation may not be very accurate. However, the assumption of neglecting the pressure-volume work in the formation of the complex should be still valid, because the value of $P\Delta V$ calculated is far smaller than the value of ΔE.

There exists an empirical, approximate expression for the entropy of formation of the complex (Lawson, 1957; Keyes, 1958), and it is written as

$$\Delta S = 4\alpha\Delta H \tag{5.7}$$

where ΔS and ΔH are the entropy and the enthalpy of the complex formation. The α is the coefficient of thermal expansion. When this equation is used to calculate the theoretical values of ΔS in NaCl and KCl with literature values of $\alpha_{NaCl} = 1.10 \times 10^{-4}$/deg and

$\alpha_{KCl} = 1.01 \times 10^{-4}$/deg (Tosi, 1964, p. 44), the following values are obtained:

$$\Delta S(NaCl{:}Ca^{2+}) = 2.5 \times 10^{-4} \text{ eV/deg},$$

$$\Delta S(NaCl{:}Sr^{2+}) = 3.0 \times 10^{-4} \text{ eV/deg},$$

$$\Delta S(KCl{:}Ca^{2+}) = 2.1 \times 10^{-4} \text{ eV/deg}$$

and

$$\Delta S(KCl{:}Sr^{2+}) = 2.3 \times 10^{-4} \text{ eV/deg}.$$

Note that Equation (5.7) is derived from crude models of crystals and provides only rough estimates of the entropy. Nevertheless the estimated values agree quite well with the experimental entropies of this work.

Mass action expressions such as (2.6), (2.7) and (2.8) were written in terms of concentrations χ_i of point defects, and assumed that the interactions were only for nearest neighbors and no account was taken of the long-range Coulomb interactions among unassociated defects. This can be taken care of by replacing a concentration in the mass action expression by an effective concentration, that is an activity a_i which is equal to $\gamma_i \chi_i$ where γ_i is an activity coefficient (Lidiard, 1957).

Hence the appropriate equations including the Coulomb interactions between the isolated defects, according to Lidiard, are given below:

$$\gamma_x \chi_c \gamma_a \chi_a = K_s = \exp(-\Delta G_s/kT) \qquad (5.8)$$

$$\frac{\chi_{k1}}{\gamma_c \chi_c \gamma_1 (c_1 - \chi_{k1})} = 12 \exp(-\Delta G_{k1}/kT) \qquad (5.9)$$

$$\frac{\chi_{k2}}{\gamma_c \chi_c \gamma_2 (c_2 - \chi_{k2})} = 12 \exp(-\Delta G_{k2}/kT) \qquad (5.10)$$

where subscripts a and c refer to anion vacancy and cation vacancy, respectively, and subscripts 1 and 2 refer to the impurity 1 and impurity 2. The γ's are the activity coefficients of the charged defects. Since the impurity-vacancy complexes are electrically neutral, their activity coefficient is unity. All concentrations are in mole fractions. Lidiard (1957) employed the Debye-Huckel theory of liquid electrolyte solutions to obtain the activity coefficients of the defects in solids, and they are expressed by

$$\log \gamma_c = 10g\ \gamma_a = \log \gamma_i = \frac{-e^2}{2\epsilon kT} \frac{K}{(1 + KR)} \qquad (5.11)$$

where

$$K^2 = \frac{8\pi e^2 \chi_c}{v\epsilon kT} \qquad (5.12)$$

Here R is the separation below which an impurity ion and a vacancy are regarded as associated, and ϵ is the dielectric constant of the medium. The volume per molecule of the pure salt is given by v, and K is the Debye-Huckel screening constant. More recently, Allnatt et al. (1972) pointed out that the Lidiard-Debye-Huckel

approximation is only valid in the low concentration limit, and it deviates from the real values quite largely at high concentrations. Hence they employed the cluster formalism to treat the Coulomb interactions between the isolated defects, and obtained the following expression for the activity coefficient:

$$-\log \gamma = \frac{1}{2} K \frac{e^2}{\epsilon kT} (1 - 0.570 \; Ka) \tag{5.13}$$

where $a = \sqrt{2}\, a_0$, and a_0 is the anion-cation separation, where K is given by Equation (5.12). Equation (5.13) is valid for $Ka \leq 0.34$. Generally it is assumed that the activity coefficients are the same for all the charged defects, that is Equation (5.11) holds. But this is not exactly true if one considers the effective charges of the different charged defects in the crystal. The effective charges may be approximately expressed by the ionicities (amounts of ionic character) of the charged defects in the crystal field. Because, at present, there is no better way to calculate the effective charges of the substitutional divalent cations in the NaCl lattice, the idea of ionicity seems to be the only tool to evaluate the effective charges of the ions. Then replacing the electronic charge e by the effective charge ef_i, the expressions for the K's are rewritten as

$$K_0^2 = \frac{4\pi e^2 \chi_c}{\epsilon kT a_0^3} \tag{5.14}$$

$$K_1^2 = \frac{4\pi e(ef_1)\chi_c}{\epsilon kTa_0^3} \tag{5.15}$$

$$K_2^2 = \frac{4\pi e(ef_2)\chi_c}{\epsilon kTa_0^3} \tag{5.16}$$

where K_0 is the Debye-Huckel screening constant for both anion- and cation-vacancy, and K_1 and K_2 are those for impurity 1 and impurity 2. The f_1 and f_2 are ionicities for impurity 1 and impurity 2, respectively, and v in Equation (5.13) was replaced by $2a_0^3$. In Equation (5.14) the ionicities of anion- and cation-vacancy are assumed to be unity. By using the Allnatt et al. form (5.13) the activity coefficients of the charged defects are represented by

$$-\log \gamma_0 = \frac{1}{2} K_0 \frac{e^2}{\epsilon kT}(1-0.570\ K_0 a) \tag{5.17}$$

$$-\log \gamma_1 = \frac{1}{2} K_1 \frac{e(ef_1)}{\epsilon kT}(1-0.570\ K_1 a) \tag{5.18}$$

$$-\log \gamma_2 = \frac{1}{2} K_2 \frac{e(ef_2)}{\epsilon kT}(1.0570\ K_2 a) \tag{5.19}$$

where γ_0 is the activity coefficient of both anion- and cation-vacancy, and γ_1 and γ_2 are those of impurity 1 and impurity 2, respectively. Now Equations (5.8), (5.9) and (5.10) can be

written as follows:

$$\chi_c \chi_a = \exp(-\frac{\Delta G_s}{kT}) \exp(\frac{\delta_0}{kT}) \tag{5.20}$$

$$\frac{\chi_{k1}}{\chi_c(c_1 - \chi_{k1})} = 12 \exp(\frac{-\Delta G_{k1}}{kT}) \exp(\frac{-\delta_1}{kT}) \tag{5.21}$$

$$\frac{\chi_{k2}}{\chi_c(c_2 - \chi_{k2})} = 12 \exp(\frac{-\Delta G_{k2}}{kT}) \exp(\frac{-\delta_2}{kT}) \tag{5.22}$$

where

$$\delta_0 = -kT \log_e \gamma_0^2 \tag{5.23}$$

$$\delta_1 = -kT \log_e \gamma_0 \gamma_1 \tag{5.24}$$

$$\delta_2 = -kT \log_e \gamma_0 \gamma_2 \tag{5.25}$$

Here δ_i is a correction factor to the effective free energy ΔG_i. In the computations, values of the lattice constant a_0 for KCl and NaCl were corrected for the thermal expansion. The equations used were

$$a_0 = 3.1466 \times 10^{-8}[1+(34.94+0.01719T) \times 10^{-6}(T-25)] \quad \text{cm}$$

for KCl (Enck et al., 1962) and

$$a_0 = 2.8194 \times 10^{-8}[1+(3.836\times10^{-5}+2.979\times10^{-8}T+1.167\times10^{-11}T^2)(T-20)]$$

for $T \leq 550°C$ or

$$a_0 = 2.8194 \times 10^{-8}[1+(6.594\times10^{-5}-7.499\times10^{-8}T+1.100\times10^{-10}T^2)(T-20)]$$

for $T > 550°C$ for NaCl (Enck and Dommel, 1965). Temperatures are all in °C.

Values of the dielectric constant were corrected for the temperature as follows:

$$\epsilon = 4.753 + 0.14748 \times 10^{-2}T + 0.48287 \times 10^{-7}T^2 + 0.20109 \times 10^{-3}T^3$$

for KCl (Smith, 1962) and

$$\epsilon = 5.4 + 2.7 \exp(-0.05(eV)/kT)$$

for NaCl (Rao and Smakula, 1965) where T is the temperature in °C.

In Equations (5.15) and (5.16) the ionicities f_i of divalent impurities were introduced. The usual method of estimating the ionicity f_i of a bond was developed by Pauling (1939) and it is expressed by

$$f_i = 1 - e^{-\frac{1}{4}(X_A - X_B)^2} \tag{5.26}$$

for a diatomic molecule AB, where X_A and X_B are the electronegativities of atoms A and B. This equation appears in the first edition of his book "The Nature of the Chemical Bond" along

with another equation which estimates f_i' for ions in crystals, and it is written as

$$1 - f_i' = (N/M)(1-f_i)$$

$$= (N/M)\exp[-1/4(X_A-X_B)^2]$$

This equation can be expanded as

$$f_i' = (N/M)f_i + (1-N/M) \qquad (5.27)$$

where N is the charge on the ion and M is the coordination number of an A^NB^{8-N} type crystal such as NaCl and also of an $A^N(B^{(8-N)/2})_2$ type crystal such as $SrCl_2$. In his 1960 edition he deleted the second equation (Equation 5.27). Several years ago Phillips (1970) developed a scheme to calculate f_i based on spectroscopic energies. This method is for crystals of A^NB^{8-N} composition. Then Phillips used an equation like (5.26) to calculate f_i for crystals and found that his theory gave f_i very different from Pauling's. Pauling pointed out to him that he had used the wrong expression. When Phillips used the correct Pauling's expression like (5.27) he obtained essentially the same f_i' as his theory gave.

Phillips' theory has some theoretical advantage over Pauling's, but can not be applied to AB_2 type crystals, while Pauling's can. Since the methods are in agreement for A^NB^{8-N} crystals, and

neglecting the vacancy, the impurity is like an AB_2 crystal site, we assign f_i the value it would have in an octahedral site in an AB_2 crystal. This does little to those situations where the normal impurity cation has 6 anions around it, but is possibly artificial for other cases. Then, using Pauling's equation (5.27) the ionicities $f_i'(Ca\text{-}Cl)$ and $f_i'(Sr\text{-}Cl)$ may be calculated with the values of electronegativity $X_{Ca} = 1.00$, $X_{Sr} = 0.95$ and $X_{Cl} = 3.16$ (Cotton and Wilkinson, 1966, p. 103), and $N = 2$, $M = 6$ for $CaCl_2$ and $SrCl_2$ crystals. The values of the ionicities calculated are 0.896 for $f_i'(Ca\text{-}Cl)$ and 0.902 for $f_i'(Sr\text{-}Cl)$, respectively. Other values of ionicities given in Table 1.1 were calculated in a similar manner.

The correction factors δ_1 and δ_2 to the effective free energies ΔG_{k1} and ΔG_{k2} in Equations (5.21) and (5.22) were calculated only for the NaCl experiments. In NaCl the smallest corrections to $\Delta G(Ca)$ and $\Delta G(Sr)$ were for the diffusion experiment at 517°C: 0.007 eV and 0.007 eV for $\Delta G(Ca)$ and $\Delta G(Sr)$ respectively. Note that the 517°C is not the lowest temperature among all the diffusion runs, but rather it is the lowest one among the vapor phase diffusions. The surface layer diffusions show larger corrections to $\Delta G(Ca)$ and $\Delta G(Sr)$ even at lower temperatures, because the impurity concentrations are much higher. The highest corrections to the free energies of association appeared for the highest temperature, that is 683°C. They were 0.021 eV and 0.021 eV for $\Delta G(Ca)$ and

$\Delta G(Sr)$, respectively. When all the corrected values of free energies of association $\Delta G(Ca)$ and $\Delta G(Sr)$ are plotted against the temperature, we obtain the corrected values of enthalpies and entropies for the Ca^{2+}- and Sr^{2+}-vacancy complex formation. The values calculated are $\Delta H'(Ca) = -0.572$ eV, $\Delta S'(Ca) = -2.81 \times 10^{-4}$ eV/deg, $\Delta H'(Sr) = -0.672$ eV and $\Delta S'(Sr) = -3.48 \times 10^{-4}$ eV/deg. These values can be compared with the uncorrected enthalpies and entropies, $\Delta H(Ca) = -0.572$ eV, $\Delta S(Ca) = -2\ 69 \times 10^{-4}$ eV/deg, $\Delta H(Sr) = -0.671$ eV and $\Delta S(Ca) = -3.35 \times 10^{-4}$ eV/deg. From this comparison it can be concluded that the inclusion of long-range Coulomb interactions in the mass action expressions did not change the enthalpies of the complex formation $\Delta H(Ca)$ and $\Delta H(Sr)$ significantly, but did change the entropies $\Delta S(Ca)$ and $\Delta S(Sr)$ slightly (about 4% changes). In Figure 5.1 the corrected and uncorrected ΔG's are plotted against the temperature.

It is important to estimate the effect of inclusion of Coulomb interactions among isolated defects on the diffusion coefficients $D_s(Ca)$ and $D_s(Sr)$. This was done as follows. The concentration along the profiles were corrected to the effect of Coulomb interactions through the activity coefficients. Then the corrected values of the concentrations, which are now the activities, are plotted against the distance to obtain the corrected diffusion profiles. Using the corrected

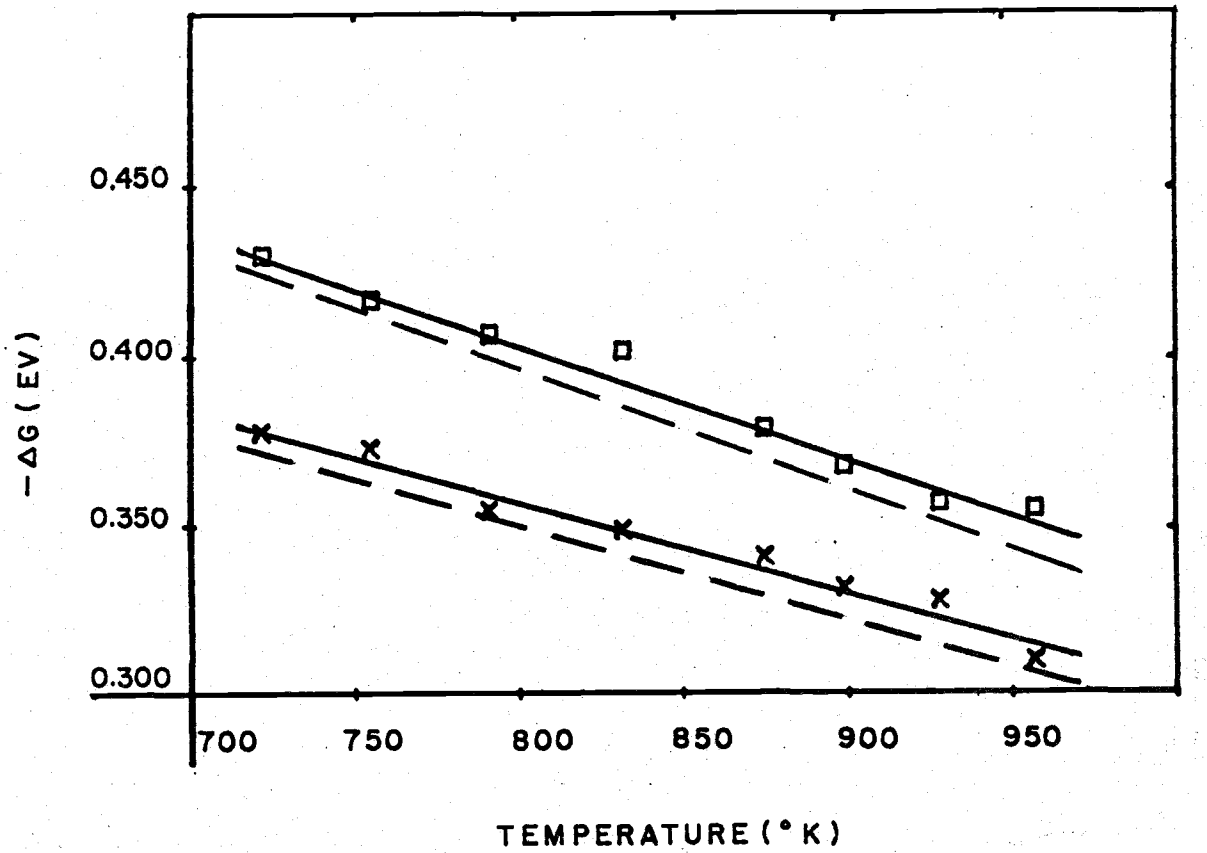

Figure 5.1. Comparison of the Gibbs free energies of association in NaCl. X:Ca^{2+}. □:Sr^{2+}. Solid lines calculated without the long-range Coulombic interactions. Dashed lines calculated with the corrections to the Coulombic interactions.

values of $\Delta G(Ca)$ and $\Delta G(Sr)$ which were obtained from the mass action equations, the new values of $D_s(Ca)$ and $D_s(Sr)$ can be determined from the corrected diffusion profiles. Figure 5.2 shows the penetration profiles of two cases at 683°C, the one without the corrections to the Coulomb interactions, and the other with the corrections. From the corrected penetration profiles the diffusion coefficients were calculated as $D'_s(Ca) = 3.79 \times 10^{-8}$ cm^2/sec and $D'_s(Sr) = 3.06 \times 10^{-8}$ cm^2/sec. These values may be compared with the uncorrected values of $D_s(Ca) = 3.84 \times 10^{-8}$ cm^2/sec and $D_s(Sr) = 3.11 \times 10^{-8}$ cm^2/sec. This shows that the inclusion of long-range Coulomb interactions did not alter the diffusion coefficients significantly.

Figure 5.3 shows the comparison of D_s vs. $1/T$ curves of the two cases. From the plot of the corrected D_s vs $1/T$ the corrected values of U' and D'_0 were obtained. They are $U'(Ca) = 0.851$ eV, $D'_0(Ca) = 1.09 \times 10^{-3}$ cm^2/sec, and $U'(Sr) = 0.926$ eV, $D'_0(Sr) = 2.28 \times 10^{-3}$ cm^2/sec. These values are compared with the uncorrected U and D_0, $U(Ca) = 0.851$ eV, $D_0(Ca) = 1.14 \times 10^{-3}$ cm^2/sec, and $U(Sr) = 0.925$ eV, $D_0(Sr) = 2.30 \times 10^{-3}$ cm^2/sec. The effect of the inclusion of Coulomb interactions on the activation energy and the pre-exponential factor was negligible in this work.

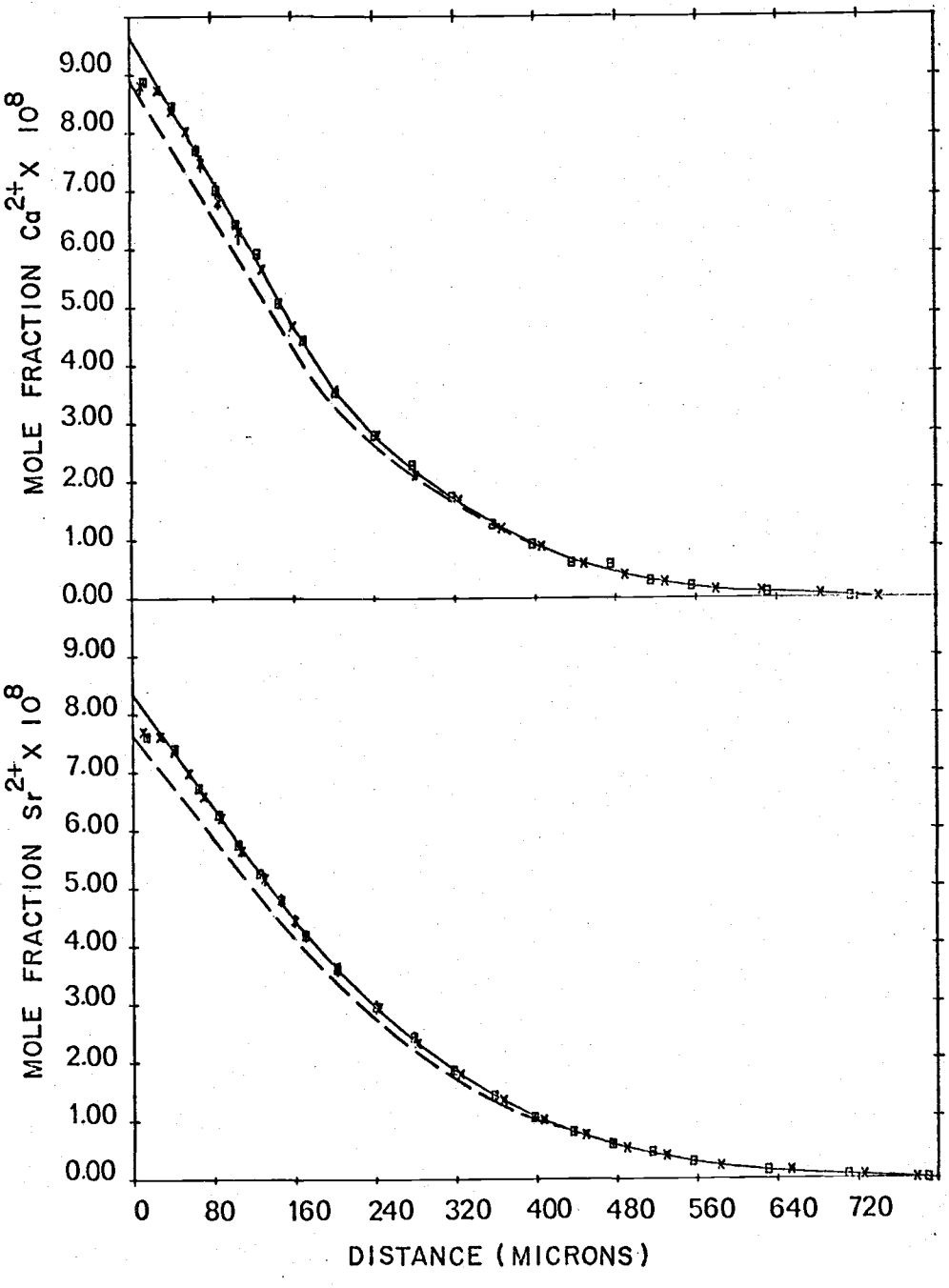

Figure 5.2. Diffusion profiles of Ca^{2+} and Sr^{2+} generated with and without the Debye-Huckel theory. Solid lines and dashed lines are profiles calculated with and without the long-range Coulombic interactions.

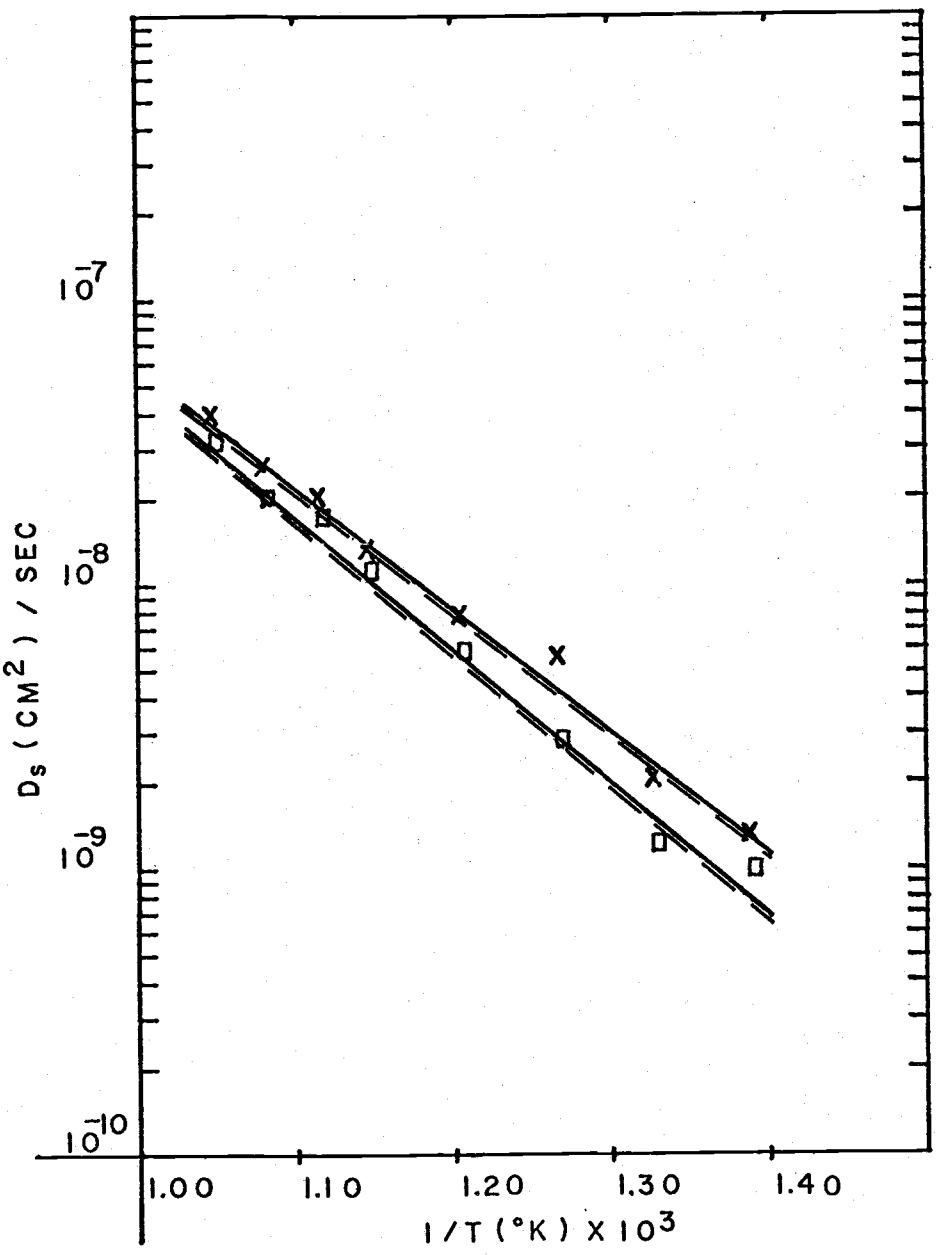

Figure 5.3. Comparison of Log D_s calculated with and without the Coulombic interactions between the isolated defects. Dashed lines are the results of the inclusion of the long-range Coulombic interactions. Solid lines are calculated without the Coulombic interactions.

In Table 5.7 the best values, that is those from experiments in which the purity of host crystals and diffusants were best and in which the experimental conditions were under best control, are given. Figures 5.4, 5.5 and 5.6 show the relationship between the activation energy of migration and the relative size of the impurity ion to the host ion. In the figures the equations which correlate the parameters and their correlation factors z are given. Figure 5.4 clearly shows the dependence of the activation energy of migration on the size of the ion, that is smaller ions need less activation energies to migrate in the crystal lattice. Figure 5.5 and 5.6 indicate rather interesting points. In NaCl the activation energies of Cd^{2+} (0.86 eV) and Ca^{2+} (0.85 eV) are very close and their ionic radii, Cd^{2+} = 0.97 Å, Ca^{2+} = 0.99 Å, are similar to that of the host ion Na^{+} (0.95 Å). On the other hand, in KCl where Cd^{2+} and Ca^{2+} replace a much bigger host ion K^{+} (1.33 Å) their activation energies differ more. In Figure 5.7 the values of activation energy are plotted against the binding energies in the impurity chlorides MCl_2. The binding energy in this case is the energy required in the reaction $MCl_2 \rightarrow MCl^{+} + Cl^{-}$. It is observed from this plot that the greater the binding energy between M^{2+} and Cl^{-} is, the more activation energy is required for M^{2+} ion to make a jump. This should be reasonable because the divalent ion M^{2+} must break bonds to the surrounding Cl^{-} ions in the NaCl crystal before it can jump to the adjacent vacancy.

Table 5.7. Values of activation energy of migration U, ionic radii and binding energies in impurity chlorides E_1.

Host	Ion	Radius (Å)[a]	$(r_i/r_h)^2$[b]	U (eV)	E_1 (eV)[c]	$(r_i-r_h)^2$[d]	References
NaCl	Cd^{2+}	0.97	1.043	0.86	2.82	0.0004	Krause and Fredericks (1971)
NaCl	Ca^{2+}	0.99	1.086	0.85	2.80	0.0016	This work
NaCl	Sr^{2+}	1.13	1.329	0.93	3.04	0.0225	This work
NaCl	Pb^{2+}	1.21	1.523	0.98	3.10	0.0529	Krause and Fredericks (1971)
NaCl	Na^{+}	0.95	---	0.65[e]	--	---	Allnatt et al. (1971)
KCl	Cd^{2+}	0.97	0.5319	0.56	2.82	0.1296	Krause and Fredericks (1973)
KCl	Ca^{2+}	0.99	0.5540	0.59	2.80	0.1156	This work
KCl	Sr^{2+}	1.13	0.7218	0.87	3.04	0.0400	This work
KCl	Pb^{2+}	1.21	0.8276	0.91	3.10	0.0144	Krause and Fredericks (1973)
KCl	K^{+}	1.33	---	0.79[e]	--	---	M. Beniere et al. (1970)

[a] Pauling radius.

[b] Square of the ratio of impurity radius to host radius.

[c] Binding energy in the reaction $MCl_2 \rightarrow MCl^+ + Cl^-$.

[d] Square root of the difference between impurity and host radii.

[e] Value of the enthalpy of the cation migration h_m^c.

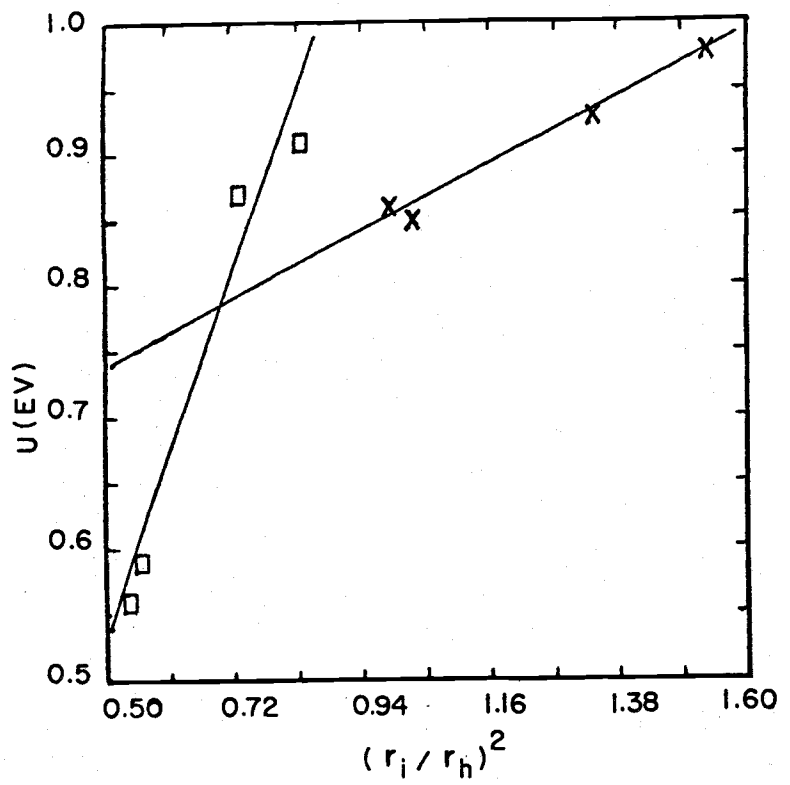

Figure 5.4. U vs. $(r_i/r_h)^2$ in NaCl and KCl.
X: NaCl. □: KCl. Straight lines are given by $U = m(r_i/r_h)^2 + b$ with
m(NaCl)=0.2349, b(NaCl)=0.6204, z=0.9910
m(KCl)=1.267, b(KCl)=-0.1023, z=0.9754
where $z=\sum_{i=1}^{n}(X_i-X)(Y_i-Y)[\sum_{i=1}^{n}(X_i-X)^2\sum_{i=1}^{n}(Y_i-Y)^2]^{-1/2}$

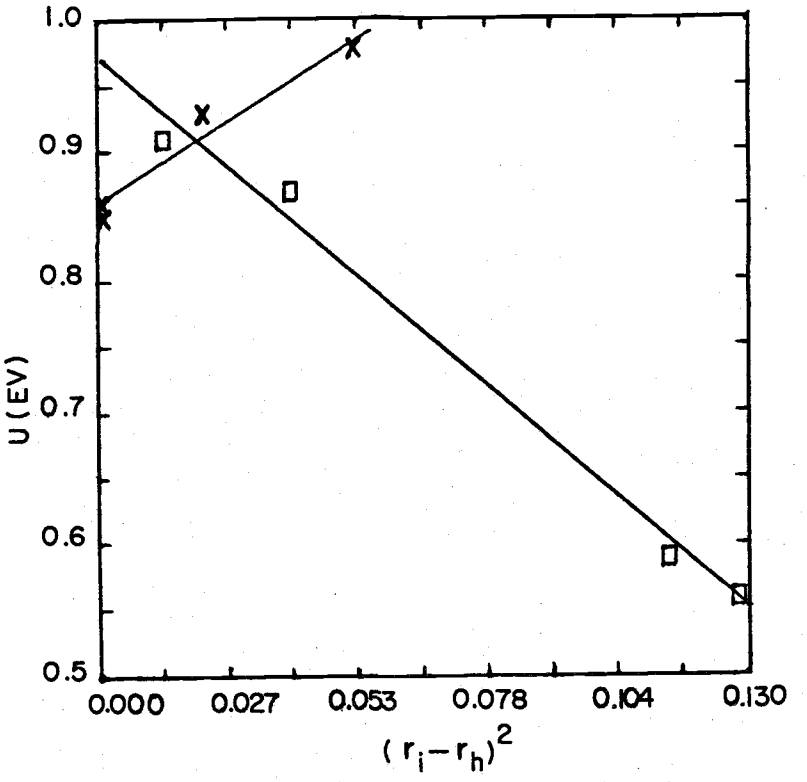

Figure 5.5. U vs. $(r_i-r_h)^2$ in NaCl and KCl.
X: NaCl. □:KCl. Straight lines are given by $U= m(r_i-r_h)^2 + b$ with
m(NaCl)=2.409, b(NaCl)=0.8594, z=0.9817
m(KCl)=-3.230, b(KCl)=0.9744, z=0.9946
where z is correlation factor as given in Figure 5.4.

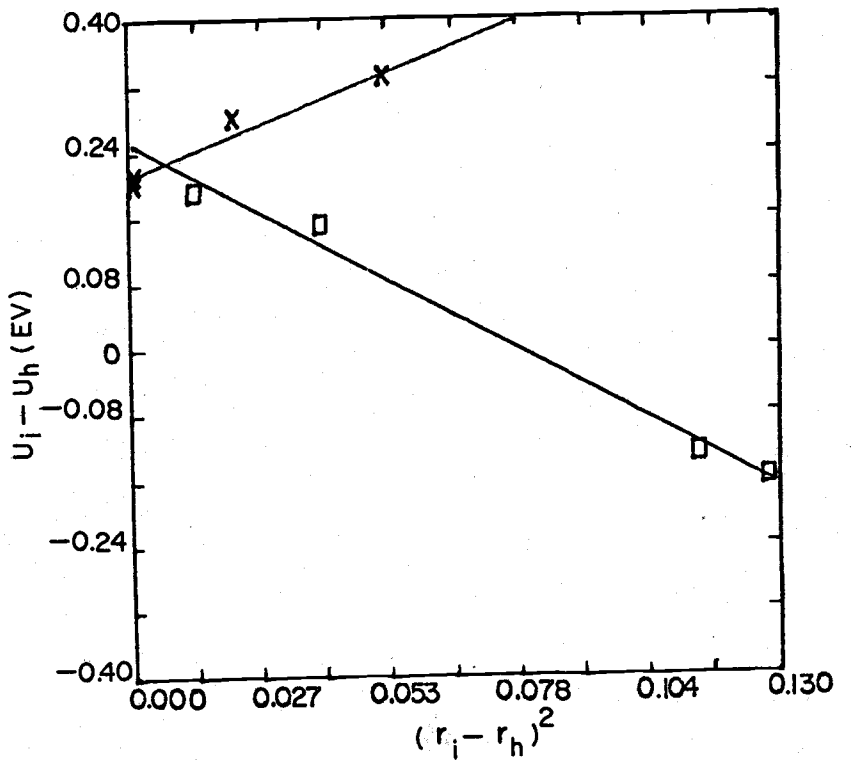

Figure 5.6. (U_i-U_h) vs. $(r_i-r_h)^2$ in NaCl and KCl. X: NaCl. □: KCl. Straight lines are given by $U_i-U_h = m(r_i-r_h)^2 + b - U_h$ with m(NaCl)=2.409, b(NaCl)=0.8594, z=0.9817 m(KCl)=-3.230, b(KCl)=0.9744, z=0.9946 where z is correlation factor as given in Figure 5.4.

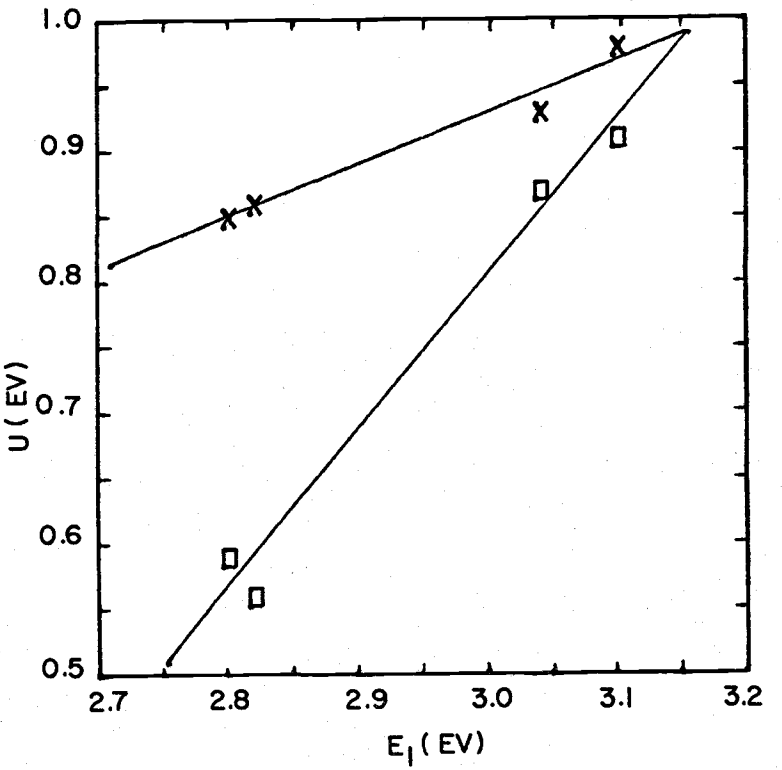

Figure 5.7. U vs. E_l in NaCl and KCl. X: NaCl. □:KCl. Straight lines are given by $U = mE_l + b$ with m(NaCl)=0.3966, b(NaCl)=-0.2609, z=0.9841 m(KCl)=1.190, b(KCl)=-2.765, z=0.9901 where z is correlation factor as given in Figure 5.4.

VI. CONCLUSIONS

Association parameters calculated from the experimental results of simultaneous diffusion of Ca^{2+} and Sr^{2+} in NaCl and KCl crystals compare favorably with most of the enthalpies, ΔH, and entropies, ΔS, of the complex formation given in Tables 5.3, 5.4, 5.5 and 5.6. For example, (see Table 5.3) the enthalpy ΔH of Ca^{2+}-vacancy complex formation in NaCl is in excellent agreement with the results of F. Beniere et al. (1969) which was obtained from well-controlled ionic conductivity experiments.

The values of the entropy of association, ΔS, in the present work appear to be of the same order of magnitude with other experimental results. Values of ΔS calculated from the empirical equation (5.7) agree very well with the results of this work, as do the values calculated from the simple model (Tables 5.3, 5.4, 5.5 and 5.6).

The effect of long-range Coulombic interactions among unassociated defects on the association parameters ΔH and ΔS and the transport parameters D_s, D_0 and U was shown to be very small Hence I conclude that for comparison of these parameters when obtained from diffusion data it is valid to neglect long-range Coulombic interactions if the impurity and free vacancy concentrations do not exceed those encountered in this work.

The importance of the size of the ion, the impurity-Cl^- binding energy, and the ionicity f_i on the activation energy U was considered. It was shown that a number of empirical relations between the relative size of the ion and the activation energy fit the data equally well. Therefore, it is not so obvious which relation among those is best to correlate these parameters at this point. The binding energy for the first Cl^- in MCl_2, that is the energy involved in the reaction $MCl_2 \rightarrow MCl^+ + Cl^-$, correlates with the activation energy U very well (see Figure 5.7). However, the correlation between the activation energy and the binding energy for the second Cl^-, that is the energy in the reaction $MCl^+ \rightarrow M^{2+} + Cl^-$, simply does not exist. The relation between the ionicity f_i and the activation energy U was examined, but no correlation seems to exist between these parameters.

In Figures 5.4, 5.5, 5.6 and 5.7, although experimental points fit the empirical equations quite well (see the values of the correlation factor, z, in the figures), only four points are plotted. In order to substantiate these correlations more data are necessary, especially those of much smaller divalent ions and much larger ions. Possible ions would be Be^{2+} (0.31 Å) for a smaller ion and Ba^{2+} (1.35 Å) for a larger ion. These are feasible experiments because both are available in suitable radioactive isotopes ($^{7}_{4}Be(t_{1/2} = 53.3d)$, $^{133}_{56}Ba(t_{1/2} = 10.7y)$) The small ion may require the inclusion of next nearest neighbor complexes as well as nearest neighbor complexes.

BIBLIOGRAPHY

Allen, C A., Ireland, D.T. and Fredericks, W.J (1967). J. Chem. Phys. Vol. 47:3068-3072.

Allen, C.A. and Fredericks, W.J. (1973). Phys. Status Solidi. Vol. 55b:615.

Allnatt, A.R. and Pantelis, P. (1968). Trans. Faraday Soc. Vol. 64: 2100.

Alnatt, A R., Pantelis, P., and Sime, S.J. (1971). Proc. Phys. Soc. London (Solid State Phys.). Vol. 4:1778.

Allnatt, A.R., Loftus, E., and Rowley, L.A. (1972). Crystal Lattice Defects. Vol. 3:77-82.

Banasevich, S.N., Lure, B.G., and Murin, A.N. (1960). Sov. Phys. - Solid State. Vol. 2:72.

Barr, L.W. and Lidiard, A.B. (1970). Defects in Ionic Crystals, in "Physical Chemistry" (H. Eyring, D. Henderson, and W. Jost, eds.), Vol. X. Academic Press, New York.

Bassani, F. and Fumi, F.G. (1954). II Nuovo Cimento. Vol. 11:274-284.

Beaumont, J.H. and Jacobs, P.W.M. (1966). J. Chem. Phys. Vol. 45:1496.

Beniere, F., Beniere, M., and Chemla, M. (1969). C.R. Acad. Sci. Paris. Vol. 268:1461.

Beniere, F., Beniere, M., and Chemla, M. (1970). J. Phys. Chem. Solids. Vol. 31:1205.

Beniere, M , Beniere, F., and Chemla, M. (1970). J. Chem. Phys. Vol. 67:1312.

Beniere, F. (1970). Thesis, Univ. of Paris, Orsay.

Beniere, F. (1972). Diffusion in Ionic Crystals, in "Physics of Electrolyties" (J. Hladik, ed.), p. 203. Academic Press, New York.

Beniere, M. (1974). Thesis, University of Paris.

Brown, N. and Hoodless, L.M. (1967). J. Phys. Chem. Solids. Vol. 28:2297.

Chandra, S. and Rolfe, J. (1970). Can. J. Phys. Vol. 48:412.

Chemla, M. (1956). Ann. Phys. (Paris). Vol. 1:959

Cotton, F.A. and Wilkinson, G. (1966). Advanced Inorganic Chemistry. A Comprehensive Text. 2nd ed. Interscience Publishers. New York.

Crank, J.C. (1970). The Mathematics of Diffusion. Oxford University Press, London.

Dreyfus, R.W (1961). Phys Rev. Vol. 121:1675.

Dusinberre, G.M. (1961). Heat-Transfer Calculations by Finite Differences. P. 14. International Textbook.

Enck, F.D., Engle, D.G., and Marks, K.I. (1962). J. Appl. Phys. Vol. 33:2070.

Enck, F.B. and Dommel, J.G. (1965). J. Appl. Phys. Vol. 36:839-844.

Etzel, H.W. and Mauerer, R.J. (1950). J. Chem. Phys Vol. 18: 1003.

Faux, I.D. and Lidiard, A.B. (1971). Z. Naturforsch. Vol. 26a:62-68.

Franklin, W.M. (1972). J. Chem. Phys. Vol. 57:2659.

Fredericks, W.J., Scheurman, L.W., and Lewis, L.C. An investigation of crystal growth processes. Corvallis, 1966. Oregon State University, Dept. of Chemistry. Final reports on Air Force Contracts AF-AFOSR-217-73 and AF-AFOSR-217-66)

Fredericks, W.J. (1975). Diffusion in Alkali Halides, in "Diffusion in Solids. Recent Developments." (A.S. Nowick and J.J. Burton, eds.) p. 381. Academic Press, Inc., San Francisco.

Fuller, R.G., Marquardt, C.L., Reilly, M.H., and Wells, J.C., Jr. (1968). Phys. Rev. Vol. 176:1036.

Fuller, R.G. (1972). Ionic Conductivity (Including Self-Diffusion), in "Point Defects in Solids" (J.H. Crawford, Jr., and L.M. Slifkin, eds.), Vol. I, p. 103. Plenum, New York.

Fumi, F.G. and Tosi, M.P. (1964). J. Phys. Chem. Solids. Vol. 25:31-43.

Gie, T.I. and Klein, M.V. (1963). Infrared and ultra violet OH bands in hydroxide-doped KCl, KBr, NaCl and NaBr. Bulletin of the American Physical Society. Vol 8:230.

Grundig, H. (1960). Z. Phys. Vol. 158:577.

Howard, R.E. and Lidiard, A.B. (1964). Rep. Progr. Phys. Vol. 27:161-240.

Hutchison, D.A. (1944). Phys. Rev. Vol. 66:144.

Jacobs, P.W M. and Pantelis, P. (1971). Phys. Rev. B. Vol. 4:3757.

Kanzaki, H., Kido, K., Tamura, S., and Oki, S. (1965). J. Phys. Soc. Japan. Vol. 20:2305.

Keneshea, F.J. and Fredericks, W.J. (1963). J. Chem. Phys. Vol. 38:1952.

Keneshea, F.J. and Fredericks, W.J. (1964). J. Chem. Phys. Vol. 41:3271.

Keneshea, F.J. and Fredericks, W.J. (1965). J. Phys. Chem. Solids. Vol. 26:501-508.

Keyes, R.W. (1958). J. Chem. Phys. Vol. 29:467-475.

Krause, J.L. An Investigation of the Simultaneous Diffusion of Pb^{2+} and Cd^{2+} in NaCl Crystals and KCl Crystals. Ph.D. thesis. Corvallis, Oregon State University, 1970. 89 numb. leaves.

Krause, J.L. and Fredericks, W.J. (1971). The simultaneous diffusion of Pb^{2+} and Cd^{2+} in Purified NaCl single crystals. J. Phys. Chem. Solids. Vol. 32:2673.

Krause, J.L. and Fredericks, W.J. (1973). J. Phys. (Paris). Vol. 34 (Suppl. 11-12):C9-25.

Lantsberry, F.C.A.H. and Page, R.A. (1920). J. Soc. Chem. Ind. Vol. 39:371. (Cited in: Levin, E.M., Robbins, C.R., and McMurdie, H.F. Phase Diagrams for Ceramists. American Ceramic Society, Columbus, Ohio, 1964)

Laredo, E. and Dartyge, E. (1970). J. Chem. Phys. Vol. 53:2214.

Lawson, A.W. (1957). J. Phys. Chem. Solids. Vol. 3:250-252.

LeClaire, A.D., "Correlation Effects in Diffusion in Solids," Chapter 6 in Physical Chemistry - An Advanced Treatise (Academic Press, New York, 1970), Vol. X.

Lidiard, A.B. (1957). Ionic conductivity. Handbuch der Physik Vol. 20:246-349

Mannion, W.A., Allen, C.A., and Fredericks, W.J. (1968). J. Chem. Phys. Vol. 48:5137-1540.

Martin, G., Lazarus, D., and Mitchell, J.L. (1973). Phys. Rev. B. Vol. 8:1726.

Menge, O. (1911). Z. Anorg. Chem. Vol. 72:162.

Murin, A.N., Banasevich, S.N., and Grushko Yu. S. (1962). Sov. Phys. Solid State. Vol. 3:1762.

Nowick, A.S. (1972). Defect Mobilities in Ionic Crystals Containing Aliovalent Ions, in "Point Defects in Solids" (J.H. Crawford, Jr., and L.M. Slifkin, eds.), Vol. I, p. 151. Plenum, New York.

Pauling, L. (1939). The nature of the chemical bond. 1st ed.

Pauling, L. (1960). The nature of the chemical bond. 3rd ed. Ithaca, Cornell University.

Phillips, J.C. (1970). Rev. Mod. Phys. Vol. 42:317-356.

Rane, A.T. and Bhatki, K.S. (1966). Rapid Radiochemical Separations of Strontium-90-Yttrium-90 and Calcium-45-Scandium-46 on a Cation Exchange Resin. Analytical Chemistry Vol 38, No. 11:1598.

Rao, K.K. and Smakula, A. (1965) J. Appl. Phys. Vol 36:3953.

Rosenbrock, H.H. (1960). The Computer Journal. Vol. 3:175.

Rothman, S.J., Peterson, N.L., Laskar, A.L., and Robinson, L.C. (1972). J. Phys. Chem. Solids. Vol. 33:1061.

Sandonnini, C. (1914). Gazz. Chim. ital. Vol. 44 I:335. (Cited in Levin, E.M., Robbins, C.R., and McMurdie, H.F. Phase Diagrams for Ceramists. American Ceramic Society, Columbus, Ohio, 1964).

Schmidt, E. (1924). Foppls Festshrift. Springer. 179 p. (Cited in: Crank, J. The Mathematics of Diffusion. London, Oxford University, 1970. p. 187).

Shoemaker, D.P. and Garland, C.W. (1967). Experiments in Physical Chemistry. McGraw-Hill. New York

Slifkin, L. and Brebec, G. (1968). Rep. CEA-DM/1750.

Smith, G.C. (1962). Materials Science Center Report, No. 51, Cornell.

Stasiw, O. and Teltow, J. (1947). J. Ann. Phys. (Leipzig). Vol.1: 261.

Table of Isotopes. Lederer, C.M., Hollander, J.M., and Perlman, I. 6th ed. New York, Wiley (1967). 594 p.

Tosi, M.P. (1964). Cohesion of Ionic Solids in the Born Model, in Solid State Phys. Volume 16.

Vendeneyev, V.I. (1966). Bond Energies, Ionization Potentials and Electron Affinities. St. Martin's Press. New York.

Vortisch, E. (1914). Neues Jahrb. Mineral, Geol. Vol. 38:220. (Cited in: Levin, E.M., Robbins, C.R., and McMurdie, H.F. Phase Diagrams for Ceramists. American Ceramic Society, Columbus, Ohio, 1964)

Wang, C.H. and Willis, D.L. (1965). Radiotracer methodology in biological science. Englewood Cliffs, N.J., Prentice-Hall. 382 p.

Watkins, G.D. (1959). Phys. Rev. Vol. 113:79.

Wells, A.F. (1962). Structural Inorganic Chemistry. 3rd ed., Oxford at The Clarendon Press.

Wert, C. and Zener, C. (1949). Phys. Rev. Vol. 76:1169.

APPENDIX

APPENDIX I

Raw Data for Diffusion Experiments in KCl and NaCl

A* has units of counts per minute.

KCl 451°C $t_t = 4.2876 \times 10^5$ sec.

For $CaCl_2$: $V_t = 0.250$ ml; $C_c = 2.010$ mg/ml; $V_c = 0.050$ ml

For $SrCl_2$: $V_t = 0.250$ ml; $C_c = 1.263$ mg/ml; $V_c = 0.100$ ml

	Crystal A, Area = 0.7422 cm^2			Crystal B, Area = 0.7673 cm^2		
	w (mg)	A*(^{45}Ca)	A*(^{85}Sr)	w (mg)	A*(^{45}Ca)	A*(^{85}Sr)
1.	5.625	194757	190436	5.237	188530	183732
2.	0.627	18521	14438	1.693	48952	37432
3.	5.793	164829	117985	1.233	35595	26849
4.	2.824	78544	50895	2.889	81123	59809
5.	2.683	72165	43621	2.838	78933	53239
6.	3.743	98796	52997	1.857	49786	32680
7.	3.746	95083	46514	3.943	103244	61376
8.	2.930	73374	29970	2.752	69551	37982
9.	4.441	106690	36102	1.556	37731	20191
10.	3.840	88958	24871	1.471	34700	16230
11.	9.939	214787	46391	4.515	99584	41543
12.	7.159	139134	22065	2.722	55690	23587
13.	12.125	199710	24913	3.715	65484	24974
14.	15.095	172173	8194	3.118	46392	14764
15.	15.367	159158	8105	6.802	75286	20205
16.	12.556	103190	3928	7.103	65318	14437
17.	10.891	61634	1218	2.411	15021	2640
18.	12.724	51338	286	9.786	33327	4591
19.	12.585	10630	283	8.323	9910	1861
20.	10.432	241		4.902	146	112
Background		52	2		52	2
Ca 0.002 ml		51504			51504	
Ca 0.010 ml		258345			258345	
Sr 0.005 ml			132658			132658
Sr 0.010 ml			265272			265272

KCl 504°C $t_t = 2.6700 \times 10^5$ sec.

For $CaCl_2$: $V_t = 0.250$ ml; $C_c = 2.010$ mg/ml; $V_c = 0.050$ ml

For $SrCl_2$: $V_t = 0.250$ ml; $C_c = 1.263$ mg/ml; $V_c = 0.100$ ml

	Crystal A, Area = 0.6741 cm^2			Crystal B, Area = 0.6848 cm^2		
	w (mg)	A*(^{45}Ca)	A*(^{85}Sr)	w (mg)	A*(^{45}Ca)	A*(^{85}Sr)
1.	4.612	98056	74199	3.225	72254	50733
2.	0.169	2899	2224	2.125	36391	28266
3.	5.152	84455	62959	2.345	38756	28951
4.	1.065	17101	11789	4.412	70208	49857
5.	6.393	99022	64076	1.546	24446	16215
6.	2.627	38954	21943	4.122	64053	39437
7.	4.210	61785	30200	2.497	37506	21147
8.	3.793	53728	22940	3.606	51908	27124
9.	4.598	62590	21524	2.530	35642	16296
10.	5.387	69123	18913	3.005	41430	16269
11.	9.537	116722	25389	6.673	88773	28554
12.	5.352	60168	9898	5.912	71472	19964
13.	7.260	74166	8498	4.933	49883	11459
14.	7.331	61727	6027	3.763	34499	4977
15.	8.329	55549	3052	5.154	42546	4468
16	8.663	40961	1472	5.133	32175	2340
17.	9.220	31755	826	5.620	26033	1458
18.	9.139	12692	84	7.144	21778	704
19.	10.486	2296		7.091	11972	65
20.	10.421	132		7.553	2649	
21.				8.032	113	
Background		52	2		52	2
Ca 0.002 ml		51504			51504	
Ca 0.010 ml		258345			258345	
Sr 0.005 ml			132658			132658
Sr 0.010 ml			265272			265272

KCl 558°C $t_t = 4.1430 \times 10^5$ sec.

For $CaCl_2$: $V_t = 0.250$ ml; $C_c = 2.010$ mg/ml; $V_c = 0.050$ ml

For $SrCl_2$: $V_t = 0.250$ ml; $C_c = 1.263$ mg/ml; $V_c = 0.100$ ml

	Crystal A, Area = 0.7907 cm^2			Crystal B, Area = 0.7896 cm^2		
	w (mg)	A*(^{45}Ca)	A*(^{85}Sr)	w (mg)	A*(^{45}Ca)	A*(^{86}Sr)
1.	1.033	3811	1138	1.668	6273	1882
2.	2.524	9218	2733	1.236	4648	1391
3.	1.821	5780	1327	2.117	6796	1645
4.	1.806	5571	1257	1.395	4357	959
5.	1.318	4019	862	1.911	5856	1257
6.	2.523	7482	1577	2.206	6544	1367
7.	3.349	9674	1859	3.032	8783	1775
8.	0.960	2739	515	2.914	8124	1496
9.	2.217	6089	1073	2.817	7540	1308
10.	2.150	5699	897	2.485	6463	967
11.	1.946	5146	803	2.997	7549	1012
12.	2.112	5394	774	4.545	10831	1210
13.	3.424	8399	1064	4.238	9654	908
14.	5.784	13272	1219	4.602	9700	717
15.	6.117	12625	832	5.951	10943	486
16.	9.414	16039	539	9.468	13300	375
17.	9.062	10741	100	8.800	8432	115
18.	9.156	6602	62	8.806	3770	3
19.	9.427	2014	3	9.092	599	
20.	8.838	60		9.162	61	
Background		52	2		52	2
Ca 0.002 ml		51504			51504	
Ca 0.010 ml		258345			258345	
Sr 0.002 ml			60160			60160
Sr 0.005 ml			150299			150299

KCl 572°C $t_t = 6.3120 \times 10^5$ sec.

For $CaCl_2$: $V_t = 6$ ml; $C_c = 2.515$ mg/ml; $V_c = 0.100$ ml

For $SrCl_2$: $V_t = 6$ ml; $C_c = 1.437$ mg/ml; $V_c = 0.100$ ml

	Crystal A, Area = 0.9961 cm^2			Crystal B, Area = 0.8694 cm^2		
	w (mg)	A*(^{45}Ca)	A*(^{85}Sr)	w (mg)	A*(^{45}Ca)	A*(^{85}Sr)
1.	5.234	8999	2170	4.815	7758	2020
2.	0.764	1198	288	0.758	1159	281
3.	0.278	442	104	1.356	2002	475
4.	2.812	4060	945	2 080	2929	640
5.	1.595	2189	468	2.784	3601	724
6.	2.645	3378	679	2.060	2464	444
7.	1.786	2133	414	1.965	2185	349
8.	2.251	2551	406	1.749	1829	252
9.	2..663	2757	366	1 658	1589	181
10.	2.520	2360	278	2.033	1777	180
11.	5.025	3992	312	3 701	2742	211
12.	3.547	2159	111	3.477	2037	91
13.	3.929	1987	63	4.300	1912	36
14.	4.667	1714	22	4.455	1446	12
15.	8.648	1883	3	4.378	890	3
16.	8.469	717		6.343	639	
17.	8.332	185		6.639	117	
18	9.638	34		7.211	33	
Background		29	2		29	2
Ca 0.005 ml		75214			75214	
Ca 0.010 ml		150702			150702	
Sr 0.005 ml			57889			57889
Sr 0.010 ml			115094			115094

KCl 595°C $t_t = 8.5950 \times 10^5$ sec.

For $CaCl_2$: $V_t = 3$ ml; $C_c = 2.010$ mg/ml; $V_c = 0.100$ ml

For $SrCl_2$: $V_t = 3$ ml; $C_c = 1.263$ mg/ml; $V_c = 0.100$ ml

	Crystal A, Area = 1.0326 cm^2			Crystal B, Area = 1.1387 cm^2		
	w (mg)	A*(^{45}Ca)	A*(^{85}Sr)	w (mg)	A*(^{45}Ca)	A*(^{85}Sr)
1.	9.516	1674	609	5.711	881	382
2.	3.024	494	150	1.700	275	106
3.	2.341	364	96	3.032	445	171
4.	1.665	257	59	3.715	508	176
5.	3.746	483	105	3.227	407	128
6.	2.551	313	51	4.129	460	132
7.	2.758	306	45	3.832	389	82
8.	3.462	333	40	2.882	282	48
9.	3.302	275	20	3.664	298	46
10.	3.484	244	14	3.362	239	25
11.	4.663	254	9	5.171	297	20
12.	6.123	237	3	4.456	202	6
13.	3.830	112	3	6.066	203	3
14.	4.786	98		5.898	84	
15.	10.435	70		10.668	95	
16.	10.229	40		10.297	49	
17.	9.963	31		10.330	31	
Background		20	2		29	2
Ca 0.002 ml		41735			41735	
Ca 0.010 ml		187969			187969	
Sr 0.002 ml			32917			32917
Sr 0.005 ml			82229			82229

KCl 602°C $t_t = 5.5272 \times 10^5$ sec.

For $CaCl_2$: V_t = 1 ml; C_c = 2.010 mg/ml; V_c = 0.050 ml

For $SrCl_2$: V_t = 1 ml; C_c = 1.263 mg/ml; V_c = 0.250 ml

	Crystal A, Area = 0.6033 cm^2			Crystal B, Area = 0.9667 cm^2		
	w (mg)	A*(^{45}Ca)	A*(^{85}Sr)	w (mg)	A*(^{45}Ca)	A*(^{85}Sr)
1.	1.834	823	621	4.795	1755	963
2.	2.155	966	456	3.500	1224	602
3.	1.299	568	243	2.187	724	318
4.	1.858	736	298	3.022	894	367
5.	1.921	701	251	2.953	785	275
6.	2.253	717	213	2.808	639	208
7.	1.830	529	129	3.007	627	153
8.	2.354	574	104	2.854	534	99
9.	1.667	361	49	3.229	514	66
10.	2.140	390	37	2.372	370	23
11.	2.229	320	14	3.817	411	9
12.	4.427	398	4	3.351	278	4
13.	3.022	161	4	3.783	225	4
14.	3.990	113		5.400	184	
15.	4.330	53		7.485	82	
16.				7.339	53	
Background		52	2		52	2
Ca 0.002 ml		51504			51504	
Ca 0.010 ml		258345			258345	
Sr 0.005 ml			132658			132658
Sr 0.010 ml			265272			265272

KCl 669°C $t_t = 5.0580 \times 10^5$ sec

For $CaCl_2$: V_t = 1 ml; C_c = 2.010 mg/ml; V_c = 0.050 ml

For $SrCl_2$: V_t = 1 ml; C_c = 1.263 mg/ml; V_c = 0.250 ml

	Crystal A, Area = 0.776 cm^2			Crystal B, Area = 0.7027 cm^2		
	w (mg)	A*(^{45}Ca)	A*(^{85}Sr)	w (mg)	A*(^{45}Ca)	A*(^{85}Sr)
1.	3.160	2223	195	4.815	3512	267
2.	4.036	2851	227	3.684	2579	187
3.	4.829	3170	218	3.892	2421	160
4.	3.703	2157	131	3.599	1980	111
5.	4.636	2415	120	4.284	2034	88
6.	4.180	1806	67	3.863	1575	54
7.	3.826	1441	41	3.912	1339	29
8.	4.345	1300	27	3.877	1000	16
9.	4.139	968	13	3.871	760	10
10.	4.647	831	5	3.864	552	6
11.	6.080	682	3	4.257	438	4
12.	6.115	360	3	4.967	289	3
13.	5.885	236		4.728	198	3
14.	9.627	144		7.795	144	
15.	10.209	56		10.741	56	
Background		52	2		52	2
Ca 0.002 ml		51504			51504	
Ca 0.010 ml		258345			258345	
Sr 0.005 ml			132658			132658
Sr 0.010 ml			265272			265272

NaCl 448°C $t_t = 6.89820 \times 10^5$ sec.

For $CaCl_2$: $V_t = 0.250$ ml; $C_c = 1.999$ mg/ml; $V_c = 0.050$ ml

For $SrCl_2$: $V_t = 0.250$ ml; $C_c = 1.277$ mg/ml; $V_c = 0.100$ ml

	Crystal A, Area = 0.6497 cm^2			Crystal B, Area = 0.6103 cm^2		
	w (mg)	A*(^{45}Ca)	A*(^{85}Sr)	w (mg)	A*(^{45}Ca)	A*(^{85}Sr)
1.	1.913	3905	3020	2.299	5894	3581
2.	0.760	1201	922	2.590	3432	2921
3.	2.363	3206	2639	0.238	334	248
4.	1.407	1674	1455	2.458	2702	2414
5.	1.941	2062	1872	5.021	4787	4559
6.	4.445	3538	3651	2.511	2161	2140
7.	1.339	910	990	5.814	4183	4523
8.	3.404	1805	2262	1.850	1208	1340
9	3.489	1187	1630	3.832	1586	2103
10.	3.179	559	853	2.616	607	921
11.	3.320	205	460	3.779	375	705
12.	3.629	105	142	1.123	102	137
13	3 038	63	26	3.541	144	252
14.	4.023	60	9	2.669	62	32
15.				5.550	62	20
Background		54	2		54	2
Ca 0.002 ml		59691			59691	
Ca 0.005 ml		149183			149183	
Sr 0.002 ml			60413			60413
Sr 0.005 ml			150912			150912

NaCl 481°C $t_t = 6.91680 \times 10^5$ sec.

For $CaCl_2$: $V_t = 0.250$ ml; $C_c = 1.999$ mg/ml; $V_c = 0.050$ ml

For $SrCl_2$: $V_t = 0.250$ ml; $C_c = 1.277$ mg/ml; $V_c = 0.100$ ml

	Crystal A, Area = 0.7369 cm^2			Crystal B, Area = 0.5329 cm^2		
	w (mg)	A*(^{45}Ca)	A*(^{85}Sr)	w (mg)	A*(^{45}Ca)	A*(^{85}Sr)
1.	3.031	23214	9232	2.169	16418	6503
2.	3.414	20116	8602	3.208	18482	7919
3.	4.021	21771	9227	3.070	16128	6844
4.	4.308	21249	9047	2.862	14056	5888
5.	4.818	21634	9004	2.769	12269	5207
6.	4.563	17800	7713	3.070	12416	5170
7.	6.063	19968	8421	2.839	10003	4220
8.	6.286	16813	7127	2.884	8932	3735
9.	6.222	12453	5120	4.593	11353	5062
10.	6.286	7742	3439	4.039	7658	3157
11.	6.288	3727	1997	4.385	4574	2323
12.	6.328	1445	749	4.570	2662	1226
13.	6.637	236	140	4.454	789	506
14.	5.999	95	21	4.523	209	89
15.				4.731	74	25
Background		54	2		54	2
Ca 0.002 ml		57812			57812	
Ca 0.005 ml		144790			144790	
Sr 0.002 ml			60099			60099
Sr 0.005 ml			149973			149973

NaCl 517°C $t_t = 1.28478 \times 10^5$ sec.

For $CaCl_2$: $V_t = 3$ ml; $C_c = 1.999$ mg/ml; $V_c = 0.005$ ml

For $SrCl_2$: $V_t = 3$ ml; $C_c = 1.277$ mg/ml; $V_c = 0.025$ ml

	Crystal A, Area = 0.7381 cm^2			Crystal B, Area = 0.8488 cm^2		
	w (mg)	A*(^{45}Ca)	A*(^{85}Sr)	w (mg)	A*(^{45}Ca)	A*(^{85}Sr)
1.	4.187	2586	1068	6.101	3593	1473
2.	7.990	4240	1690	2.821	1503	589
3.	2.493	1211	471	3.087	1520	605
4.	1.694	722	265	2.095	895	336
5.	2.333	828	291	3.859	1278	469
6.	2.141	591	192	3.438	957	318
7.	1.662	383	109	5.196	891	265
8.	5.785	770	217	3.889	456	127
9.	1.023	113	24	4.946	505	97
10.	6.648	356	62	4.617	252	52
11.	5.119	146	26	6.248	187	38
12.	5.524	63	23	6.983	88	29
13.	5.630		22	6.873	63	15
14.				6.446		12
Background		53	2		53	2
Ca 0.002 ml		58063			58063	
Ca 0.005 ml		144873			144873	
Sr 0.002 ml			59984			59984
Sr 0.005 ml			150340			150340

NaCl 558°C $t_t = 1.05918 \times 10^6$ sec.

For $CaCl_2$: $V_t = 3$ ml; $C_c = 1.999$ mg/ml; $V_c = 0.005$ ml

For $SrCl_2$: $V_t = 3$ ml; $C_c = 1.277$ mg/ml; $V_c = 0.025$ ml

	Crystal A, Area = 0.9940 cm^2			Crystal B, Area = 0.8533 cm^2		
	w (mg)	A*(^{45}Ca)	A*(^{85}Sr)	w (mg)	A*(^{45}Ca)	A*(^{85}Sr)
1.	4.043	5862	1541	1.237	1817	463
2.	4.151	5539	1437	3.251	4617	1180
3.	4.852	5405	1411	3.387	4329	1137
4.	3.815	3814	887	3.626	4046	1036
5.	3.640	2494	692	4.541	3651	980
6.	3.754	2077	546	4.388	2512	691
7.	5.107	2025	564	3.846	1652	451
8.	4.858	1282	367	4.615	1296	380
9.	5.083	938	276	4.368	770	234
10.	4.880	501	161	4.043	497	143
11.	4.894	334	84	4.680	329	94
12.	5.434	186	47	3.870	173	40
13.	4.626	105	34	4.664	113	27
14.	5.260	78	18	4.551	82	16
15.	4.589	62	12	4.372	63	11
16.	5.652		12	4.559		12
Background		52	2		52	2
Ca 0.002 ml		57602			57602	
Ca 0.005 ml		144445			144445	
Sr 0.002 ml			59515			59515
Sr 0.005 ml			148693			148693

NaCl 601°C $t_t = 9.44640 \times 10^5$ sec.

For $CaCl_2$: $V_t = 3$ ml; $C_c = 1.999$ mg/ml; $V_c = 0.005$ ml

For $SrCl_2$: $V_t = 3$ ml; $C_c = 1\ 277$ mg/ml; $V_c = 0.025$ ml

	Crystal A, Area = 0.6930 cm^2			Crystal B, Area = 0.6229 cm^2		
	w (mg)	A*(^{45}Ca)	A*(^{85}Sr)	w (mg)	A*(^{45}Ca)	A*(^{85}Sr)
1.	4.036	7776	2515	2.773	5467	1710
2.	2.454	4288	1388	1.270	2398	766
3.	3.082	4766	1543	1.647	2934	919
4.	2.694	3711	1183	1.583	2580	816
5.	2.946	3327	1138	1.556	2365	752
6.	2.833	2654	907	2.091	2840	934
7.	3.213	2539	866	2.271	2691	896
8.	3.006	1859	650	2.401	2395	824
9.	2.757	1358	508	3.123	2580	851
10.	2.826	1149	424	3.328	2126	746
11.	3.009	876	380	2.830	1866	505
12.	2.676	691	263	2.633	986	389
13.	2.894	636	234	2.529	753	293
14.	3.277	537	226	2.475	639	247
15.	2.759	331	135	2.602	538	209
16.	2.931	299	107	4.259	546	230
17.	2.997	204	73	2.645	275	106
18.	2.846	144	72	2.844	196	84
19.	2.930	102	41	3.822	181	62
20.	3.978	106	38	2.504	95	30
21.	3.634	77	29	2.612	75	22
22.	3.949	60	10	2.566	57	6
Background		53	2		53	2
Ca 0.002 ml		58823			58823	
Ca 0.005 ml		147433			147433	
Sr 0.002 ml			58333			58333
Sr 0.005 ml			145668			145668

NaCl 625°C $t_t = 8.58060 \times 10^5$ sec.

For $CaCl_2$: $V_t = 3$ ml; $C_c = 1.999$ mg/ml; $V_c = 0.005$ ml

For $SrCl_2$: $V_t = 3$ ml; $C_c = 1.277$ mg/ml; $V_c = 0.025$ ml

	Crystal A, Area = 0.6275 cm^2			Crystal B, Area = 0.6115 cm^2		
	w (mg)	A*(^{45}Ca)	A*(^{85}Sr)	w (mg)	A*(^{45}Ca)	A*(^{85}Sr)
1.	2.265	5649	2135	3.023	7381	2817
2.	2.073	4838	1843	1.313	3060	1154
3.	2.766	5969	2288	1.645	3604	1365
4.	2.531	4900	1898	2.575	5177	1975
5.	2.365	4151	1593	1.963	3591	1406
6.	2.822	4330	1720	2.400	4033	1554
7.	2.557	3403	1351	2.875	4162	1645
8.	2.562	2950	1192	2.565	3162	1279
9.	2.681	2591	1080	2.635	2710	1101
10.	2.635	2172	909	2.381	2082	896
11.	2.494	1715	756	2.221	1710	730
12.	2.488	1501	657	2.373	1568	672
13.	2.725	1372	608	2.589	1453	645
14.	2.448	1056	477	2.609	1221	547
15.	2.480	917	408	2.788	1098	499
16.	2.415	782	329	2.632	882	384
17.	2.492	644	293	2.588	701	310
18.	2.408	540	226	2.518	558	247
19.	2.697	460	203	3.165	578	249
20.	3.475	445	196	3.519	450	203
21.	4.257	448	125	5.569	496	168
22.	3.271	243	51	3.739	220	58
23.	3.592	178	31	3.019	123	24
24.	4.358	140	18	4.352	67	12
25.	5.237	79	6			
Background		53	2		53	2
Ca 0.002 ml		58234			58234	
Ca 0.005 ml		145315			145315	
Sr 0.002 ml			58446			58446
Sr 0.005 ml			145465			145465

NaCl 654°C $t_t = 5.65440 \times 10^5$ sec.

For $CaCl_2$: $V_t = 3$ ml; $C_c = 1.999$ mg/ml; $V_c = 0.005$ ml

For $SrCl_2$: $V_t = 3$ ml; $C_c = 1.277$ mg/ml; $V_c = 0.025$ ml

	Crystal A, Area = 0.8811 cm^2			Crystal B, Area = 0.9118 cm^2		
	w (mg)	A*(^{45}Ca)	A*(^{85}Sr)	w (mg)	A*(^{45}Ca)	A*(^{85}Sr)
1.	4.171	6201	2358	2.852	4181	1607
2.	2.610	3697	1393	2.012	2919	1120
3.	3.467	4536	1714	2.989	4171	1576
4.	3.305	4003	1520	2.841	3538	1372
5.	3.707	3967	1509	3.413	4081	1554
6.	4.717	4430	1685	3.639	3919	1470
7.	3.896	3099	1177	3.799	3641	1378
8.	3.929	2669	952	3.971	3290	1221
9.	8.208	4345	1497	7.345	4832	1728
10.	7.609	2706	882	7.654	3750	1279
11.	7.748	1880	631	7.933	2792	913
12.	7.331	1076	457	7.959	1837	636
13.	8.039	734	334	8.344	1176	468
14.	8.583	610	239	8.099	766	324
15.	8.044	388	168	8.200	585	241
16.	7.800	287	80	8.362	401	149
17.	7.961	279	45	8.431	320	92
18.	8.515	195	15	8.370	193	47
19.	7.753	80	8	8.344	151	15
20.	8.118	68		8.228	68	8
Background		54	2		54	2
Ca 0.002 ml		58560			58560	
Ca 0.005 ml		144750			144750	
Sr 0.002 ml			60243			60243
Sr 0.005 ml			149693			149693

NaCl 683°C $t_t = 5.62380 \times 10^5$ sec.

For $CaCl_2$: $V_t = 3$ ml; $C_c = 1.999$ mg/ml; $V_c = 0.005$ ml

For $SrCl_2$: $V_t = 3$ ml; $C_c = 1.277$ mg/ml; $V_c = 0.025$ ml

	Crystal A, Area = 1.0020 cm^2			Crystal B, Area = 1.0042 cm^2		
	w (mg)	A*(^{45}Ca)	A*(^{85}Sr)	w (mg)	A*(^{45}Ca)	A*(^{85}Sr)
1.	4.474	6566	2589	6.223	9174	3563
2.	2.726	3985	1562	6.226	8746	3466
3.	3.203	4483	1052	4.535	5815	2293
4.	2.926	3930	1538	4.389	5137	2071
5.	3.371	4214	1670	4.704	5043	2036
6.	4.178	4754	1953	4.783	4731	1894
7.	4.689	4926	1994	4.955	4204	1790
8.	5.053	4778	1966	5.959	4415	1879
9.	7.860	6118	2626	8.485	5016	2305
10.	10.176	6072	2795	9.076	4252	2022
11.	8.022	3764	1781	8.287	3188	1522
12.	8.617	3057	1518	9.519	2789	1340
13.	9.934	2827	1347	8.999	1941	976
14.	8.432	1724	864	9.118	1453	729
15.	8.914	1363	686	8.728	932	534
16.	9.185	948	527	9.068	921	411
17.	8.633	623	346	9.069	502	316
18.	8.538	447	259	9.594	385	218
19.	8.442	261	148	8.831	198	102
20.	6.168	174	72	9.838	85	54
21.	6.916	132	33	9.426		9
22.	5.994	63	7			
Background		52	2		52	2
Ca 0.002 ml		57912			57912	
Ca 0.005 ml		145150			145150	
Sr 0.002 ml			59127			59127
Sr 0.005 ml			147163			147163